Dissertations (2016-Present)   Dissertations

5-2022

Preclinical Development of a Novel Antileishmanial Agent OJT007: Bioanalytical Assay, in Vitro Studies and Pharmacokinetics

Maria Eugenia Rincon-Nigro

Recommended Citation

PRECLINICAL DEVELOPMENT OF A NOVEL ANTILEISHMANIAL AGENT

OJT007: BIOANALYTICAL ASSAY, IN VITRO STUDIES AND

PHARMACOKINETICS

DISSERTATION

Presented in Partial Fulfillment of the Requirements for

the Degree Doctor of Philosophy in the Graduate School

of Texas Southern University

By

Maria Rincon Nigro, B.S.

Texas Southern University

2022

Approved By

_____
Dong Liang

Chairperson Dissertation Committee

_____
Gregory H. Maddox

Dean, Graduate School

Approved By

Dong Liang	3/2/2022
Chairperson, Dissertation Committee	Date

Song Gao	02/28/2022
Committee Member	Date

Selvam Chelliah	02/28/2022
Committee Member	Date

	02/25/2022
Huan Xie	
Committee Member	Date

Mario Hollomon	02/24/2022
Committee Member	Date

PRECLINICAL DEVELOPMENT OF A NOVEL ANTILEISHMANIAL AGENT OJT007: BIOANALYTICAL ASSAY, IN VITRO STUDIES AND PHARMACOKINETICS

By

Maria Rincon Nigro, Ph.D.

Texas Southern University, 2022

Professor Dong Liang, Advisor

Current treatments for cutaneous leishmaniasis suffer from toxic side effects, high cost, parenteral administration, and drug resistance. Thus, there is a critical need to develop oral drugs for the treatment of leishmaniasis. OJT007 is a novel class of drug with potent antiproliferative effects against *Leishmania Major*. The purpose of this project is to conduct preclinical drug development studies for OJT007 including bioanalytical assay development, pre-formulation studies, in vitro hepatic drug metabolism and in vivo pharmacokinetics.

A sensitive, specific, and reproducible ultra-high performance liquid chromatography-tandem mass spectrometry (LC-MS/MS) method was developed and validated. The separation was achieved on a UPLC BEH C_{18} column (2.1 × 50 mm, 1.7 µm) using a mobile phase consisting of 0.1% formic acid in acetonitrile and 0.1% formic acid in water as gradient elution at a flow rate of 0.4 mL/min. The mass analysis was performed with a 4000 QTRAP® mass spectrometer using multiple-ion reaction

monitoring (MRM) in the positive mode, with the transition of m/z 325 → m/z 205 for

OJT007 and m/z 350 → m/z 101 for voriconazole (as internal standard). Rat plasma and

urine were extracted for OJT007 by protein precipitation in acetonitrile for quantification.

Plasma protein binding of OJT007 was determined using the ultrafiltration

method. In vitro phase I and II hepatic metabolism of OJT007 was evaluated in rat liver

microsomes using standard reaction protocols. OJT007 metabolites were identified by

LC-MS/MS using Q1MI, product ion, precursor ion and neutral loss scan and by β-

glucuronidase hydrolysis. The OJT007 glucuronidation rates were determined by

quantifying OJT007 glucuronide using UPLC, and the kinetic parameters of OJT007

were determined by measuring the initial glucuronidation rates.

. Oral bioavailability of OJT007 was evaluated using a crossover study design.

Serial plasma samples were collected at predetermined time points. Total urine samples

were also collected from each rat for 24 hours after each dose. The pharmacokinetic

parameters were calculated using Phoenix WinNonlin® 8.0 software.

The intra- and inter-day precision and accuracy were within the acceptable limit

of ≤20% for LLOQ and ≤15% for high, medium and low QC. The extraction recovery in

rat plasma and urine samples were 95.1% and 83%, respectively. OJT007 exhibited a

matrix factor in plasma and urine of 7.96% and 12.4%, respectively. The fraction of

OJT007 bound to plasma protein had a mean value of 99.1%, suggesting the drug is

highly bound to plasma proteins.

OJT007 is glucuronidated rapidly in rat liver microsomes to form a mono-

glucuronide, which was confirmed by LC-MS/MS and β-glucuronidase hydrolysis. The

kinetic parameters of glucuronidation V_{max} and K_m were 1.125 nmol/min/mg and 10.73 µM., respectively.

After intravenous administration, OJT007 displayed a bi-exponential disposition with a rapid distribution followed by a slower elimination. The mean AUC, volume of distribution, and clearance were 2.06 h.mg/L, 6.90 L/Kg and 2.30 L/hr/Kg, respectively. Following oral administration, OJT007 was rapidly absorbed with a t_{max} of 1.4 hours. After oral dosing the mean AUC, volume of distribution, and clearance were 0.45 h.mg/L, 78.6 L/Kg and 23.19 L/hr/Kg, respectively. Mean oral bioavailability of OJT007 in the co-solvent formulation was 10.9%. The mean percentage of OJT007 dose excreted unchanged in urine after 24 hours following intravenous and oral administration was less than 1%, suggesting OJT007 was extensively metabolized in vivo.

A sensitive, specific and reproducible LC-MS/MS method was developed and validated to quantify OJT007 in rat plasma and urine. The method was successfully used for pharmacokinetic studies. This is the first time that oral bioavailability of OJT007 after oral administration in rat is determined. These results may prove valuable for further preclinical and clinical evaluation of OJT007

TABLE OF CONTENTS

LIST OF FIGURES

LIST OF TABLES

LIST OF EQUATION

LIST OF ABBREVIATIONS

%	Percentage
μg	Microgram
μL	Microlitre
μM	Micromolar
μmol	Micromole
ADME	Absorption-Distribution-Metabolism-Elimination
CL	Cutaneous leishmaniasis
Cl	Clearance
MCL	Mucocutaneous Leishmaniasis
VL	Visceral leishmaniasis
L	*Leishmania*
DCL	Disseminated cutaneous leishmaniasis
LCL	Localized cutaneous leishmaniasis
FDA	US Food and Drug Administration
IS	Internal standard
IV	Intravenous
PO	Per os (oral)

DP	Declustering potential
CE	Collision energy
CXP	Collision cell exiting potential
EP	Entrance potential
ESI	Electro-spray ionization
LC-MS/MS	Liquid chromatography tandem mass spectrometry
MRT	Mean residence time
PK	Pharmacokinetics
MetAP	Methionine aminopeptidase
HPLC	High performance liquid chromatography
UV	Ultraviolet
GC	Gas chromatography
MS	Mass spectrometry
CYP	Cytochrome P450
UGT	UDP-glucuronosyltransferase
NCE	New chemical entity
LLOQ	Lowe limit of quantification
GIT	gastrointestinal tract

GI	Gastrointestinal
KPI	Potassium phosphate
NME	N- Terminal excision
RE	Relative error
CV	Coefficient of variation
LIT	Linear ion trap
MRM	Multiple reaction monitoring
QC	Quality control
SD	Sprague Dawley
AUC	Area under the curve
mL	Milliliter
RPM	Revolutions per Minute
VMAX	Maximum Velocity
KM	Michaelis Constant
MS2	Product ion
NL	Neutral loss
LdMT	*Leishmania donovani* miltefosine transporter

DMSO   Dimethyl sulfoxide

DI   Deionized

HLM   Human liver microsomes

RLM   Rat liver microsomes

R&D   Research and Development

MetAP   Methionine Aminopeptidase

VITA

2016…………………………………………………… Bachelor of Science,
University of Houston, Texas

2017-2022…………………………………………….. Graduate Research Assistant,
College of Pharmacy and
Health Science, Texas
Southern University

Major Field……………………………………………. Pharmaceutical Science

DEDICATION

To the unconditional love and support of Eugenia, Gonzalo,

Mario, Jose, Mario Rene and Raul.

ACKNOWLEDGEMENT

In the process of writing this dissertation, I have received a great deal of support and assistance. I would like to take a moment to thank the many people who helped in one way or another on this journey.

I want to express my deepest gratitude to my advisor Dr. Dong Liang. Thank you for your guidance and for believing in me throughout graduate school. Your support, mentorship and enthusiasm has helped me to stay motivated through this journey. I greatly appreciate you taking me into your lab and molding me into a more independent scientist.

I would also like to express my deepest appreciation to my committee members Dr. Huan Xie, Dr. Mario Hollomon, Dr. Selvam Chelliah and Dr. Song Gao for your guidance, scientific advice and sharing your valuable expertise.

I sincerely appreciate Dr. Song Gao and Dr. Huan Xie for giving me access to equipment and supplies in their labs.

I want to thank Dr. Omonike Olaleye for being a great mentor and for entrusting me with OJT007, you were always very encouraging, and your enthusiasm was always contagious. I am extremely thankful to Dr. Jing Ma, Dr. Yang Wang, Dr. Ting Du and Dr. Yuan Chen for illustrating various lab techniques and helping throughout the conduct of in vitro and in vivo animal studies.

I would like to thank give a special thanks to Dr. Ololade Awosemo for her help when I called upon her. Thank you for being a great senior student in the lab. Working till late together or waking up early for animal studies was always a bit more fun when we were together. I want to also thank Manvir Kaur for her discussions and her friendship.

CHAPTER 1

INTRODUCTION

Preclinical studies play a crucial role in the development of new chemical entities (NCE) and serve as the bridge that connects drug discovery to clinical studies. During preclinical development a wealth of data on safety and efficacy is amassed for its potential extrapolation into humans. Undoubtedly, the main goal of drug development is to understand the pharmacologic response and toxicity of the lead molecule to guide in the rational design and conduct of clinical studies. In order to accomplish these goals, typical preclinical development efforts comprehend six major activities: synthesis/manufacture of the drug substance, safety and toxicology, pharmacology, manufacture of drug product, method development and validation, pre-formulation and formulation, metabolism, and pharmacokinetics (Singh, 2018). In this work, we will focus on the last four activities.

Bioanalytical assay development and validation is a critical prequel to the various preclinical studies. In fact, the analytical method provides the means to quantitate the analyte or drug in the relevant biological matrix. Not surprisingly, the FDA recommends a full validation of any new bioanalytical method (*USFDA*, 2018). The method validation is done with the purpose of ensuring the veracity of the data collected during the drug development studies.

Maximization of exposure, and thus efficacy, can be accomplished by the intelligent design of a suitable formulation. The rational design of a formulation entails pre-formulation studies to assess physicochemical properties of the NCEs to develop a formulation that will enable *in-vivo* evaluations. The drug's physicochemical characteristics and the intended route of administration are key driving factors in the formulation of an NCE.

Pharmacokinetics studies what the body does to a drug. It encompasses four basic processes: absorption, distribution, metabolism, and excretion of a drug. Early characterization of each of these processes enables the selection of the best candidates for further development. An important byproduct of pharmacokinetic evaluations is that the information accumulated can be used to predict plasma concentrations, target dose, and the fate of the administered dose.

Part of a drug's pharmacokinetic evaluation comprehends an assessment of drug metabolism. Drug metabolism is a significant determinant of a drug's clearance since generally drugs undergo biotransformation for its elimination. The ultimate purpose of a preclinical metabolism assessment is to predict the behavior of a drug in humans and to ensure safe clinical studies. In addition, early in drug development, drug metabolism studies can help select drugs more likely to have appropriate exposure *in vivo* by identifying drugs which are resistant to extensive metabolism.

In this work, we aimed to apply the guiding principles of pharmacokinetics for the rational development of a novel antileishmanial agent. The treatment of leishmaniasis relies on drugs that suffer from toxic effects, high costs, mixed efficacy, and parenteral administration. Notwithstanding the need for R&D of drugs for CL, the pipeline remains

poor (Golgher et al., 2011). Recently, OJT007 was identified as a potent and selective methionine aminopeptidase inhibitor against *L.major*. Furthermore, the compound demonstrated efficacy in vivo following oral administration with no toxicity (Rodriguez et al., 2020). The dearth of oral chemotherapeutic agents for CL and the promising *in vivo* results makes OJT007 an attractive candidate for further development.

In this dissertation, we seek to evaluate the feasibility of OJT007 as a novel chemotherapeutic candidate. Accordingly, the development and validation of a bioanalytical assay for the quantification of OJT007 in urine and plasma is reported. The results of pre-formulation studies to characterize physicochemical properties of OJT007 and its application to the development of a cosolvent are outlined. The in vitro metabolism of OJT007 in rat liver microsomes is investigated. The bioanalytical method and formulation were applied to investigate the pharmacokinetics of OJT007 in rats.

CHAPTER 2

LITERATURE REVIEW

2.1 Leishmania Species and Leishmaniasis

Leishmaniases are vector-borne parasitic diseases caused by more than 20 *Leishmania* species and are spread to humans by over 90 species of infected sand flies. About 12 million people suffer from leishmaniasis (Mohammadi & Soltani, 2019).The disease is endemic across all continents except Australia and affects the most vulnerable populations. Some risk factors associated with the disease include poverty, poor housing and domestic sanitary conditions, malnutrition, and immunosuppression (Burza et al., 2018).

Though tropical areas are more prone to leishmaniasis infection, migration and travel have put at risk previously unaffected populations. As a result, leishmaniasis is an emerging concern in the United States with authors reporting non-endemic and endemic infections. (Barry et al., 2014; McIlwee et al., 2018; Wortmann et al., 2002; Wright et al., 2008)

There are different forms of leishmaniasis in people: Cutaneous leishmaniasis, visceral leishmaniasis and mucocutaneous leishmaniasis. Visceral Leishmaniasis (VL), or Kala-azar, is one of the deadliest diseases among the neglected tropical diseases if left untreated (Pandey et al., 2020). Depending on the transmission characteristics, VL is

classified as zoonotic or anthroponotic. The zoonotic form, which is caused by *L. infantum*, uses dogs as main reservoir, and generally affects children and immunocompromised individuals. The anthroponotic form, which is caused by *L. donovani* and *L. chagasi,* is more common and affects all age groups. (van Griensven & Diro, 2012). Clinical manifestations consist of fever, malaise, weight loss, hepatomegaly, splenomegaly and pancytopenia (Pearson & Sousa, 1996). Visceral leishmaniasis has an incidence of 50000 to 90000 cases per year worldwide with the majority of the cases occurring in Brazil, Ethiopia, Eritrea, India, Iraq, Kenya, Nepal, Somalia and Sudan. (World Health Organization, 2021).

Cutaneous Leishmaniasis (CL) is the most common form of leishmaniasis. It is characterized by skin lesions, mainly ulcers, on exposed body parts. An estimated 600,000 to 1 million cases occur worldwide annually (World Health Organization, 2021). Approximately 66,941 patients of CL are reported annually in the Americas which accounts for approximately 30% of the total patients of CL worldwide (Pan American Health Organization, 2018).

Mucocutaneous Leishmaniasis (MCL), a sequela of infection with CL, leads to partial or complete destruction of the mucosal membranes of the nose, mouth and throat. Approximately a few thousand cases occur worldwide each year (Karunaweera et al., 2020).

The causative agents for CL have been classified as 'Old World' and 'New World'. In Africa and Eurasia ('Old World'), leishmaniasis is generally caused by *L. major, L. tropica, L. aethiopica, L. infantum,* and *L. archibaldi*. In the Americas or 'New World' leishmaniasis is caused by *L. mexicana, L. venezuelensis, L. amazonensis, L.*

braziliensis, L. panamensis, L. chagasi, L. guyanensis, and *L. peruviana.* (Akilov et al., 2007)

2.1.1. Parasite life cycle

Figure 1 summarizes the life cycle of *Leishmania*. Leishmania parasites have two major cell morphologies: the promastigote which is characterized by a long motile flagellum, and the amastigote which is characterized by a short immotile flagellum. *Leishmania* infected sand flies inoculate the promastigote stage of the parasite during blood meals. The promastigotes at the puncture site are phagocytized by macrophages, monocytes, and neutrophils. Once inside the macrophage the promastigotes differentiate into the amastigote stage, proliferate by simple division, and proceed to infect other cells and tissues. During a blood meal, the sand fly ingests the amastigote stage of the parasite, which then begins to differentiate into the motile promastigote form (Séguin & Descoteaux, 2016; Sunter & Gull, 2017).
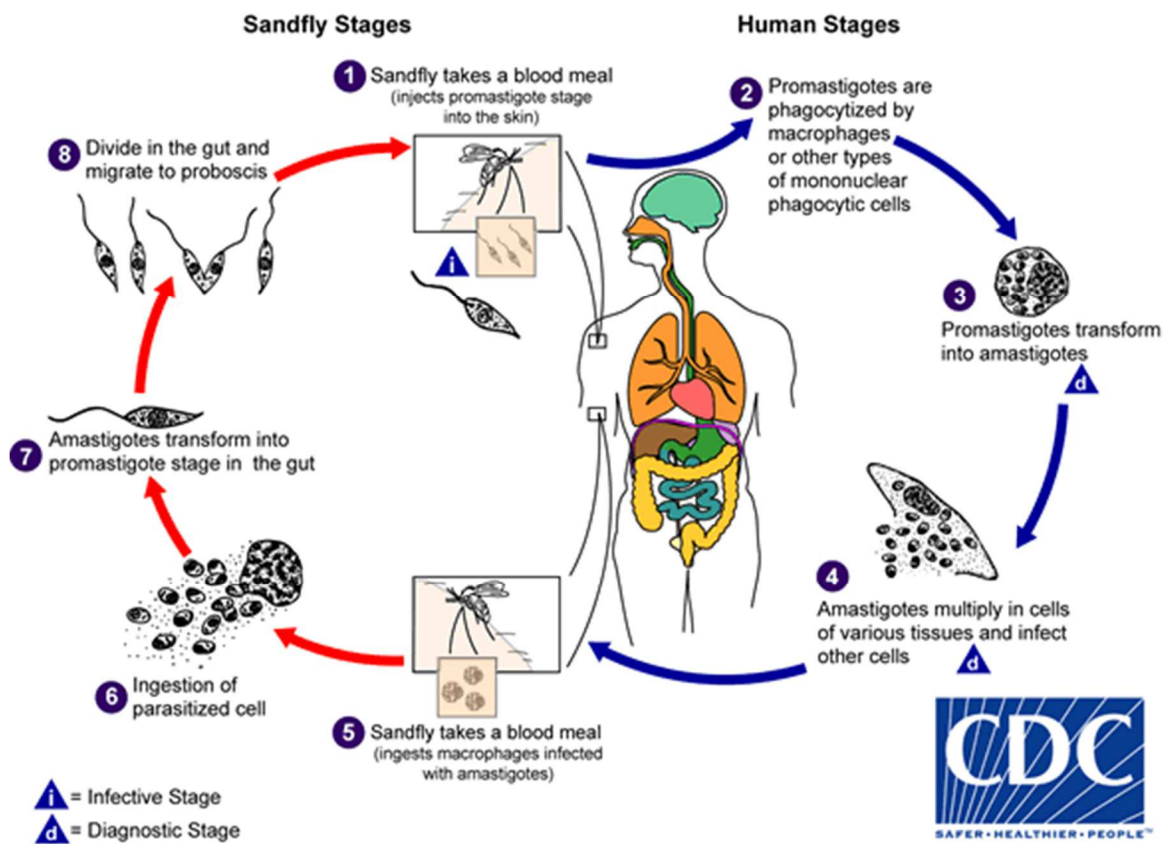
Figure 1. *Leishmania Life Cycle,*
Center for Disease Control and Prevention,2021. Leishmaniasis Biology. Retrieved from
CDC - Leishmaniasis - Biology

2.1.2 Vectors and transmission

The *Leishmaniases* are transmitted by the bite of small, hairy, soundless, and blood-feeding insects named sand flies. Vectors in the 'Old World' and 'New World' belong to the genus *Phlebotomus* and *Lutzomyia*, respectively. *Pheblotomus* sandfly species live in semi-arid ecosystems or deserts while *Lutzomyia* sandflies live in forests (Sharma & Singh, 2008). Transmission is both anthroponotic or zoonotic, and it depends on whether human is the main reservoir (Reithinger et al., 2007).

2.2 Cutaneous leishmaniasis (CL)

2.2.1 Clinical manifestations

The clinical manifestations of the disease are the product of the complex interaction between the parasite virulence characteristics, vector biology, and host factors (i.e., immune response). Intracellular infection of dermal macrophages by *Leishmania* parasites causes an excessive host immune response leading to tissue damage and disease (Wijnant et al., 2018). The varied clinical forms include localized cutaneous lesions, disseminated cutaneous lesions, and mucosal lesions.

In simple, localized, uncomplicated localized cutaneous leishmaniasis (LCL), the first sign of an infection is typically a small erythema that develops into a red papule at the site where sandfly bit the host. The papule slowly evolves into a firm nodule with an iceberg configuration. The nodule enlarges and ulcerates into a lesion that resembles a flattened volcano (Figure 2, Panel A). Ulcerative lesions generally self-heal 5-12 months after initial appearance leaving cribriform scars. Secondary bacterial infections are

possible, especially in ulcerated lesions, which exacerbate the symptoms of leishmaniasis (Akilov et al., 2007).

The appearance of disseminated cutaneous leishmaniasis (DCL) was first described in Venezuela in 1948 (Convit & Lapenta,1948). It is caused by *L. aethiopica* in the 'Old World' and by *L.amazonensis* in the 'New World'(Vélez et al., 2015). DCL may occur due to the parasite's ability to migrate via the lymph or blood to different areas of the body (Figure 2, Panel B). Lesions in DCL are mostly papules and nodules that do not ulcerate. DCL is more serious than LCL due to an inhibition of specific cellular immunity (Vélez et al., 2015).

Mucocutaneous Leishmaniasis (MCL), occurs as a sequela of CL infection, though it can co-occur. Inadequate therapy of LCL is a risk factor for MCL. In the New World, it is caused by *L. braziliensis* , although *L. panamensis* , *L. guyanensis* , and *L. amazonensis* can also be involved. In the Old World, it is caused by *L*, *major* and viscerotropic *L. infantum* (Goto & Lauletta Lindoso, 2012). The symptoms associated with MCL include nasal inflammation, ulceration, and perforation of the septum (Figure 2,Panel C). In occasions, the lesions may extend, and parts of the face, soft palate, pharynx, and larynx may be affected (Goto & Lindoso, 2010).
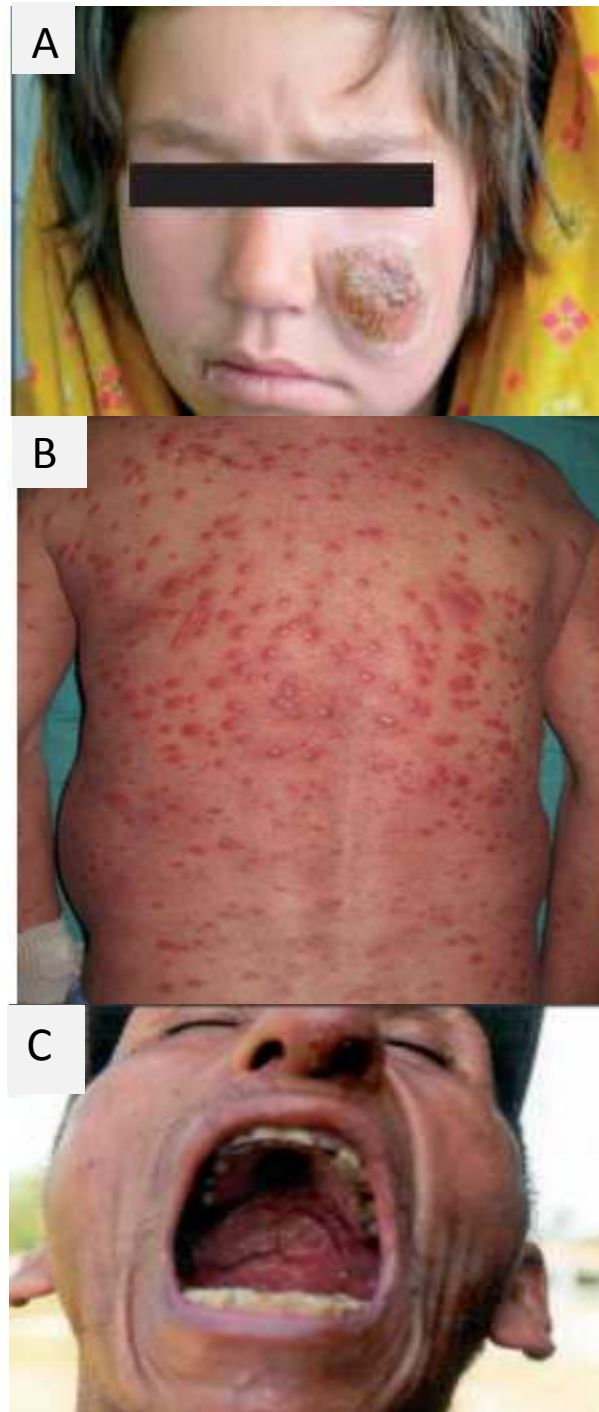
Figure 2. *Cutaneous leishmaniasis clinical manifestations. A) Localized lesions. B) Disseminated lesions. C) Mucocutaneous lesions.*
Adapted from "Cutaneous Leishmaniasis" by R. Reithinger et al. 2007

2.3 Current treatment of CL

Generally, CL lesions self-heal without treatment; however, self-healing may take several months and can leave disfiguring scars (Scorza et al., 2017). Therapeutic interventions are used in order to accelerate cure and to prevent scarring and mucocutaneous disease. Due to the heterogeneity of the causative infectious agent, there is no universal treatment for leishmaniasis (Minodier & Parola, 2007). Pharmacological treatment options can be local or systemic.

2.3.1 Local chemotherapeutics

Local treatments are the treatment of choice in Old World Leishmaniasis, while for New World CL, systemic treatments are preferred because of the risk of developing MCL. Drug administration through the skin is particularly appealing as it could deliver doses of the drug to the target while preventing adverse effects due to the drug acting off target.(Khalil et al., 2019)

2.3.1.1 Paromomycin Sulfate

Aminoglycosides inhibit bacterial protein biosynthesis (van Hees & Naafs, 2016). Paromomycin topical treatment has displayed mixed efficacy and modest benefits. Skin permeation is an important problem limiting the efficacy of topical paromomycin (Khalil et al., 2019). Paromomycin 15% with methylbenzethonium 12% was effective for 72% of the patients as therapy for *L. major* infection in Israel (El-On et al., 1986). In a study in Colombia that treated patients with topical 15% paromomycin plus 0.5% gentamicin cure rates were similar to those obtained in placebo. Nonetheless, it appeared that cure time

was faster in patients treated with paromomycin (J. M. Soto et al., 2002). Local irritation has been the most common side effect associated with paromomycin use.

2.3.1.2 Intralesional pentavalent antimony

Intralesional pentavalent antimony is widely used in the treatment of Old World and New World CL. It is applied alone or in combination with cryotherapy. The basic aim of local infiltration is to fill infected parts in the dermis with the drug, making sure not to inject onto the subcutaneous tissue, as this would prevent the drug from reaching the site of action (van Hees & Naafs, 2016). Pentavalent antimony is recommended for simple CL cases where lesions do not involve face of joints (Vera et al., 2021). Intralesional administration results advantageous because a high concentration of the Sb(V) can be delivered into the diseased tissue, which would be toxic if treated systemically (Oliveira-Neto et al., 1997).

2.3.2 Systemic chemotherapeutics

Systemic chemotherapeutics include parenteral treatments, mainly intravenous (IV) or intramuscular (IM), and oral treatments.

2.3.2.1. Pentavalent antimonial (IV, IM)

Pentavalent antimonial (Sb(V)) compounds such as sodium stibogluconate (Pentostam) and meglumine antimoniate (Glucantime) are the first-line drugs in the treatment of leishmaniasis. The mechanism of action of Sb(V) is not entirely understood, though it seems to involve inhibition of macromolecular biosynthesis in amastigotes via perturbation of energy metabolism (van Hees & Naafs, 2016). Pentavalent antimony is given as an intramuscular or intravenous injection in a dose of 20 mg/kg/day for up to 30

days. Sb(V) has a cure rate of 90% when it is used at an appropriate dose (Thakur et al., 1988). Nonetheless, the appropriate dose and duration of treatment have changed over the course of years to prevent therapeutic failure caused by antimony resistance (Ryan & Magill, 2020).

The use of pentavalent antimonial is often accompanied by severe side effects such as cardiotoxicity, hepatotoxicity, nephrotoxicity, and pancreatitis (Kato et al., 2014). Furthermore, these side effects have been exacerbated by the increased dose and length of treatment necessary for maintaining the cure rate. For instance, QT prolongation has been observed in patients treated with Sb(V) and this prolongation in the QT interval appears to be directly related to the dose administered (Ryan & Magill, 2020).

2.3.2.2. Amphotericin B (IV)

Conventional Amphotericin B (Amphotericin B deoxycholate) is a polyene antibiotic used in systemic fungal infections. It is used as a second-line treatment for mucosal or localized cutaneous leishmaniasis, especially with pentavalent antimony treatment failure. The dose of amphotericin B is 1 mg/Kg/day infused over two hours every other day up to 30 days (Sundar & Chakravarty, 2013). The drug binds to leishmania parasites' membrane sterol (ergosterol), creating pores that lead to cell death. Nonetheless, because mammalian and leishmanial membranes contain sterols, amphotericin B causes toxicity in humans by binding to cholesterol. Although the activity of amphotericin B is higher against ergosterol than cholesterol, it can cause serious side effects against the host, such as nephrotoxicity, hypokalemia, and myocarditis (Eriksson, 2001).

The various side effects are minimized by using lipid formulations that decrease the free drug's exposure to organs. Short courses of liposomal amphotericin B at a dose of 3-4 mg/kg/day on days 1-5 and a sixth dose on day 10 have shown to be effective (Solomon et al., 2011). Liposomal amphotericin B has been shown to be less nephrotoxic because it is selectively taken up by macrophages, the *Leishmania* parasite target cell (Solomon et al., 2011). Although toxicity is minimized in liposomal amphotericin B, high cost becomes a significant problem in developing countries (Sundar et al., 2001).

2.3.2.3. Pentamidine (IV, IM)

Pentamidine isethionate is a diamidine drug. Its mechanism of action is not entirely understood, but it appears to interfere with DNA synthesis and modify the morphology of kinetoplast (Kaur & Rajput, 2014). It is the drug of choice for the treatment of cutaneous leishmaniasis caused by infection with *L. guayanensis* and *L. panamensis* (Soto-Mancipe et al., 1993; van Hees & Naafs, 2016). Three or four 4 mg/Kg injections every other day are well tolerated via IV infusion or deep IM injection. Toxicity seems to be dose-related and includes adverse effects such as hypotension, phlebitis, permanent diabetes mellitus, nephrotoxic effects, arrhythmia, and mild cardiac toxicity (Piccica et al., 2021).

2.3.2.4 Paromomycin

Paromomycin is an aminoglycoside that binds to 16S ribosomes RNA and inhibits protein synthesis. Systemic use of paromomycin for cutaneous leishmaniasis is rare due to mixed efficacies depending on the causative infectious species. For instance, a dose of 20 mg/Kg/day for 20 days was shown efficacious in infection caused by *L. braziliensis*

(Correia et al., 1996); However, *L. panamensis* showed resistance and efficacy was insubstantial (J. Soto et al., 1994). In addition, side effects such as ototoxicity and nephrotoxicity limit its use to treat CL.

2.3.2.5 Azoles (PO)

The antifungals ketoconazole, fluconazole, and itraconazole have shown variable results in the treatment of leishmaniasis. Their mechanism of action is inhibition of lanosterol 14-α-demethylase, which blocks the formation of ergosterol, a fundamental component of the cell membrane (Ghannoum & Rice, 1999).

A dose of 400 mg daily for 28 days was found efficacious in treating cutaneous leishmaniasis caused by *L. major*. Reported adverse effects are mild and limited to reversible abnormalities in hepatocellular function test and decreased serum testosterone values (Saenz et al., 1990; Weinrauch et al., 1983). Oral fluconazole at a dose of 5 mg/Kg/day for 12 days has been shown efficacious against disseminated cutaneous leishmaniasis in Venezuela, and the merits of this treatment deserve future studies (Daly et al., 2014). Itraconazole has shown merits in the treatment of mucosal leishmaniasis due to its better bioavailability and ability to achieve higher exposure in tissue and mucosa. For instance, itraconazole displays 65% and 51% efficacy in localized cutaneous leishmaniasis and mucocutaneous leishmaniasis, respectively (Galvão et al., 2017).

2.3.2.6 Miltefosine (PO)

An alkyl phospholipid, initially developed as an oral antineoplastic agent, inhibits phospholipid and sterol biosynthesis (van Hees & Naafs, 2016). It is the only oral treatment of leishmaniasis approved by the FDA. The FDA regimen is 2.5 mg/kg/day

with a maximum dose of 150 mg/day. Miltefosine displays mixed efficacy, with high variability between countries and *leishmania* species (Garza-Tovar et al., 2020). The reported cure rates range from 50% (L. braziliensis and *L. Mexicana* in Guatemala) to 88% (L. *panamensis* in Colombia)(J. Soto et al., 2004). Likewise, miltefosine has shown a modest efficacy of 65% against CL infection caused by *L. tropica* (J. Soto et al., 2004).

Even within same species, efficacy variations have been observed (J. Soto et al., 2007). The drug non susceptibility of certain *leishmania* species to miltefosine has been associated with low expression of the putative *L. donovani* miltefosine transporter (LdMT) and the protein LdRos3 both of which aid in drug internalization into the parasite (Dorlo et al., 2012). Of particular concern is that miltefosine has a long half-life, this leads to subtherapeutic levels of miltefosine in blood for several weeks and could potentially cause drug resistance (Dorlo et al., 2008). The toxicity associated with miltefosine treatment is mild, including adverse effects such as vomiting and diarrhea, which occur in a dose-dependent matter (Machado & Penna, 2012).

2.4 Drug discovery and development in CL

Clinical drug development is a costly and lengthy process. The cost to develop New Chemical Entities (NCE) is around 2.6 billion (Mohs & Greig, 2017) . Preclinical drug discovery and development aims to deliver candidate molecules that have appropriate efficacy at target site, safety and drug-like properties. Approximately 63% of all preclinical compounds nominated for clinical development fail due to poor pharmacokinetics and toxicity (Han et al., 2010). Nonetheless, the discovery and development of new antileishmanial agents remains a commercially unattractive area of R&D; thus, it has been explored primarily in the realm of academic research.

2.4.1 Methionine aminopeptidase as a target for infectious disease

Methionine aminopeptidase (MetAP) is a metalloprotease that catalyzes N-terminal methionine cleavage from proteins during translation. Protein synthesis is initiated with a formylated methionine in prokaryotes or methionine in eukaryotes. Methionine is usually removed from mature proteins in eukaryotes by MetAP (Methionine aminopeptidase). In prokaryotes , formyl methionine is removed by formyl methionine deformylase resulting in N-terminal methionine, which MetAP.then processes (O. A. Olaleye et al., 2009).

There are two types of MetAPs, 1 and 2; prokaryotes have homologs of either type, while eukaryotes have both (O. A. Olaleye et al., 2009). Nonetheless, eukaryotes develop lethal phenotypes if either MetAP gene is deleted (X. Li & Chang, 1995). N-terminal excision (NME) is necessary for post-translational modifications, stability, folding, and the localization of nascent proteins. The essentiality of NME in eukaryotes and prokaryotes makes it a promising target for infectious diseases. Various types of MetAP have been validated as targets for a variety of infectious diseases caused by *Mycobacterium Tuberculosis* (*Mtb*, the causative agent of TB) (O. Olaleye et al., 2010), *Plasmodium falciparum* (the causative agent of malaria)(Gardiner et al., 2009), *Acinetobacter baumannii* (a Gram-negative bacillus resistant to most of the antibiotics in use) (Yuan et al., 2011)and *Cryptosporidium parvum* (a parasite that infects epithelial cells and causes diarrhea)(Kang et al., 2012). Recently, MetAP1 inhibitors have shown promising results against *Leishmania donovani*, giving evidence for the use of MetAP1 inhibitors for the treatment of Leishmaniasis (Bhat et al., 2018).

2.4.2 Identification of OJT007 as a methionine aminopeptidase inhibitor.

The identification used a target-based approach. Briefly, a high-throughput screen of 175,000 structurally diverse compounds against MetAP1 was conducted. A total of 439 hits that exhibited 30-40% inhibition were identified. The IC_{50} was determined for 81 compounds. The most potent inhibitors were then tested on the growth of M. tuberculosis culture. This effort led to the discovery of eight potent MetAP1 inhibitors against M. tuberculosis (O. Olaleye et al., 2010, 2011).

2.4.3 Identification and characterization of OJT007 as a treatment for Cutaneous Leishmaniasis caused by L. major.

As part of the drive to find new antileishmanial treatments, the antiparasitic activity of these eight novel MetAP1 inhibitors against CL infection caused by *L. major* was screened and characterized. The screen led to the identification of OJT007, a MetAP1 inhibitor with potent and selective leishmanicidal activity against *L. major* (Rodriguez et al., 2020).

OJT007 displayed an EC_{50} of 500nM against *L.major* promastigotes and amastigotes with no cytotoxicity to hosts cells. Furthermore, the drug demonstrated oral efficacy in a preclinical mouse model. In a BALB/c animal mode, OJT007 decreased parasite load and decreased lesion size. In addition, it did not generate changes in weight, nor did it cause cardiac or hepatic damage. These promising results made OJT007 an attractive candidate for the oral treatment of cutaneous leishmaniasis (Rodriguez et al., 2020).

2.5 OJT007

OJT007 is known by the IUPAC as 2-[(*E*)-(5,6,7,8-tetrahydro-[1] benzothiolo

[2,3-d]pyrimidin-4-ylhydrazinylidene)methyl] phenol. It has a molecular formula of

$C_{17}H_{16}N_4OS$, and a calculated molecular weight of 324.4 g/mol (Figure 3). OJT007

occurs as yellow fine needle-like crystals with no noticeable odor and unknown taste. The

studies reported in this work were conducted using the free base of OJT007.

2.5.1 Physicochemical characteristics of OJT007

The calculated physicochemical properties of a drug are paramount in identifying

the most druggable lead during drug discovery and development. Furthermore, these

properties serve as early predictors of orally active drugs. As we will learn in the

following section, the physicochemical properties of a drug affect the drug permeability

and solubility, which consequently affects drug absorption.

The physicochemical properties of OJT007 were obtained using the American

Chemical Society (ACS) database, SciFinder®. These properties are summarized in

Table 1. OJT007 is a lipophilic compound, suggesting that the compound shows

preference to be associated with lipid phase and, by extension, will likely permeate

biological membranes easily by passive diffusion.

OJT007 has a calculated water solubility of 8.1 μg/ml, making OJT007 sparingly

soluble in water. Low water solubility may have important implications in drug

absorption. Solubility of the drug is a prequel to permeation across the GI tract. Thus,

solubility may become a limiting factor in the absorption process. The calculated melting

point for OJT007 is 200°C. High melting points have been associated with poor

solubility due to the strong cohesive forces between molecules (Semalty, 2014).

The drug is amphoteric; it has three calculated ionizable groups, two basic, and

one acidic pKa. At physiological pH, the drug would be primarily unionized. The pH

range found in the gastrointestinal tract from the stomach to the colon is about 1-8. The

very weakly acid ionizable group in OJT007 (pKa 8.7) would theoretically be unionized

across the GI tract. On the other hand, the weakly basic amine (pKa -2.2) would

theoretically be unionized across the GI tract, while the basic amine (pKa 5.8) would be

primarily ionized at low pH (i.e., fasting conditions pH) and unionized in the intestines.

2.6 Physicochemical characteristics of successful oral drugs

Oral efficacy is dependent on potency and oral bioavailability. An important

distinction must be made between absorption and bioavailability. Absorption refers to the

drug penetration across the intestinal membrane. On the other hand, bioavailability refers

to the appearance of unaltered drug in the systemic circulation (beyond the liver).

Physicochemical characteristics, and the characteristics of the environment in the GI

tract, affect the inherent absorbability and the bioavailability of a drug.

In a retrospective analysis, Christopher Lipinski analyzed a database of 50,000

compounds. A subset of over 2245 compounds that had entered Phase II were selected

under the hypothesis that those compounds with poor physicochemical properties would

fail preclinical and phase I evaluation. An analysis of the physicochemical properties of

these compounds yielded several observations: 11% of the 2245 compounds had a

molecular weight above 500 Da. Approximately 10% of the compounds had a calculated

log P <5. High log P are associated with low solubility.
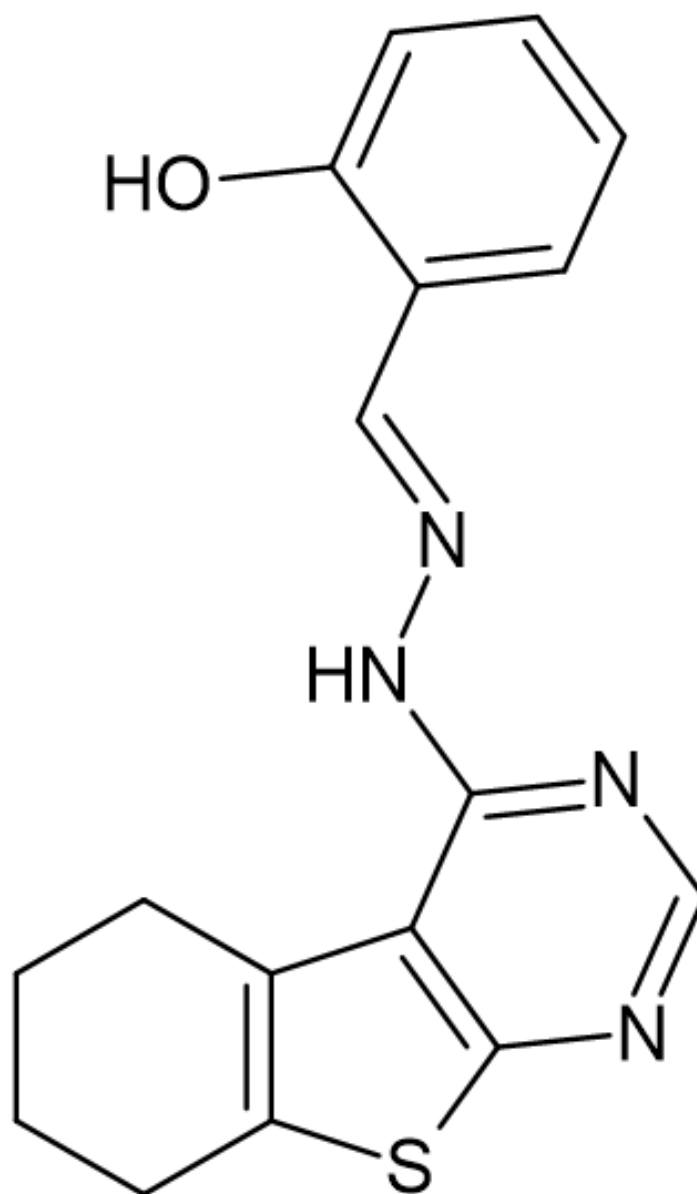
Figure 3. *Chemical structure of OJT007*

Table 1. *Calculated Physicochemical Properties of OJT007*

Property	Value	Condition
Density	1.46 g/cm^3	Temp: 20 °C Press: 760 Torr
Melting point	200.5	-
Log P	4.89	Temp: 25ºC
Solubility	-4.6 (8.1 µg/ml)	Temp: 25ºC pH=7.0
pKa	8.7±0.3	Most Acidic Temp: 25ºC
	5.8±0.2	Most Basic Temp: 25ºC

*Calculated using Advanced Chemistry Development (ACD/Labs) Software v11.02 (© 1994-2020 ACD/Labs

In addition, 8% of the molecules had more than 5 hydrogen bond (H-bond) donor groups (i.e., NH or OH).12% of the compounds had more than 10 H-bond acceptors atoms. (Lipinski et al., 1997)

This analysis led to the rule of five, which has helped pharmaceutical scientists reach early decision regarding developability of drug candidates across the years. The `Rule of Five' (RO5) states that poor absorption is more likely when a compound possesses:

- ClogP greater than five

- Molecular mass over 500 Da.

- More than five H-bond donors (sum of Nitrogen and Oxygen attached to one or more hydrogen atoms)

- More than ten H-bond acceptors (sum of Nitrogen and Oxygen)

Oral bioavailability (Figure 4) is a function of the fraction absorbed by the gut wall (F_a), Fraction escaping intestinal metabolism (F_g) and fraction escaping hepatic metabolism (F_h) (Equation 1). F_a is a function of the drug solubility, intrinsic permeability of the drug, GI stability. F_g is affected by active efflux into the intestinal lumen and by intestinal wall metabolism. F_h is a function of metabolism and transport.

$$F = F_a \times F_g \times F_h \tag{1}$$

The biological membranes lining the GI tract is described as a phospholipid bilayer interrupted by water pores; Thus, enabling lipid soluble molecules to readily penetrate the lipid region while small water soluble molecule cross through the aqueous channels (Song et al., 2004). In general, membrane permeability increases with an

increased Log P; This is because the attractive forces between drug-membrane interactions are greater than the attractive force between drug-solvent (Mayersohn, 2002).

Although a high log P is good for passive membrane permeability, values that are too high (>6 log P) may indicate poor aqueous solubility (since the drug preferentially associates in lipophilic regions) which in turn can cause poor absorption. Likewise, they may indicate the compound is susceptible to metabolism and biliary clearance.

High molecular weight of compounds (>500) has been associated with a decreased passive diffusion. Likewise, high molecular weight compounds may be associated with low solubility, an important prequel to membrane permeability(Navia & Chaturvedi, 1996). The hydrogen bonding ability of a drug is used as an estimate of its hydrophilicity. In this way, both hydrogen bond acceptor and donor atoms are associated with decreased drug permeability (Song et al., 2004).

2.6.1   Drug likeness of OJT007

Lipinski's rule of five is informative in early decision-making regarding drug candidates at early stage. OJT007 meets all the criteria of the RO5 (Table 2) suggesting that the molecule is likely to be active when administered orally to humans. Nonetheless, this should be interpreted with caution as these predictions do not always equate to success in experimental models. This phenomenon may be attributed to, among other things, the RO5 missing to consider important disposition factors such as the involvement of transporter (C.-Y. Wu & Benet, 2005).
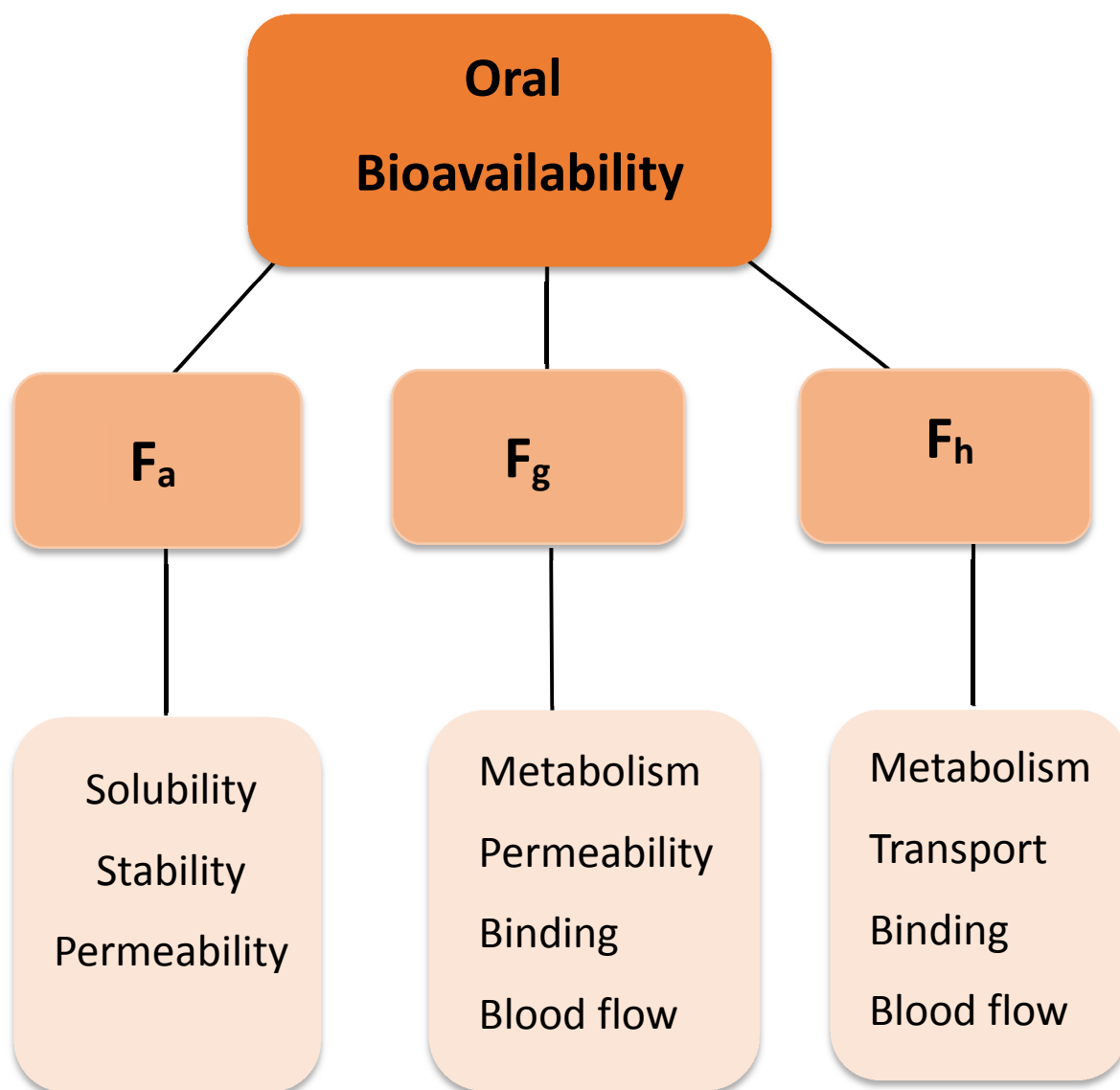
Figure 4. *Oral Drug Bioavailability: A Schematic*

Table 2: *Lipinski Properties of OJT007*

Property	Predicted Value
Molecular Weight	324.4 g/mol
Hydrogen bond acceptors	5
Hydrogen bond donors	2
Calculated log P (Clog P)	4.89

*Calculated using Advanced Chemistry Development (ACD/Labs) Software v11.02 (© 1994-2020 ACD/Labs

2.7 Bioanalytical Assay Development

Bioanalytical assay development plays an essential role in drug development. The ability to quantitate the parent drug and/or metabolite in the relevant biological matrices is a prerequisite to conduct robust pharmacokinetic, toxicokinetic and pk/pd studies. An important feature of bioanalysis in drug development is the need for quantification at very low concentrations levels: in the ng/ml or even pg/ml concentration range. LC-MS/MS has become the standard instrument for bioanalytical quantification replacing other analytical techniques such as HPLC and GC (Abdel-Hamid, 2000).

LC-MS/MS has several advantages over UPLC-UV. Classical UPLC methods rely on the UV absorbing properties of a drug. For drugs with weak UV absorbing properties, quantification at low concentration is problematic. In LC-MS/MS, detection relies on monitoring the specific mass of the molecular or fragment ion which results in higher sensitivity and specificity.

The LC-MS/MS offers greater sensitivity and specificity; however, there are limitations to its use. The electrospray ionization source is highly susceptible to contaminants. Furthermore, nonvolatile buffers are not amenable for LC-MS/MS analysis. Even low concentrations of nonvolatile buffers in the LC-MS/MS can cause severe signal suppression (Sterling et al., 2010). In addition, excipients such as PEG 400 and Tween 80 are not amenable for direct quantification in LC-MS/MS (Temesi et al., 2003). The signal suppression phenomenon is observed due to a competition in the ionization process between the analyte of interest and the contaminant (Choi et al., 2001).

2.7.1 Quantification without a reference standard

New chemical entities seldom have commercially available authentic standards for their metabolites. This situation becomes an important hurdle in enzyme kinetic studies because, ideally, all quantification must be conducted against a reference standard. Overcoming this difficulty using LC-MS/MS is not advisable. The addition of polar ionizable groups like glucuronides during metabolism dramatically impacts the molecule's ionization resulting in an over or underestimation of metabolism. (Blanz et al., 2017)

Quantification of metabolite by LC-UV is a more sensible approach. Each compound has an extinction coefficient. Extinction coefficients are a function of its chemical moieties or chromophores. If these structural motifs do not change significantly in the metabolite compared to the parent molecule, it is reasonable to assume that the metabolite's extinction coefficient has not changed. In this case, metabolite concentrations can be compared to the parent molecule using the standard curve built for the parent molecule. On the other hand, stark changes in λ_{max} would indicate that quantification cannot be performed without having an authentic standard (Y. Li et al., 2014).

Many studies assume that molar extinction coefficients remain the same as their corresponding parent; therefore, quantification was accomplished in each of those cases using the calibration curve of the parent drug (P. Li et al., 2015). More precise estimations can be accomplished by determining the conversion factor (K), which is the ratio between the molar extinction coefficient of the metabolite and the parent drug. (Gao et al., 2011; Zhang et al., 2006)

According to Beer-Lambert Law

$$A = \varepsilon \times C \qquad\qquad (2)$$

Where A, ε and C are the UV absorbance, molar extinction coefficient and the concentration of absorbing species, respectively. At equal molar concentration, the following equality can be established $A_p/\varepsilon_p = A_m/\varepsilon_m$. Where A_p, A_m represent the UV absorbance of parent and metabolite, while ε_p and ε_m represent the molar extinction coefficient of parent and metabolite, respectively. If we assume 1 mole of OJT007 generates 1 mol of glucuronide during glucuronidation, then A_m and A_p can be represented as $\Delta_{OJT007Glu}$ and Δ_{OJT007}, where $\Delta_{OJT007Glu}$ is the peak area change for OJT007 Glucuronide and Δ_{OJT007} is the peak area change for OJT007. Thus, a conversion factor $K = \Delta_{OJT007Glu} / \Delta_{OJT007} = A_m/A_p = \varepsilon_m / \varepsilon_p$ can be established in the study. The metabolite concentration can be established by using the conversion factor K and the parent standard curve (Zhang et al., 2006).

2.7.2 Method Validation

Validation of bioanalytical methods helps to ensure the reliability of the obtained results. Likewise, validation covers the steps pertinent to PK studies, including sample collection, handling, storage, and preparation. The U.S. FDA recommends that all methods be validated for standard (calibration) curve, selectivity, accuracy and precision, stability under normal storage and handling conditions, extraction recovery and matrix effect, and dilution integrity (USFDA, 2018). A summary of the validation parameters is shown in figure 5.

Sensitivity refers to the lowest concentration that can be accurately and precisely quantitated (i.e., LLOQ). The calibration curve is defined as the relationship between instrument response and the known calibrators concentration within an intended quantitation range. As per guidance, it should consist of a blank (matrix sample without IS), a zero calibrator (matrix sample processed with IS), and at least six standards covering the expected range including the LLOQ.

Selectivity refers to the ability to determine and unambiguously assess an analyte in the presence of all expected matrix components (Tiwari & Tiwari, 2010). Accuracy is the closeness of the measured value to the nominal concentration. It is typically measured as relative error (%RE) (Deshpande et al., 2019). Precision reflects the closeness of agreement of individual samples run multiple times under the same operating conditions expressed as percentage coefficient of variation (CV%) (Tiwari & Tiwari, 2010).

The percentage recovery refers to the extraction efficiency, reported as response obtained from an extracted sample to the results obtained by analyzing unextracted samples. The primary purpose of extraction is removing the proteins and interfering substances to assist in chromatographic separation, minimizing matrix effect during ionization in MS, and increasing sensitivity. Although recovery does not need to be 100%, the agency highlights it is important for recovery percentage to be consistent and reproducible across concentrations (USFDA, 2018). The Matrix effect is the suppression or enhancement of analyte ionization due to the presence of unintended analytes or interfering substances in the sample.

Bioanalytical validation methods	US FDA guidelines
Selectivity (specificity)	Analyses of blank samples of the appropriate biological matrix (plasma, urine or other matrix) should be obtained from at least six sources. Each blank should be tested for interference and selectivity should be ensured at LLOQ
Accuracy	Should be measured using a minimum of six determinations per concentration. Minimum of three concentrations in the range of expected concentrations is recommended for determination of accuracy. The mean should be ±15% of the actual value except at LLOQ, where it should not deviate by ±20%. This deviation of mean from the true values serves as the measure of accuracy
Precision	Precision should be measured using a minimum of five determinations per concentration. Minimum of three concentrations in the range of expected concentrations is recommended. The precision determined at each concentration level should not exceed 15% of the CV except for the LLOQ, where it should not exceed 20% of the CV
Recovery	Recovery experiments should be performed at three concentrations (low, medium and high) with unextracted standards that represent 100% recovery
Calibration curve	Should consist of a blank sample (matrix sample processed without internal standard), a zero sample (matrix sample processed with internal standard) and six to eight non-zero samples covering the expected range, including LLOQ
LLOQ	Analyte response should be five times the response compared to blank response. Analyte peak should be identifiable, discrete and reproducible with a precision of 20% and an accuracy of 80–120%
Freeze–thaw stability	Analyte stability should be determined after three freeze–thaw cycles. At least three aliquots at each of the low and high concentrations should be stored at intended storage temperature for 24 hours and thawed at room temperature. When completely thawed, refreeze again for 12–24 hours under same conditions. This cycle should be repeated two more times, then analyze on third cycle. Standard deviation of error should be <15%. If analyte is unstable, freeze at -70°C for three freeze–thaw cycles
Short-term stability	Three aliquots of each of the low and high concentrations should be thawed at room temperature and kept at this temperature for 4–24 hours and analyzed. Percent deviation should be <15%
Long-term stability	At least three aliquots of each of low and high concentrations at same conditions as study samples. Analyze on three separate occasions. Storage time should exceed the time between the date of first sample collection and the date of last sample analysis
Stock-solution stability	Stability of stock solutions of drug and the internal standard should be evaluated at room temperature for at least 6 hours. Percent deviation should be <15%
QC samples	QC samples in duplicates at three concentration levels (one near the 3× LLOQ, one in mid range, one close to high end) should be incorporated at each assay run. At least four out of every six should be within 15% of the respective nominal value. Two of the six may be outside of 15% but not both at the same concentration. Minimum number QCs should be at least 5% of total number of unknown samples or six total QCs, whichever is greater

Figure 5. *Validation Parameters FDA*

From "Bioanalytical Method Validation: an updated review" by Tiwari et al. 2010

2.8 Formulation for preclinical studies

2.8.1 Pre-formulation studies

The use of high-throughput screening and combinatorial chemistry during drug discovery has resulted in new chemical entities characterized by low water solubility. Consequently, the preparation of suitable formulation for in vivo studies is a significant hurdle in drug development. Investigational new drug (IND) applications require a description of the physical and chemical characteristics of the NCE (USFDA, 2006). The typical pre-formulation studies include physicochemical characterization of the solid and solution properties of a drug with the purpose of amassing pharmaceutical information that would be useful in the development of a suitable delivery system. Some of the pre-formulation studies consist of pKa, solubility, stability tests, log P, melting point (Niazi, 2019)

2.8.2 Cosolvent Formulation

In the early stages of drug development, solution dosage forms offer the important advantage of minimizing dissolution limited absorption. Several techniques can be used to solubilize poorly water-soluble molecules: pH manipulations (acid or base drugs), cyclodextrin complexations, cosolvents. PH manipulation techniques suffer from precipitation upon dilution after dosing; Likewise, in occasions, the pH for optimal solubility is extreme and could potentially cause side effects (Bosselmann & Williams, 2012). Inclusion complexes may not achieve the desired solubility, especially because of the drug conformations constraints for successful complexation (Davis & Brewster, 2004). Cosolvents result attractive due to their dramatic increase in solubility and their simplicity.

Cosolvency is a common approach to improve the solubility of poorly water-soluble drugs. Cosolvents are a mixture of miscible solvents that increase a nonpolar molecule's water solubility. The mechanism by which cosolvents achieve this task is by reducing the surface tension between the water and hydrophobic solute. Many of the water-miscible solvents used in cosolvent formulations are toxic; because of this, the following criteria must be met during formulation: nontoxicity, compatibility with blood, non-sensitizing, physically and chemically stable and inert.

Following this further, during formulation excipients must be selected carefully especially since formulation vehicles may have effects on pharmacokinetic studies due to their ability to affect metabolic enzymes, transporters, and distribution. (Trivedi & Yue, 2017)

2.9. Pharmacokinetics Studies

2.9.1 Role of pharmacokinetics in preclinical drug discovery and development

One of the main reasons drugs fail during clinical development is unsatisfactory pk/bioavailability or toxicity. Pharmacokinetics is defined as what the body does to the drug. Pharmacokinetics comprehends four main processes: absorption, distribution, metabolism, and excretion. A relevant pharmacokinetic characterization of a drug is necessary prior to exposing human subjects to a new chemical entity. In fact, pharmacokinetic data in two species (rodent and nonrodent) are generally required for IND application. Generally, this pharmacokinetic data in two species is generated concurrently with toxicity studies (USFDA, 2010).

An important question needs to be addressed early in drug development: what dose is safe and efficacious? Answering this question requires the combined evaluation of pharmacodynamics and pharmacokinetics. Ideally, PK/PD correlations sampling is done in the same animal. In occasions, this is not possible due to the nature of PD biomarker, in this case, a satellite group can be used. These animals must match species, strain, gender, dose, route of administration, disease state, and sample time to match the study design as much as possible.

Depending on the disease, animal models can be limited in such a case a "bridging experiment" in a different strain or species can be carried out to demonstrate similarity in PK behavior between groups (F. Li et al., 2019; Tuntland et al., 2014). The gold standard for *L. major* infection animal model are BALB/c mice. Although infection with *L. major* infection has been reported in SD rats, rats did not develop skin ulcerations (Rostamian & Niknam, 2019).

Pharmacokinetic and pharmacodynamic data in animals can be used to propose a dosing regimen in humans. The success of this task will be largely dependent on the selection of an appropriate animal model. For instance, if pharmacokinetic properties are species-dependent (i.e., in terms of disposition), then extrapolation to humans will be inaccurate.

Ultimately, the underlying need for studying a drug's pharmacokinetics is to establish a relationship between dose and exposure. This relationship is established by evaluating a concentration time profile, which basically describes the amount of drug in a biological matrix (i.e., blood, plasma) following drug administration over a period of

time. From the concentration time profile, several PK parameters can be derived. Table 3 summarizes the most essential PK parameters.

After intravenous administration, the life cycle of a drug in the body starts with its distribution to different organs and tissues. The drug is eliminated from the body by the interplay of metabolism and excretion. The disposition of a drug, or how a drug distributes to tissues and is eliminated from the body, can be determined from an IV bolus dose. Complete characterization of the pharmacokinetics of a drug entails sampling the relevant matrix 3-5 half-lives. (Ronald Schoenwal, 2002). Three important pk parameters characterize disposition at minimum: clearance, volume of distribution and half-life. Both clearance and volume of distribution are primary pharmacokinetic parameters, which means they are not derived from other pharmacokinetic parameters.

After oral administration, the drug is absorbed across the intestinal membrane. An important difference between IV and oral administration is that metabolism can occur before the drug reaches systemic circulation and site of action.

2.9.2 Pharmacokinetic challenges of new chemical entities

Clearance and volume of distribution have critical implications in half life; thus, they significantly affect the duration of action. These three parameters, along with rate and extent of absorption, are key in dose and dose regimen.

Conceptually, clearance refers to the volume cleared of drug per unit time. It is a function of how efficiently an organ, like the kidney or the liver, excretes or metabolizes a drug and the blood flow rate to said organ (Gibaldi, 1991). In other words, it describes how efficiently a drug is eliminated from the body. Clearance establishes a

Table 3. *Fundamental PK Parameters*

Parameter	Symbol	Description	Example Units	Calculation
Dose	D	Administered dose	mg, mg/Kg	Design parameter
C_{max}	C_{max}	Maximum concentration attained after drug administration	ng/mL	Direct observation
C_0		Initial concentration	ng/mL	Calculated by back extrapolation or by direct measurement if first time point occurs at t=0
T_{max}	T_{max}	The time at which C_{max} occurs	Hr, min	Direct observation
Volume of Distribution	Vd	The apparent volume in which a drug distributes. Relates the drug concentration to the amount of drug in the body	L	D/(Kel x AUC)
Elimination rate constant	Kel	The rate at which a drug is removed from the body	1/hr	Estimated by linear regression
Clearance	Cl	The volume of body fluid cleared per unit time	L/hr	D/AUC
Half-life	$T_{1/2}$	The time it takes for the drug concentration to decrease by half of its previous value	hr	Ln(2)/Kel
AUC	AUC	A measure of exposure, area under the curve	Hr x ng/L	Trapezoidal rule
Bioavailability	F	The fraction of an administered dose that reaches the systemic circulation	Fraction	$\dfrac{AUCpo/po\ dose}{AUCiv/IV\ dose}$

critical connection between dose and exposure (in terms of AUC), as such any changes in clearance can have important implications.

Achieving appropriate exposure is imperative for efficacy. Successful NCEs should achieve and maintain effective drug concentration at the site of action. NCEs with high clearance values remove drug immediately from the body which translates into short duration of action. Nonetheless, too stable compounds may also become problematic due to interactions or even toxicity.

Unsurprisingly, metabolic stability studies assessing a compound's susceptibility to metabolism have become standard in the industry. "Softs spots" can be optimized to decrease metabolic turnover rates (Słoczyńska et al., 2019). For drugs cleared by the liver, low bioavailability due to high extraction is an important challenge for many oral drugs. For drugs with clearance approaching blood flow, hepatic extraction ratio approaches 1 (Benet & Zia-Amirhosseini, 1995), which translates into low bioavailability.

2.10 Drug metabolism

Drug metabolism constitutes one of the most important components of the pharmacokinetic properties of an NCE. The importance of metabolism resides on its effect on activity and toxicity. Understanding the metabolism and excretion of a drug early in drug development provides valuable information during drug development. This information is key in identifying potential drug interactions, interindividual difference and the need for further pharmacological characterization or structure modifications.

Drugs undergo metabolic biotransformations that generally increase the compound's polarity to facilitate excretion. Two important PK parameters are dependent on metabolism: oral bioavailability and half-life. Consequently, knowledge on the route of elimination can help drug developers make informed decisions in terms of proper doses that are both safe and efficacious.

The FDA encourages early in vitro evaluation of drug metabolism and excretion to prevent unnecessary testing at later stages in drug development. Likewise, FDA urges scientists to investigate metabolic pathways that account for more than 25% of systemic clearance (US Food and Drug Administration, 2012).

Drug metabolism is generally classified in phase I and phase II reactions. Phase I reactions comprehend functionalization reactions either by adding or by unmasking polar functional groups like hydroxyl, carboxyl or amino in the molecule. On the other hand, phase II reactions correspond to conjugation reactions in which endogenous compounds such as glucuronic acid, glutathione, sulfate, or acetyl are covalently linked to functional groups in the drug (A. Rowland et al., 2013).

In vitro methods for drug metabolism studies are generally carried out on cellular systems such as hepatocytes or enzyme systems such as microsomal or cytosolic subcellular fractions. Microsomes express cytochrome P450 (CYP) and UDP-glucuronosyltransferase (UGT), which are two major drug metabolizing enzymes (Knights et al., 2016). Metabolic activity of either enzyme can be evaluated by monitoring the depletion of parental compounds or the formation of metabolites.

2.10.1 Phase I metabolism

Phase I metabolism primarily involves oxidation reactions mediated by cytochrome P450 (CYP). To a lesser extent, flavin monooxidation (FMO), alcohol dehydrogenase, aldehyde dehydrogenase, and aldehyde oxidase. Nonetheless, other metabolic reactions such as reduction or hydrolysis of the parent drug by esterases or amidases may also occur (Sensenhauser, 2014). The cytochrome P450 family is the most important class of enzymes in drug metabolism.

CYPs are membrane-bound proteins found in the endoplasmic reticulum. CYP enzymes are found in almost all tissues; however, the liver contains the highest expression of CYPs (Hrycay & Bandiera, 2008). CYP enzymes metabolize approximately 90% of the clinically used drugs in the market (Lynch & Neff, 2007); Thus, their evaluation is critical in drug development.

Cytochrome P450 has a heme bound non-covalently to the enzyme's active site, which binds to molecular oxygen via its iron atom. This binding initiates a catalytic cycle in which protons and electrons are transferred from NADPH and heme-associated aminoacids side chains to yield, typically, a mono-oxygenated product (Sensenhauser, 2014).

2.10.2 Phase II metabolism

In phase II reactions, phase I metabolites or parent drug undergo conjugation reactions with hydrophilic moieties such as glucuronic acid, sulfate, or glutathione. Glucuronidation represents a significant pathway for the drug metabolism of many drugs.

U-glucuronosyltransferase catalyzes the conjugation of glucuronic acid from UDP- glucuronic acid (UDPGA) to hydroxyl, carboxyl, or amine groups of drugs. The elimination of glucuronides comprehends biliary, urinary, and intestinal excretion. UGTs are divided into two families, UGT1 and UGT2, which are divided into subfamilies UGT1A, UGT2A and UGT2B.

UGTs are primarily distributed in the liver and intestine. However, they are also found on the stomach, esophagus, kidney, colon, lung and epithelium. Although UGTs are primarily located in the ER of cells, they are not exposed to cytosol like CYPs but rather they predominantly reside in the luminal face of the ER (Caldwell & Yan, 2014).

Glucuronide metabolites are highly hydrophilic and unable to permeate cell membranes via passive permeation. Thus, the parent compound's elimination is dependent on efflux transporters located in various disposition organs. In enterocytes, the efflux transporters MRP2 and BCRP mediate the efflux of intracellularly formed glucuronides into the lumen. In the lumen, the glucuronide metabolites can be excreted in feces or hydrolyzed back into the aglycone. In hepatocytes, MRP2 and BCRP mediate the efflux of intracellular glucuronides into bile, or they enter systemic circulation via basolateral efflux transporters such as MRP3. From systemic circulation, organic anion transporters can uptake glucuronides into the kidney proximal tubular cells to be excreted via MRP2 or MRP4 (G. Yang et al., 2017).

CHAPTER 3

DESIGN OF THE STUDY

3.1 Central Hypothesis

OJT007 is a MetAP$_1$ inhibitor containing the hydrazine-1-ylidene pharmacophore. The compound had potent activity against *L.major* promastigotes and amastigotes, both *in vitro* and *in vivo* (Rodriguez et al., 2020). OJT007 was identified as an excellent candidate for the oral treatment of cutaneous leishmaniasis based on its promising efficacy in a mice animal model (Rodriguez et al., 2020). We plan to determine the feasibility of OJT007 as a drug candidate for clinical application as a new mechanism of action for the treatment of cutaneous leishmaniasis. We will conduct various types of preclinical drug development studies including physicochemical characterization, formulation development, bioanalysis, drug metabolism, and pharmacokinetic evaluations for OJT007 (Rogge, 2010). We hypothesize that OJT007 is a potential chemotherapeutic candidate with favorable chemical and biopharmaceutical properties for the oral treatment of cutaneous leishmaniasis. We propose the following specific aims.

3.2 Specific Aims

3.2.1 Aim 1

Develop and validate a bioanalytical assay using LC-MS/MS for the quantification of OJT007 in rat plasma and urine.

Rationale

To accurately evaluate the absorption, distribution, metabolism, and excretion of OJT007 in a rat model, we need a sensitive, specific, and reproducible bioanalytical assay to quantitate OJT007 concentrations in plasma and urine. Unlike conventional HPLC with UV detection systems, which were limited by sensitivity and significant interference from biological media, LC-MS/MS offers high sensitivity, excellent specificity, and good reproducibility. Furthermore, LC-MS/MS requires very small quantity of biological samples (i.e., 10 uL – 20 uL plasma) for quantification. In this aim we develop a bioanalytical assay suitable for characterization of pharmacokinetics of OJT007 in rats after oral and intravenous administration.

3.2.2 Aim 2

Investigate the physicochemical properties of OJT007 and develop a suitable formulation for preclinical studies in animals.

Rationale

A suitable formulation of OJT007 is a prerequisite for successful in vivo studies. This task entails a thorough understanding of the physicochemical characteristics of the drug in order to design of a suitable formulation. All formulation efforts are especially

important and challenging for drugs with poor solubility. Furthermore, formulation must be designed with suitable excipients. In this aim we develop a cosolvent formulation for intravenous and oral administration of OJT007.

3.2.3 Aim 3

Investigate the in vitro hepatic metabolism of OJT007 in human microsomes and rat liver and intestine microsomes.

Rationale

Drug metabolism is an integral part of drug development. Understanding how and via what pathways a drug candidate is/are metabolized would help not only to know the behavior of the drug in vivo but also to design optimal dosage regimen. In vitro metabolism studies using liver microsomes is an authentic way of estimating intrinsic hepatic clearance of a compound and identifying potential metabolites. It also provides mechanistic information about pre-systemic metabolism in relation to oral bioavailability of the drug. In this aim we explore metabolic processes of OJT007.

3.2.4 Aim 4

Determine pharmacokinetic profiles of OJT007 following intravenous and oral administration using rat as an animal model

Rationale

Poor pharmacokinetic properties accounts for 40% of attrition in phase I clinical trials (Ajavon & Taft, 2010). An understanding of preclinical drug disposition in animal

models aids in the knowledge base for a drug candidate to determine whether it is feasible to move into clinical evaluations or recommend for early elimination.

We will characterize the disposition and elimination profiles of OJT007 following intravenous administration. Oral bioavailability of OJT007 will be assessed accordingly. Furthermore, the impact of stomach acid degradation on OJT007 bioavailability will also be evaluated.

3.3 Materials

3.3.1 Chemicals and Drugs

- Acepromazine (10 mg/mL) injection, purchased from Hospira (Lake Forest, IL), was used as part of the anesthetic cocktail for jugular vein cannulation surgery.

- Alamethicin purchased from Sigma-Aldrich (St. Louis, MO), was used for preparation of solution B for the UGT regenerating system.

- Bupivacaine HCl injection USP (0.5%, 5mg/mL), purchased from Hospira (Lake Forest, IL), was used to provide post-surgery analgesia to the animals.

- Deionized water, produced in the lab with a Barnstead TM Smart2Pure TM water purification system (Thermo Fisher Scientific, Waltham, MA), was used in OJT007 formulation.

- Dimethyl sulfoxide (DMSO), purchased from Sigma-Aldrich (St. Louis, MO), was used for studying solubility of OJT007.

- β- Glucuronidase, from *Escherichia coli*- Type IX-A, lyophilized powder, 1434438 units / g protein purchased from Sigma-Aldrich (St. Louis, MO), was used for glucuronide hydrolysis

- Formic Acid, purchased from Sigma-Aldrich (St. Louis, MO), was used to enhance the ionization of OJT007 in the LC-MS/MS method development.

- Heparin sodium injection (1000 units/mL), purchased from Hospira (Lake Forest, IL), was used as anticoagulant in animal experiments.

- Human liver microsomes, 20-Donor Pool, Mixed Gender purchased from Corning Gentest (Corning, NY), were used for in vitro incubations.

- Ketamine injection (100 mg/mL), purchased from Hospira (Lake Forest, IL), was used as part of the anesthetic cocktail for jugular vein cannulation surgery.

- LC-MS grade acetonitrile, purchased from J.T. Baker Chemical Co. (Phillipsburg, NJ), was used to prepare mobile phase for the quantification of OJT007 by LC-MS/MS.

- LC-MS grade water, purchased J.T. Baker Chemical Co. (Phillipsburg, NJ), was used to prepare mobile phase for the quantification of OJT007 by LC-MS/MS.

- LC-MS grade methanol, procured from Mallinckrodt Baker (Phillipsburg, NJ, USA), was used for solubility studies of OJT007.

- Monopotassium phosphate (KH_2PO_4), Dipotassium phosphate (K_2HPO_4) and KPI buffer was made using KH_2PO_4 and K_2HPO_4 and the pH was adjusted to 7.4 using

sodium hydroxide and hydrochloride. All of which were purchased from VWR (Radnor, PA).

- Magnesium Chloride purchased from Sigma (St. Louis, MO), was used for Solution A UGT regenerating system preparation

- OJT007 (purity ≥ 98%) was purchased from MolPort (Riga, Latvia).

- Polyethylene glycol (PEG 400), purchased from Wood Scientific (Houston, TX), was used to prepare OJT007 formulations.

- Polysorbate 80 (Tween 80®), purchased from Sigma-Aldrich (St. Louis, MO), was used for the solubility test of OJT007.

- Rabeprazole sodium, purchased from Sigma-Aldrich (St. Louis, MO), was used to control gastric acid secretion in rats.

- Rat (Sprague-Dawley) pooled liver microsomes, male, purchased from Corning Gentest (Corning, NY), were used for in vitro incubations.

- Rat (Sprague-Dawley) pooled intestinal microsomes, male, were prepared in-house according to previously published methods for in vitro incubations.

- Saccharolactone purchases from Sigma-Aldrich (St. Louis, MO), was used for preparation of solution B for the UGT regenerating system.

- Sodium chloride solution, 0.85 %, (normal saline) purchased from Sigma-Aldrich (St. Louis, MO), was used to dilute dosing solutions for animal dosing.

- Solution A, purchased from Corning Gentest (Corning, NY), was used for NADPH regenerating system for microsomal incubations.

- Solution B, purchased from Corning Gentest (Corning, NY), was used for NADPH regenerating system for microsomal incubations.

- Uridine 5'-diphosphoglucuronic acid trisodium salt purchased from Sigma (St. Louis, MO), was used for solution B UGT regenerating system for microsomal incubations.

- Voriconazole, purchased from Sigma-Aldrich (St. Louis, MO), was used as internal standard for LC-MS/MS method.

- Xylazine injection (100 mg/mL), purchased from Hospira (Lake Forest, IL), was used as part of the anesthetic cocktail for jugular vein cannulation surgery.

3.3.2 Supplies

- 1 cc sterile tuberculin slip tip syringes and PrecisionGlide® 23 G TW needles, purchased from Becton Dickinson & Co. (Franklin Lakes, NJ), were used during animal experiments for intra-venous dosing and blood sampling.

- Amber scintillation vials (20 mL), purchased from VWR (West Chester, PA), were used as storage containers.

- Amicon Ultra – 0.5 mL Centrifugal Filters, MWCO 3k, purchased from EMD Millipore (Billerica, MA), were used to determine the plasma protein binding of OJT007.

- Auto-sampler propylene injection vials (Clear; 100 µL), purchased from ChromTech (Apple Valley, MN), were used to hold samples for injection in the LC-MS/MS assays.

- Cotton tipped applicators (6"), purchased from Baxter Healthcare Co (McGaw Park, IL), were used during animal surgeries to stop bleeding and apply topical contents during surgery.

- Face masks, purchased from AlphaProTech, Inc. (Salt Lake City, UT), were worn while using chemicals and handling animals.

- Gauze (3 in x 3 in), purchased from Tyco Healthcare (Mansfield, MA), were used to suppress bleeding and clean-up incision sites during animal surgeries.

- Insulin syringe (1 mL, sterilized), purchased from Becton Dickinson & Co. (Franklin Lakes, NJ), were used for administration of anesthesia agents during animal experiments.

- Membrane filters (47 mm, 0.45 µm, hydrophilic polypropylene, Pall Corp., Ann Arbor, MI) were used to filter mobile phase for LC-MS/MS analysis.

- Microcentrifuge tubes (amber, clear and assorted colors, 1.5 mL), purchased from VWR (West Chester, PA), were used in sample preparation for microsomal incubations and LC-MS/MS analysis.

- Nylon 2/0 and 3/0 surgical sutures, purchased from Henry Schein Inc. (Melville, NY), were used during animal surgery to close incisions and secure the jugular vein cannula.

- Pipette tips (10 μL, 20 μL, 250 μL, and 1000 μL), purchased from Rainin Instrument (Oakland, CA), were used along with the appropriate mechanical pipettes for volumetric transfer of liquids.

- Polyethylene tube (I.D. 0.023", O.D. 0.038"), purchased from Becton Dickson Intramedic & Co. (Franklin Lakes, NJ), were used for blood sampling via jugular vein cannula

- Powder-free latex examination gloves, purchased from VWR (West Chester, PA), were worn during all laboratory and animal experiments.

- Standard silicone tubing (I.D. 0.025", O.D. 0.047"), purchased from HelixMark (Carpinteria, CA), were used as the soft front of the polyethylene tubing.

- Syringe filters (0.45 μm, HPLC certified), purchased from VWR (Radnor, PA), were used to sterilize anesthesia cocktail.

- Syringes (1 ml, sterilized, single use), purchased from Becton Dickson &Co. (Sparks, MD), were used for blood sampling.

3.3.3 Equipment, Apparatus and Software

- Analyst® software v1.6.2, purchased from SCIEX (Foster City, CA), was used to control and acquire data from the LC-MS/MS system.

- Electronic Weighing Balances (AB204-S and AT261 Delta Range), purchased from Mettler Toledo (Columbus, OH), were used to weigh all solid-state excipients and drugs.

- Empower 3® software (Milford, MA) was used to control and acquire data from the UPLC system.

- Eppendorf Centrifuge 5427 R (Enfield, CT) was used to centrifuge samples and working solutions to enable collection of supernatants.

- Gastight glass syringe, purchased from Hamilton Company (Reno, NV), was used to tune the mass spectrometer parameters for OJT007 and IS.

- Sigma Plot v11.0, purchased from Graph Pad Software Inc. (La Jolla, CA), was used to generate plots and for statistical analysis of data.

- LC-MS/MS system consisting of the following was used for the quantification of OJT007

  o 4000 QTRAP MS/MS system purchased from SCIEX (Foster City, CA)

  o Genius ABN2ZA Tri Gas Generator purchased from Peak Scientific (Billerica, MA)

  o Shimadzu Nexera X2 UHPLC System (Columbia, MD)

  o Acquity UPLC® BEH C$_{18}$ UHPLC column (1.7μm, 2.1 x 50 mm) purchased from Waters (Milford, MA)

- Phoenix WinNolin® 8.3, purchased from Certara (St. Louis, MO), was used to estimate pharmacokinetic parameters from rat data.

- Pipettes, purchased from Rainin Instrument (Oakland, CA) and Eppendorf (Hamburg, Germany), were used for volumetric measurements.

- Precision™ Shaking Water Baths, Thermo Scientific™ (Waltham, MA) was used to incubate samples during *in-vitro* metabolism studies.

- Syringe Pump 11 PLUS, purchased from Harvard Apparatus (Holliston, MA), was used to tune the mass spectrometer parameters for OJT007 and IS.

- Vortex machines (Vortex-Genie® 2), purchased from Scientific Industries (Bohemia, NY), were used mix sample preparations.

- Waters Acquity UPLC with photodiode array detector (Milford, MA)

3.3.4 Animals

The animal protocol used in this work was reviewed and approved by the Institutional Animal Care and Use Committee (IACUC) at Texas Southern University. Additionally, all animal studies were conducted in compliance with the National Institute of Health "Guide for the Care and Use of Laboratory Animals, 8th Edition". Experiments were carried out using adult male Sprague-Dawley rats (mean body weight 350g) purchased from Envigo RMS, LLC, Alice, TX. Upon arrival, the animals were housed under normal conditions which includes free access to food and water, a room temperature environment with 12-hour light-dark cycles from 6 am to 6 pm daily.

These conditions were maintained for one week before starting animal experiments to allow for adequate acclimatization of the animal. The animals were implanted with a cannula tube in the left jugular under anesthesia and allowed to recover for 24 hours before initiating dosing.

3.4 Methods

3.4.1 LC-MS/MS Assay Development

A LC-MS/MS analytical method was developed to quantitate OJT007 concentrations in plasma and urine samples collected from pharmacokinetic studies of OJT007 in rats. The method development required optimization of the mass-spectrometric conditions to achieve the best signal to noise ratio and optimization of the chromatographic conditions to ensure the best selectivity and minimize matrix effect due to interference in the biological matrix.

3.4.1.1 Chromatography

The LC analysis was accomplished using a Shimadzu Nexera X2 UHPLC system (Columbia, MD, USA). The chromatographic separation was achieved using an Acquity UPLC BEH C_{18} column (50 × 2.1 mm, 1.7 μm) with a gradient mobile phase at flow rate of 0.4 mL/min. The sample injection volume was 2 μL, and the mobile phase consisted of 0.1% v/v formic acid in water (A) and 0.1% v/v formic acid in acetonitrile (B). Gradient elution was employed with 5% to 98% B from time 0 to 1.8 min and was kept constant at 98% B for 1.7 min, then 98% B was changed to 5% B from 3.5 to 3.7 min and kept constant at 5% from 3.7 min to 5 min (Table 4).

Table 4: *Summary of Gradient Elution Profile Applied to the Chromatographic Separation of OJT007 and IS*

Time (min)	Flow Rate (mL/min)	Mobile Phase A (%)	Mobile Phase B (%)
0	0.4	95	5
1.80	0.4	2	98
3.50	0.4	2	98
3.70	0.4	95	5
5.0	0.4	95	5
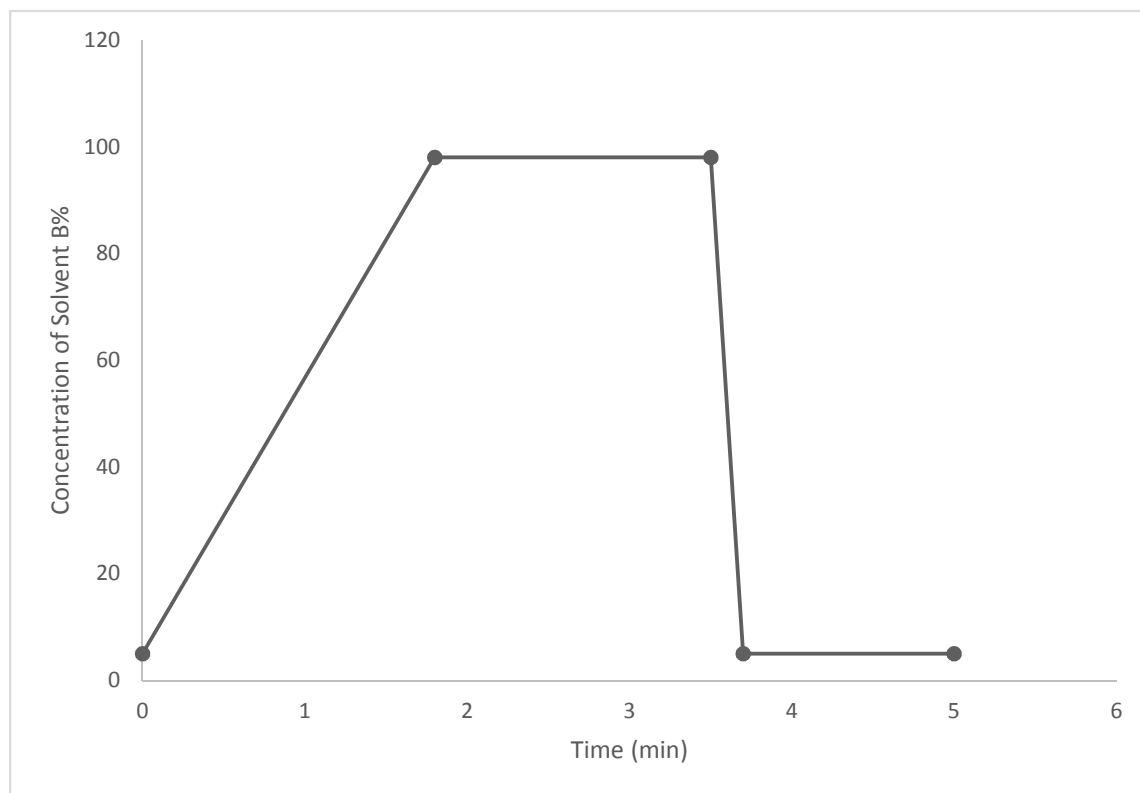
Figure 6: *Gradient elution plot depicting changing concentration of solvent B (0.1% formic acid in Acetonitrile)*

3.4.1.2 MS/MS Detection

The MS/MS analysis was performed on a 4000 QTRAP® triple quadrupole mass spectrometer system equipped with a Turbo Ion Spray ion source (Sciex, Redwood City, CA). The hybrid triple quadrupole LIT (linear ion trap) mass spectrometer is equipped with a Turbo V™ ion source. Pure nitrogen used as curtain gas, and source and exhaust gases were generated by a Peak Scientific (GENIUS ABN2ZA) Tri Gas Generator. Voriconazole was used as internal standard (IS). The quantification was performed using multiple-ion reaction monitoring (MRM) in positive mode, with the transitions of m/z 325 → m/z 205 for OJT007 (Fig. 2) and m/z 350 → m/z 101 for IS. The source parameters were set as follows: ion spray voltage, 4500 V; ion source temperature, 500°C; nebulizer gas, 50 psi; heater gas, 40 psi; curtain gas, 25 psi; and the collision gas, high. The compound-dependent parameters for OJT007 and IS were optimized with entrance potential (EP), 10 V and 10 V; declustering potential (DP), 105 V and 56 V; collision energy (CE), 30 V and 105 V; and collision cell exit potential (CXP), 11 V and 8 V, respectively. Analyst® Software 1.6.2 (Redwood City, CA, USA) was used to control the LC-MS/MS system and analyze the data. The compound dependent electronic parameters for the MS/MS acquisition of OJT007 and IS are summarized in Table 5.
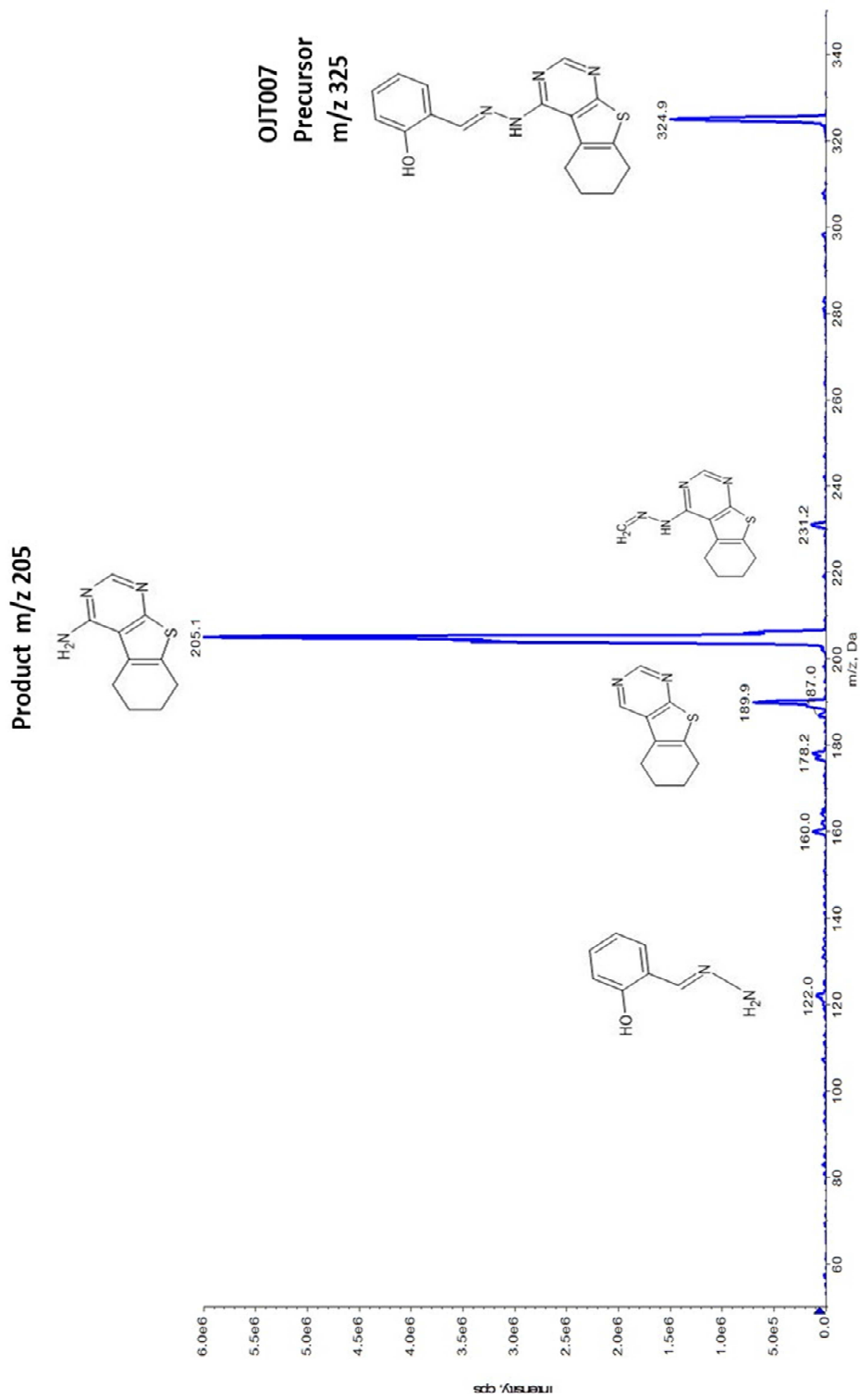
Figure 7: *Product ion spectra of OJT007*

Table 5: *Electronic Parameters for MS/MS Acquisition of OJT007 and IS*

Parent	Transition (m/z)	Dwell Time (msec)	DP (V)	CE (V)	EP (V)	CXP (V)
OJT007	325→205	150	105	30	10	11
IS	350→101	150	56	105	10	8

3.4.1.3 Standard and Quality Control Samples

The stock solution of OJT007 was prepared by dissolving the solid compound in 5% DMSO and 95% methanol at a concentration of 1 mg/mL and was stored at −80 °C until it was used. The IS was prepared by dissolving voriconazole in acetonitrile at the concentration of 1 mg/mL. The OJT007 working solutions were prepared by diluting the stock solution in 50% acetonitrile in water at final concentrations of 10, 5, 2.5, 1, 0.5, 0.25, 0.10, and 0.05 µg/mL. The OJT007 quality control (QC) working solutions were prepared by diluting the stock solution in 50% acetonitrile in water at final concentrations of 0.15, 0.75 and 7.5 µg/mL. The IS working solution was prepared by diluting the 1 mg/mL stock solution with 100% acetonitrile to obtain a concentration of 300 ng/mL. Plasma and urine samples were processed by protein precipitation. A series of standard samples were prepared by spiking the working solutions (5 µL) into blank rat plasma or urine (45 µL) to obtain the following concentrations of OJT007: 5, 10, 25, 50, 100, 250, 500, and 1000 ng/mL. The QC samples were prepared by spiking QC working solutions into blank rat plasma or urine to obtain concentrations of 15 ng/mL (low), 75 ng/mL (medium) and 750 ng/mL (high), respectively. The mixture was vortexed for 30 seconds and then centrifuged at 14,000 rpm for 15 minutes. The resulting supernatant was then transferred to an auto-sampler vial for LC−MS/MS analysis.

3.4.1.4 Plasma and Urine Sample Preparation

Plasma samples stored at −80 °C were thawed at room temperature. An aliquot (50 µL) of plasma was extracted for OJT007 using protein precipitation by adding 250 µL of acetonitrile containing the internal standard (300 ng/mL). The mixture was vortexed for 30

seconds and centrifuged at 14,000 rpm for 15 min at 4°C. An aliquot of the supernatant was injected into the LC-MS/MS for quantitative analysis.

3.4.2 LC-MS/MS Method Validation

The LC-MS/MS assay was validated according to Center for Drug Evaluation and Research (CDER) "Guidance for Industry: Bioanalytical Method Validation" with respect to specificity, lower limit of quantification (LLOQ), linearity and range, accuracy and precision, extraction recovery, matrix effect, carryover effect, stability and dilution integrity (*USFDA*, 2018).

3.4.2.1 Linearity and Sensitivity

Linear calibration curves in rat plasma and urine were generated by plotting the peak area ratio of OJT007 to IS against known standard concentrations of OJT007. The slope, intercept, and coefficient of determination were estimated using least squares linear regression method. The lower limit of quantification (LLOQ) was evaluated based on the signal to noise ratio of at least 5.

3.4.2.2 Calibration Curve

Calibration curves in blank rat plasma or urine were obtained by plotting the peak area ratio of OJT007 to IS versus the known concentration of OJT007. Least-squares linear regression method with $1/x^2$ weighting was applied to obtain the slope, intercept, and correlation coefficient. The lower limit of quantification (LLOQ) was evaluated based on the signal-to-noise ratio of at least 5. The LLOQ is the minimal quantifiable concentration point in the calibration curve at which precision (coefficient of variation, CV) should be within 20%, and accuracy (relative error, RE) should be within 20% of nominal value.

3.4.2.3 Stability in Plasma and Urine

All stability studies were evaluated in blank rat plasma or urine at low, medium, and high QC levels (15, 75, and 750 ng/mL, respectively) using triplicates at each concentration level. All the samples were compared to freshly prepared samples at the same concentrations. Short-term QC samples in blank rat plasma or urine were freshly prepared and left on the benchtop at room temperature for 4 hours (short-term benchtop). Freeze-thaw (FT) stability samples were exposed to three cycles of freeze (-80°C) and thaw (RT, room temperature). The auto-sampler stability of processed samples was determined by comparing processed plasma or urine that remained in the auto-sampler for 24 hours at 15°C. Long-term storage stability samples were freshly prepared and stored at -80°C for 14 days.

3.4.2.4 Extraction Recovery and Matrix Effect

To examine the extraction recovery and matrix effect, QC samples were evaluated at three concentration levels (15, 75 and 750 ng/mL, n=6, respectively). The extraction recovery and matrix effect were calculated according to Equation 3 and Equation 4.

$$\text{Extraction Recovery } \% = \frac{Response_{pre-extraction\ spike}}{Response_{post-extraction\ spike}} x100\% \tag{3}$$

Where $Response_{pre\text{-}extraction\ spike}$ is the average area count for OJT007 that has undergone the extraction process; and $Response_{post\text{-}extraction\ spike}$ is for OJT007 samples spiked into extracted matrix after the extraction procedure. The matrix factor of OJT007 was calculated according to:

$$\text{Matrix Factor }\% = \left(\frac{Response_{post-extraction\ spike}\ -\ Response_{matrix-free\ spike}}{Response_{matrix-free\ spike}} \right) \times 100\%$$

(4)

Where $Response_{\text{post-extraction spike}}$ is the average area count for OJT007 spiked into matrix after the extraction procedure, and $Response_{\text{matrix-free spike}}$ is the average area count for OJT007 samples at the same concentration of OJT007 in neat solution (50% acetonitrile in water).

3.4.2.5 Accuracy and Precision

To evaluate the intra-day or inter-day assay accuracy and precision, the LLOQ and QC samples were analyzed on the same day or three subsequent days. Experiments were conducted in replicates of N=6 for each testing level. The assay accuracy and precision were expressed in relative error from the theoretical drug concentration (RE%) and coefficient of variation (CV%), respectively.

3.4.2.6 Dilution Integrity

The dilution integrity was assessed by determining the accuracy and precision of the measurement of rat plasma spiked with OJT007 5X upper limit of quantification (ULOQ). The effect of 1:5, 1:10, 1:20 and 1:50 dilution with blank rat plasma was measured. Following LC-MS/MS analysis, the quantitated concentrations were corrected with their respective dilution factor, and accuracy and precision were determined. This experiment was conducted in sextuplets.

3.4.3 UPLC Quantification Method Development

Nonvolatile buffers (i.e., phosphates) and salts have the tendency to remain deposited on the ion source, which contaminates the electrodes in the ion source in turn resulting in a reduction in signal intensity (Mannur et al., 2011). Furthermore, PEG, surfactants and PEG-like solvents have the tendency to decrease signal by interfering with ionization (Keller et al., 2008). To prevent ion source contamination in the buffered *in vitro* metabolism experiments and during solubility studies, a UPLC analytical method was developed to quantitate OJT007 and metabolites concentrations. The UPLC system consisted of Waters Acquity UPLC with photodiode array detector and Empower software; column, BEH C$_{18}$, (1.7μm, 2.1 × 50 mm. The mobile phase consisted of 100% acetonitrile (B) and 0.1% formic acid in water (A). Gradient elution was employed with 5% to 98% B from time 0 to 2.8 min and was kept constant at 98% B for 1.2 min, then 98% B was changed to 5% B from 4 to 5.2 min, and kept constant at 5% from 5.2 min to 6 min. UV detection wavelength was 343 nm, and 10 μL injection volume. The Standard curve samples containing OJT007 were prepared in solution or phosphate buffer and injected into UPLC for quantification.

3.4.4 Preformulation Studies

3.4.4.1 Solubility in Common Solvents

The solubility of OJT007 in common pharmaceutical excipients were determined using the shake-flask method. Briefly, excess amounts of OJT007 were added into 1 mL of solvent and placed on a mechanical shaker at room temperature for 24 hours. Each sample was centrifuged at 14000 rpm at 4°C for 15 minutes. The supernatant was collected

and filtered using sterile 0.22 μm syringe filters before UPLC injection. The following solvents were evaluated: DMSO, polysorbate 80, ethanol, labrasol, PEG 400 and deionized (DI) water.

3.4.4.2 pH Solubility Profiles

The solubility of OJT007 was determined under pH conditions ranging from 3-7. Standard USP buffers were prepared and used for this experiment: 0.2 M Hydrochloric acid for pH 1.2, 0.2 M acid phthalate buffer for pH 3-4, neutralized phthalate buffer for pH 5, and 0.2 M phosphate buffer for pH 6-7. Excess OJT007 was added to buffered systems. The mixtures were placed in a water bath at room temperature for 24 hours shaking at 50 rpm to reach solubilization equilibration. The samples were centrifuged and filtered using sterile 0.22 μm syringe filters. The filtrates were injected onto the UPLC system for quantification of OJT007 concentrations, and subsequently calculating solubility of OJT007 in various pH conditions. Each buffered cosolvent was tested in triplicate.

3.4.4.3 Solution State pH Stability

The effect of varying pH conditions on the stability of the drug was evaluated by incubating OJT007 in buffers of various pH. Standard USP buffers (USP-NF) were prepared and used for this experiment: 0.2 M Hydrochloric acid for pH 1.2 and 2, 0.2 M acid phthalate buffer for pH 3-4, neutralized phthalate buffer for pH 5, 0.2 M phosphate buffer for pH 6-8 and 0.2 M borate buffer for pH 9-10. Buffers spiked with OJT007 (100 μg/mL) were incubated at 37°C. Aliquots of the buffer solution were collected at 0, 0.25, 0.5, 0.75, 1, 2, 3, 4, 5, 7 and 24 hrs. The collected samples were diluted with 50% acetonitrile in water to obtain appropriate concentrations and analyzed by the UPLC.

3.4.4.4 UV-metric pKa measurements

The experimental pKa was determined by UV-metric method with a Sirius T3 automated titrator instrument (Pion, Woburn, MA). This method measures the UV absorbance changes of chromophores of the substance as a function of pH. The Sirius T3 machine is equipped with an Ag/AgCl double junction electrode to measure the pH, a dip probe attached to the UV spectrophotometer, a stirrer, and titration capabilities. The stock solution for OJT007 were prepared by dissolving the drug in DMSO. During the experiment 5 uL of stock solution were delivered to the Sirius T3 glass vial to achieve a final concentration of 20 mM (to ensure appropriate absorbance without saturating the detector). The titration experiments were conducted at 25°C in 0.15 M KCl solution under argon flow to prevent CO_2 absorption that could potentially affect pH. The pH was titrated between 1.8 and 12.2 via de addition of 0.5 M HCl and 0.5 M KOH starting from low to high pH (so titration would start when the compound was more soluble). The UV absorbance data was collected from 160-760 nm; However, the region of 250-450 nm was used for pKa determination.

3.4.4.5 Cosolvent Formulation

Water-miscible solvents in which OJT007 has good solubility were used to develop a cosolvent formulation to improve the poor aqueous solubility of the drug. Several solvents with varying ratios and compositions were tested to make the cosolvent formulation of OJT007. Varying concentration of OJT007, ranging from 1-10 mg/mL were incorporated in the cosolvent system. The optimal formulation to be used in the preclinical studies was selected on the basis of precipitation upon dilution with normal saline and formulation stability.

3.4.5 Plasma Protein Binding

Plasma protein binding (PPB) was evaluated using a modified ultra-filtration technique (Bowers et al., 1984; Robinson et al., 2015; Toma et al., 2021). Three different concentrations (50, 75 and 100 µg/mL) of OJT007, were selected to ensure that unbound fraction could be accurately quantitated with the developed method. Briefly, stock solutions of three different concentrations (50, 75 and 100 µg/mL) prepared in 50% acetonitrile were spiked into blank rat plasma. The plasma was incubated at 37°C for 30 min. The mixture was transferred into Amicon Ultra-0.5 mL centrifugal filters of 30kD (EMD Millipore Corporation, Billerica, MA) for ultrafiltration at 14,000 rpm for 15 min at 4°C. Filtrate and non-filtrate samples were spiked with internal standard and analyzed using the LC-MS/MS. Percent PPB was calculated according to Equation 5.

$$\text{Plasma protein binding\%} = \left(\frac{C_b}{C_b + C_u} \right) \times 100\% \qquad (5)$$

Where C_b and C_u are bound and unbound OJT007 concentrations measured in the un-filtrated sample and filtrated, respectively. Experiments were conducted in triplicate.

3.4.6 Metabolism of OJT007 in Hepatic Cytochrome P450 Phase I and II Reaction Systems

To determine whether OJT007 is metabolized by cytochrome P450 (CYP) or uridine glucuronosyltransferase enzymes (UGT), rat and human liver microsomes and intestine microsomes were used.

3.4.6.1 In Vitro Metabolic Studies - CYP Reaction System

The NADPH regenerating system consists of solution A and solution B which after mixing, generate the NADPH needed for oxidation reactions. Solution A contains 26 mM NADP+, 66 mM glucose-6-phosphate, and 66 mM magnesium chloride in water while and solution B contains 40 U/mL glucose-6-phosphate dehydrogenase in 5 mM sodium citrate for generating NADPH. The *in vitro* cytochrome P450 phase I oxidation metabolism of OJT007 was evaluated according to previously described incubation procedures (Yang et al, 2010). Briefly, rat liver microsomes (final concentration 10 mg protein/mL), 50 mM phosphate buffer at pH 7.4 (KPI), test compound (50 µM), 30 µL NADPH regenerating solution A and 6 µL NADPH regenerating solution B were incubated for 28 hours at 37°C (600 µL total assay volume). Aliquots of 100 µL were taken at different time points and quenched with 50 µL of ice-cold acetonitrile containing 0.6% formic acid. The samples were vortexed for 30 seconds, centrifuged at 14,000 rpm and the supernatant was injected into UPLC system for analysis. A negative control was prepared without addition of NADPH.

3.4.6.2 In Vitro Metabolic Studies - UGT Reaction System

The *in vitro* uridine glucuronosyltransferase (UGT) phase II glucuronidation of OJT007 was evaluated according to previously described incubation procedures (Jiamboonsri et al., 2016) . Rat liver microsomes (final concentration of 0.035 mg protein/mL or 0.5 mg protein/mL), rat intestine microsomes (final concentration of 0.5 mg protein/mL) or human liver microsomes (final concentration of 0.5 mg protein/mL) were mixed with 0.88 mM magnesium chloride, 4.4 mM saccharolactone, 0.022 mg/mL alamethicin, 15 µM, test compound and 3.5 mM UDPGA, which was added last. The

mixture (final volume=200 μL) was incubated at 37°C for 1 hr or 2 hr. The reaction was stopped by addition of 50 μL acetonitrile containing 0.6% formic acid. The samples were vortexed for 30 seconds, centrifuge at 14,000 rpm and the supernatant was injected into UPLC system for analysis of OJT007 and metabolites. Genistein (15 μM) was used as a reference substrate for UGT. A negative control was prepared without addition of cofactor.

3.4.7 Determination of Molar Extinction Coefficient of OJT007 Glucuronide

Because of the lack of OJT007 glucuronide authentic standards, the OJT007 standard curve was used for quantification of OJT007 glucuronide using a conversion factor (K). Determination of conversion factors has been described previously (Gao et al., 2011; Z. Yang, Zhu, et al., 2010). Briefly, an OJT007 standard curve was prepared in KPI without microsomes. The conversion factors were determined by comparing the UV absorption peak area of OJT007 and those of the glucuronide at absorption wavelength of 343 nm with following its 100% conversion to after a complete glucuronide. The difference in peak area of glucuronide metabolite (PA_c) and peak area of OJT007 (PA_o) was calculated to be the ratio K. The average conversion factor (K) at three different concentrations (2.5, 10 and 50 μM) was used for estimating metabolite concentration.

$$K = \frac{PA_c}{PA_o} \tag{6}$$

The calculated conversion factor can be used to calculate the metabolite concentration using peak area of metabolite and the slope of the calibration curve obtained from parent compound (a1).

$$C = \frac{PAc}{Kxa1} \tag{7}$$

3.4.8 Metabolite Identification

3.4.8.1 Hydrolysis by β-glucuronidases

β-glucuronidases are enzymes which catalyze the hydrolysis of O- or S-glycosidic moieties allowing for the liberation of aglycones from glycosides (Sui et al., 2021). Following OJT007 biosynthesis of the glucuronide metabolite using liver microsomes for 2 hours, the incubates were centrifuged at 14,000 rpm for 15 min. The supernatant (200µL) was added to 50µL of the β-glucuronidase solution, which was prepared in KPI pH 7.4 at a concentration of 4,000 units/mL. Then, the mixtures were incubated at 37°C for 2 hr to hydrolyze the glucuronide into parent compound. Aliquots of the mixture were collected at 0, 1 and 2 hours and added into the ice-cold 0.6%formic acid in acetonitrile solution to stop the reaction. The mixtures were then vortexed for 30 seconds and centrifuged at 14,000 rpm for 15 min. The supernatant of this mixture was analyzed for OJT007 and glucuronide concentrations by a UPLC method. The control reaction consisted of an equivalent volume of KPI instead of the enzyme solution. The remaining glucuronide metabolite after hydrolysis was expressed as residual percent: the peak area of the analyte at different time points relative to the peak area of the same analyte at time zero multiplied by 100. The produced aglycone or unconjugated molecule was expressed as the concentration of the analyte at each time point.

3.4.8.2 Identification of Metabolites

After biosynthesis of the glucuronide, the metabolite solution was analyzed by
LC-MS/MS to identify the glucuronide. UPLC analysis was accomplished using a
Shimadzu Nexera X2 UHPLC system (Columbia, MD, USA) coupled with a 4000
QTRAP® triple quadrupole mass spectrometer system equipped with a Turbo Ion Spray
ion source (AB Sciex. Redwood City, CA, USA) using the instrument conditions
optimized on section 3.4.1.2. The mass spectrometer used Q1MI, product ion (MS2),
Neutral Loss (NL) and Precursor ion (PI) scan to identify the metabolites.

3.4.9 Metabolic Stability Data Analysis

The half life was calculated based on a single time point assay as done by others (Di et
al., 2004). Briefly, half-life was calculated based on first-order reaction kinetics using
Equation 8, which allows to calculate the percentage of the parent remaining at certain
incubation time. For screening purposes, 60 minutes was selected as optimal time for
incubation as it would give a higher predictive limit and would allow to differentiate
OJT007 microsomal stability.

$$Half - life\ (t_{\frac{1}{2}}) = \frac{\ln 2\ x\ (Incubation\ time)}{\ln(\%\frac{Remaining}{100})} \quad (8)$$

3.4.10 Glucuronidation Metabolic Kinetics

The kinetic parameters of OJT007 glucuronidation were determined by measuring
the initial glucuronidation rates of OJT007 at 1 hour after incubation with liver
microsomes according to the glucuronidation assay described in section 3.6.2. OJT007
concentrations evaluated ranged from 1.25−100 μM at a 0.035 mg of protein/mL. The

glucuronidation rates were calculated as the amount of formed glucuronide per reaction time per protein amount (nmol/min/mg). Kinetic data were analyzed according to the Eadie-Hofstee plot for selection of the appropriate equation (Seibert & Tracy, 2014). If the Eadie-Hofstee plot was linear, the formation rate at different substrate concentration were fit to the standard Michaelis-Menten equation:

$$V = \frac{V_{max} x\ C}{K_m + C} \qquad (9)$$

Where K_m is the Michaelis-Menten constant, and V_{max} is the maximum rate of glucuronidation. GraphPad Prism software (version 7.3 for Windows; GraphPad Software, La Jolla, CA) was used. Visual inspection of fitted functions was used to select the best-fit enzyme kinetic model.

3.4.11 Prediction of In Vivo Clearance From In Vitro Hepatic Data

The in vitro intrinsic clearance was scaled-up to predict the in vivo intrinsic clearance. For microsomes a standard value of 45 mg of protein/g of liver weight is used. The intrinsic clearance values were based on total concentrations not on free concentrations (Brian Houston, 1994; Obach, n.d.). Likewise, a value of 40 g of liver/Kg of body weight was applied in the calculation. (Davies & Morris, 1993)

$$Cl_{IntVivo} = Cl_{IntVitro} x\ \frac{microsome\ mg}{liver\ (g)} x\ \frac{liver\ weight\ (g)}{body\ weight\ (Kg)} \qquad (10)$$

Conversion of the intrinsic clearance to clearance in rats was done using the well-stirred model of hepatic clearance. It has been reported that for highly protein bound lipophilic amines or neutral molecules, inclusion of PPB data yielded severe Cl underpredictions. It appears that for compounds highly bound to microsomes, the

intrinsic clearance is underestimated. In this case, inclusion of the free fraction term

leads to an underprediction of clearance (Obach, 1999; Obach et al., 1997). Due to this

we will use the well stirred model as follow:

$$Cl_H = \frac{Cl_{int} \times Q}{Cl_{int} + Q} \qquad (11)$$

3.4.12 Pharmacokinetic Studies

3.4.12.1 General animal procedures

Jugular vein cannulation was performed under anesthesia using an aqueous

anesthetic cocktail composed of ketamine: acetopromazine: xylazine (50:3.3:3.3 mg/Kg)

at a dose of 1 mL/Kg the day before the study. A cannula, composed of silicone elastic

tubing (0.02" I.D. and 0.037" O.D.) was inserted into the right jugular vein, secured with

a silk suture tunneled subcutaneously and exteriorized in the dorsal infrascapular area.

The surgical incision was closed with surgical sutures. Cannula patency was maintained

by flushing the cannula line daily with 0.5 mL of sterile heparinized saline solution (100

units/mL).

3.4.12.2 Evaluation of Oral Bioavailability

Cross-over design was used in this study to evaluate the oral bioavailability of

OJT007. Adult male SD rats (n=5) weighing 300 – 350 g were cannulated through the

jugular vein under anesthesia one day before the study. Each rat received a 5 mg/kg

intravenous dose of OJT007 cosolvent formulation. Serial blood samples (100-150 µL

each) were collected from each rat before dose and at 2, 5, 15, 30, 60, 90 minutes, and 2,

4, 6, 8, 10, and 24 hours post dose. After blood centrifugation at 13000 rpm for 3

minutes, the plasma supernatants were collected, and immediately stored in -80^{0}C and analyzed within 14 days. We also collected urine samples up to 24 hours post dose and immediately stored in -80^{0}C and analyzed within 14 days. Following a week washout period, the rats were fasted overnight and for four hours after receiving a 10 mg/kg oral dose of OJT007 cosolvent formulation. Water was always available to the rats. Again, serial blood samples were collected before dose and at 0.25, 0.5, 0.75, 1, 1.5, 2, 3, 4, 6, 8, 10, 24 hours post dose. Blood samples were centrifuged at 13000 rpm for 3 minutes, and the supernatants were collected. Urine samples were collected up to 24 hours after dose. Urine and plasma samples were stored at -80^{0}C and analyzed by LC-MS/MS analysis within 14 days.

3.4.12.3 Drug Interaction Studies following Co-administration of OJT007 and Rabeprazole

Determination of Gastric pH

We evaluated the effect of rabeprazole, a proton pump inhibitor that reduces stomach acid, on oral bioavailability of OJT007 in another crossover study design. Briefly, adult male SD rats (n=4) weighing 296-338 g were cannulated through the jugular vein under anesthesia one day prior to the study. The rats were fasted overnight prior to and for four hours after drug administration. Water was always available to the rats. Fasting rats were pretreated with an intravenous bolus administration of 10 mg/kg rabeprazole (dissolved in saline) 30 minutes before each rat received a 25 mg/kg oral dose of OJT007 cosolvent formulation. Under anesthesia, the abdominal cavity was opened, and the stomach was located. The antrum cardiacum and pylorus of the stomach

were ligated. An incision to the stomach wall was made and the gastric juice pH was measured with a pH meter at 0.5, 1 and 2 hours after rabeprazole administration.

Dosing and Sampling

Fasting rats were dosed with 25mg/kg oral dose of OJT007 cosolvent formulation. Serial blood samples (100 µL each) were collected before dose and at 0.25,0.5, 0.75, 1, 1.5, 2, 3, 4, 6, 8, 10 and 24 hours post dose. Plasma samples were separated and stored at -80°C pending LC-MS/MS analysis of OJT007 concentrations. Urine samples were collected up to 24 hours post dose pending LC-MS/MS analysis of OJT007. Following a week washout period, fasting rats were pretreated with an intravenous bolus administration of 10 mg/kg rabeprazole (dissolved in saline) 30 min before the oral administration of OJT007 cosolvent formulation (25 mg/kg). Serial blood samples (100 µL each) were collected before OJT007 dose and at 0.25,0.5, 0.75, 1, 1.5, 2, 3, 4, 6, 8, 10 and 24 hours post dose. Plasma samples were separated and stored at -80°C pending analysis. Urine samples were collected up to 24 hours post dose.

3.13 Pharmacokinetic Analysis

Plasma OJT007 concentration versus time data were analyzed for each rat using a non-compartmental model (WinNonlin v8.1, Pharsight Corp, Mountain View, CA). The noncompartmental pharmacokinetic parameters derived after intravenous administration were maximum plasma concentration (C_0), terminal elimination half-life ($T_{1/2}$), systemic plasma clearance (CL), apparent volume of distribution (Vd), the total area under the plasma drug concentration-time curve from 0 to last sampled point (AUC_{Last}), the total area under the plasma drug concentration-time curve from 0 to infinity ($AUC_{0-\infty}$), MRT

- $AUC_{0-\infty}$ - The area under the concentration-time curve from time zero to infinity was calculated using the trapezoidal method using the plasma drug concentration vs time data from time zero to the last experimental time plus the excess area (from last experimental time to infinity).

- $T_{1/2}$ – The terminal half-life of the drug was calculated as

$$T_{1/2} = 0.693/K \qquad (12)$$

The terminal phase rate constant (K) was determined from the slope of the terminal linear segment of a semilogarithmic plot of plasma drug concentration vs. time.

- C_0- Initial plasma concentration of drug was determined by back extrapolation.

- V_d- Volume of distribution was calculated as

$$V_d = \text{Dose} / (K \times AUC_{0-\infty}) \qquad (13)$$

- Cl – The total body clearance was calculated as

$$Cl = \text{Dose} / AUC_{0-\infty} \qquad (14)$$

- MRT- The mean residence time extrapolated to infinity was calculated using moment analysis according to the equation

$$MRT = AUMC_{0-\infty} / AUC_{0-\infty} \qquad (15)$$

where $AUMC_{0-\infty}$ is the area under the first moment curve extrapolated to infinity and $AUC_{0-\infty}$.

- V_{ss}- The volume of distribution at steady state was calculated according to the following equation

$$V_{ss}= Cl \times MRT \qquad (16)$$

- ER- The hepatic extraction ratio calculated as the ratio of systemic clearance (Cl) to liver blood flow (Q)

$$ER=\frac{Cl}{Q} \qquad (17)$$

After extravascular administration, the following pharmacokinetic parameters were calculated using phoenix WinNonlin non-compartmental analysis:

- T_{max}- Time of maximum observed concentration. It is determined by observation of the entire concentration time- profile.

- C_{max}- Maximum observed concentration, occurring at Tmax. It is determined by observation of the plasma- concentration time profile.

- CL/F – The total body clearance after extravascular administration calculated as defined above.

- V_d/F- Volume of distribution for extravascular administration calculated as defined above.

- F - The absolute oral bioavailability was estimated according to the following equation:

$$F\% = \frac{AUCpo/Oral\ dose}{AUCiv/IV\ dose} \times 100\% \qquad (18)$$

- F_{rel} - The relative oral bioavailability with versus without gastric acid inhibition was calculated using the following equation:

$$Relative\ F\% = \frac{AUC\ with\ rabeprazole}{AUC\ without\ rabeprazole} \qquad (19)$$

- F_h- Hepatic bioavailability calculated according to the following equation

$$F_h= 1-ER \hspace{3cm} (20)$$

3.14 Statistical analysis

Statistical results were performed using Sigma Plot v11.0 (La Joya, CA). Paired *t*-test at a 0.05 level of significance was used to determine statistical significance across treatments on exposure pharmacokinetic parameters.

CHAPTER 4

RESULTS AND DISCUSSION

4.1. LC-MS/MS Method Development

The method development process entails three main tasks. First, the mass spectrometric conditions need to be optimized to achieve the best signal-to-noise ratio for the analyte of interest. Second, the chromatographic conditions must be optimized to achieve the best selectivity while minimizing matrix effect. Third, the sample preparation process must be optimized to ensure sufficient sample cleaning.

4.1.1. Mass Conditions

Positive ion mode and electrospray ionization (ESI) provided the best peak intensity compared to the negative mode and atmospheric chemical ionization (APCI). During Q1 scan, the presence of the analyte of interest (i.e., OJT007) was confirmed as indicated by a pseudo-molecular ion $[M+H]^+$ at 325.

The compound dependent parameters were optimized based on the compound ionization efficiency and fragmentation pattern. Through Q1MI scan mode, the XIC signal of the pseudo-molecular ion at m/z 325 was monitored, ramping the DP values from 0-400 V. The best signal intensity was found with DP of 105 V, because it effectively eliminates ion clusters (Figure 8).

Likewise, the EP was set at 10 V. In a subsequent experiment, using product ion scan, the fragmentation of the precursor ion was evaluated by ramping the CE values from 10 to 100V. The optimal CE value for the formation of the fragment 205 was 30V (Figure 9). Similarly, the collision exit potential (CXP) was optimized to 11 V by ramping the value from 5-100V to ensure optimal sensitivity.

The source parameters were optimized in order to obtain the most suitable conditions for the analyte while ensuring signal stability and sensitivity. Curtain gas (CUR) was set at 25 psi to prevent the entrance of neutral contaminants. The ion spray voltage was set at 4500 V to ionize sample. CAD gas was set on high for optimal pressure of collision gas in Q2. Source temperature was set at 500. The nebulizer gas (GS1) was set at 50 psi to ensure optimal generation of small droplets during sample flow. The heater gas was set at 40 psi to ensure evaporation of the generated small droplets and to prevent solvent from entering the mass analyzers.
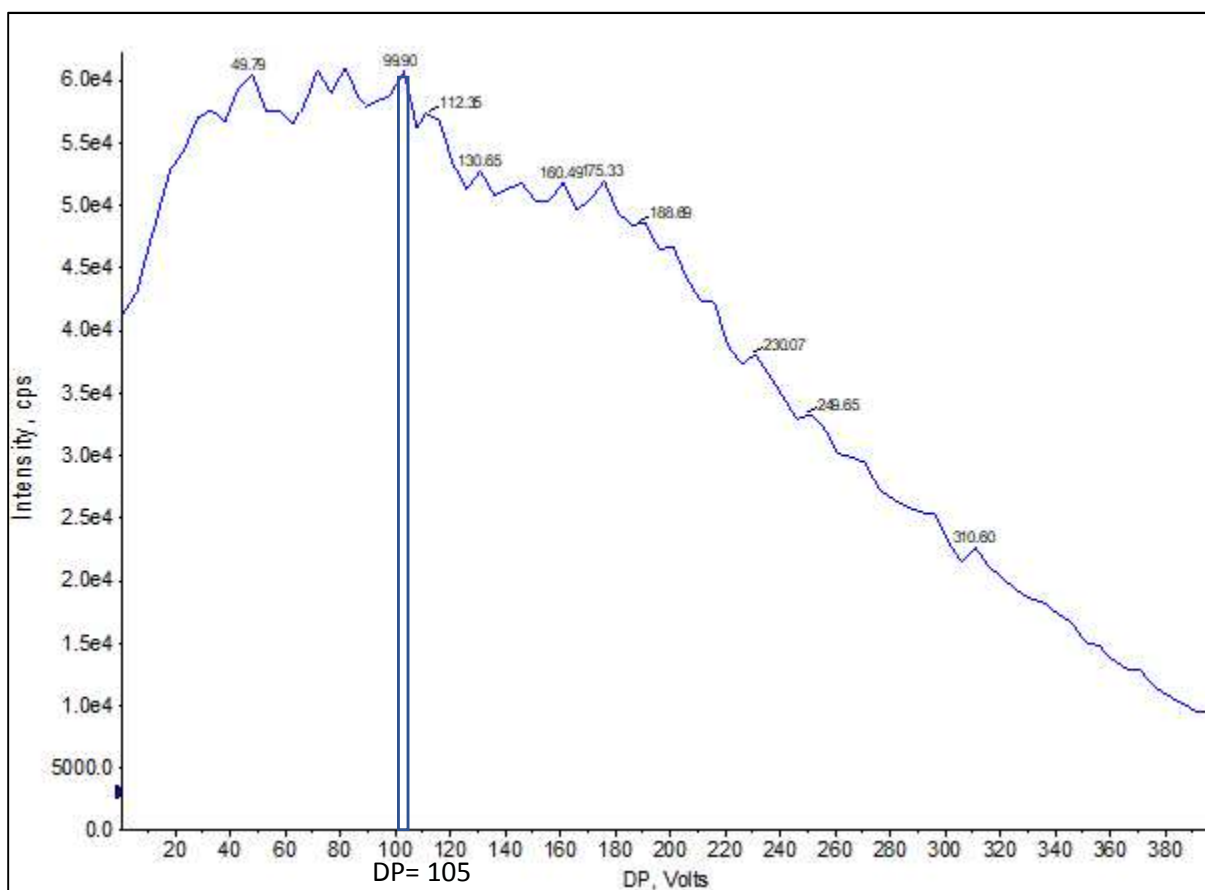
Figure 8: *Optimal DP Value: XIC for 325 m/z. The apex of the XIC trend was reached at the optimal DP value of 105 V.*
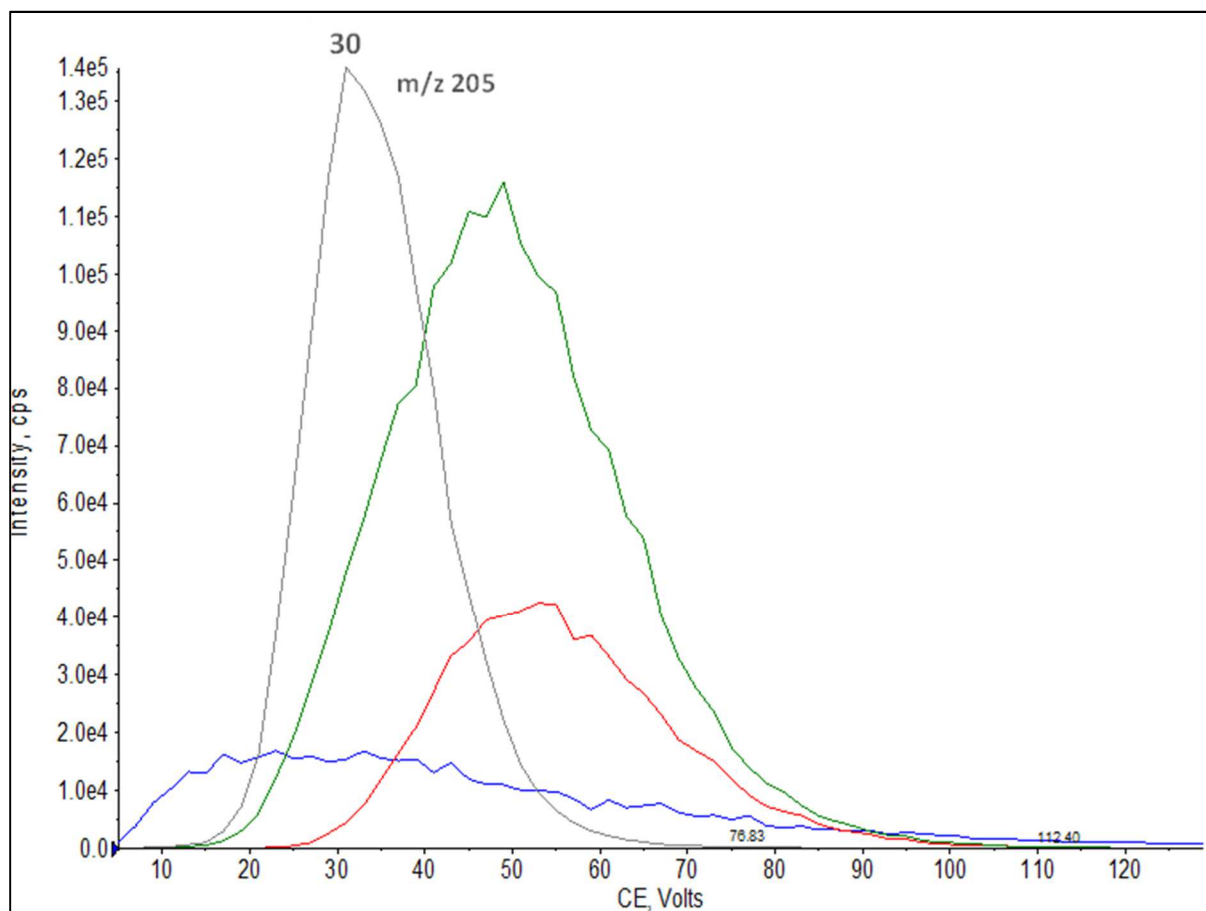
Figure 9: *Optimal CE. Intensity signal obtained in MRM mode following the transition from the precursor ion at 325 m/z to the selected product ions 205.*

4.1.2. Chromatographic Conditions

OJT007 does not have a commercially available stable isotope-labeled analog. As such, we selected voriconazole as the internal standard, which has a similar ionization mode, sensitivity, and lipophilicity to OJT007 (M. Li et al., 2018). Several mobile phase compositions and columns were tested until an optimal intensity and peak shape were attained. The best response and peak shape were achieved with an Acquity UPLC BEH C_{18} column (50 × 2.1 mm, 1.7 μm) using 0.1% formic acid in acetonitrile and water as the mobile phase. OJT007 is a weak base analyte; the addition of 0.1% formic acid to the mobile phase aids in the formation of ions in the solution in order to achieve the optimal response in ESI.

Figure 10 illustrates the chromatograms obtained under the established chromatographic conditions. Although the analyte was in an ionized form, an adequate chromatographic performance was observed. This may be due to the analyte's hydrophobic moiety maintaining the ability to interact with the stationary phase. Likewise, a good peak shape may be attributed to the Acquity UPLC BEH C_{18} column's endcapping effectively eliminating unbounded silanol groups preventing ionic interactions with the positively charged analyte.

The gradient was optimized to ensure appropriate chromatographic retention and separation while preventing carryover. The chromatographic run time for the developed assay was 5 min, with retention times of 2.16 and 1.74 for OJT007 and IS, respectively, in plasma (Figure 10, A) and urine (Figure 10, B).

Potential carryover interference peaks between the injections were prevented using an organic solvent mixture comprising 50% acetonitrile and 50% methanol as a

needle wash between the injections. The purpose of the needle wash was that of solubilizing any remaining analyte that adhered onto the needle. The adherence or adsorption of analyte onto the needle has been reported as a source of carryover, which can be prevented by optimization of needle wash during LC method development (DesJardins et al., 2019).

4.1.3 Sample Preparation

An important component of the method development effort is sample preparation. Often during ADME evaluations, samples consist of complex biological matrices which contain endogenous components (i.e., proteins and lipids) which might interfere with the detection of the drug. Basically, this interference could affect the ionization of the drug causing variation in response. Moreover, the endogenous components can dirty and damage the chromatographic column and the source.

As sample extraction method, protein precipitation was selected for its simplicity and to ensure a high throughput workflow. It was tested both the efficiency of methanol and acetonitrile at cleaning samples using different ratios of precipitant organic solvent to plasma. Precipitant to plasma ratio of 1.5 for acetonitrile and 2.5 for methanol has been reported to remove approximately 90% of plasma proteins (Liu & Aubry, n.d.). A precipitant to plasma ratio of 10:1 and 5:1 yielded clear supernatants for methanol and acetonitrile, respectively. The need for larger volumes necessary for protein precipitation with methanol led to diluted samples, which translated into low signal intensity. The best compromise between sample clean-up and signal intensity was found using acetonitrile.
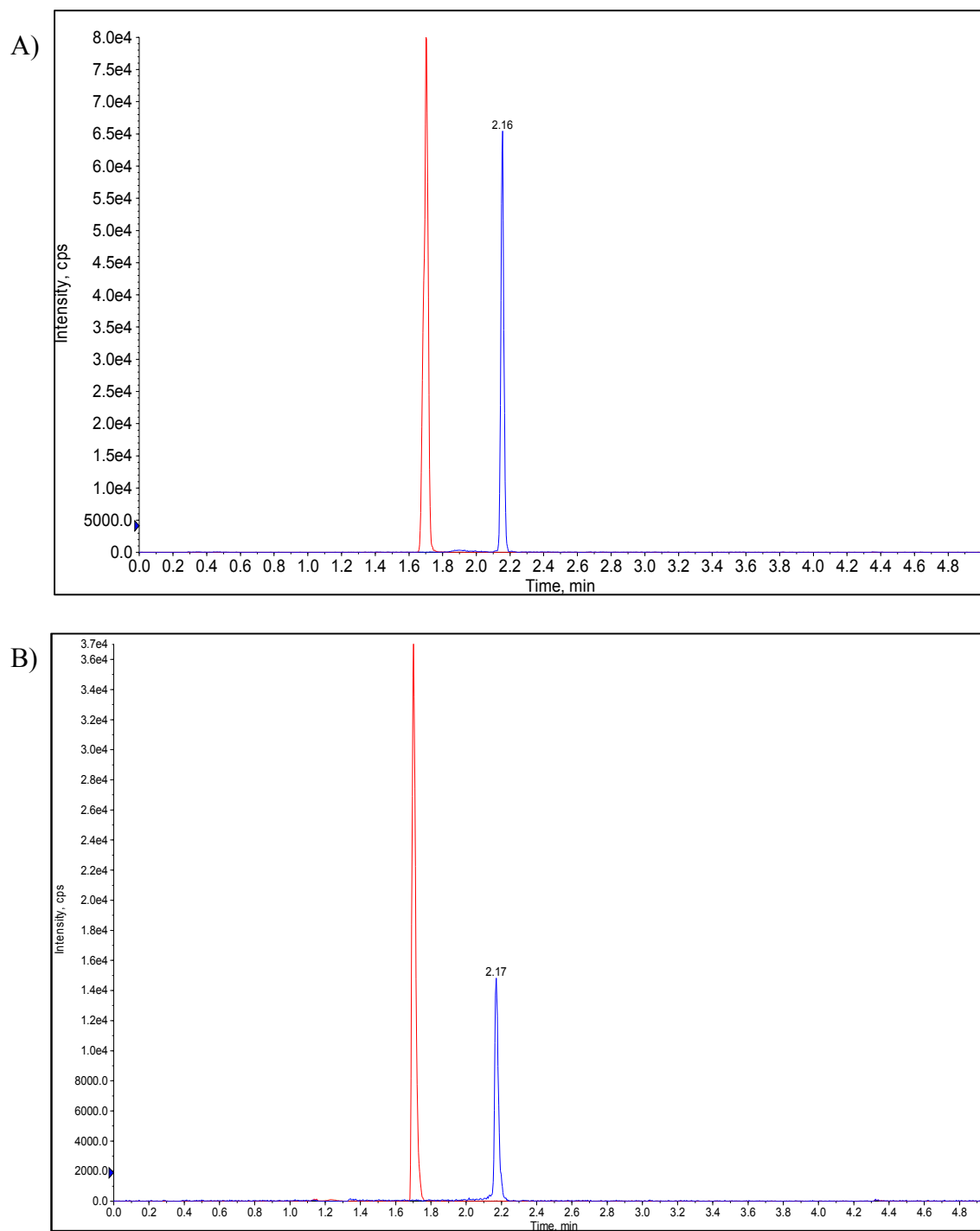
Figure 10: *Representative chromatograms in A) rat plasma spiked at 50 ng/ml and B) spiked rat urine at 50 ng/mL*

4.2. Method Validation

4.2.1. Linearity and Sensitivity

Linear calibration curves in rat plasma and urine were generated by plotting the peak area ratio of OJT007 to IS against known standard concentrations of OJT007. Because the standard curve spans several orders of magnitude, a weighting factor of $1/x$ was used to construct the standard curves. Generally, unweighted regressions are used whenever errors from the instrument response (dependent variable) are independent of each other, uncorrelated with the dependent variable (concentration) and response have equal variance or standard deviation across the different concentrations. However, at higher concentrations, standard deviation and variance are larger. Consequently, homoscedasticity is violated, and weighting is used to address the heteroscedastic error (Gu et al., 2014).

The slope, intercept, and coefficient of determination were estimated using least-squares linear regression method. Linear correlation coefficients greater than 0.99 were considered acceptable for the quantification of the analyte in the biological matrix.

The lower limit of quantification (LLOQ) was evaluated based on the signal-to-noise ratio of at least 5:1. Based on a signal-to-noise ratio of at least 5:1, the LLOQ for the developed assay was 5 ng/mL in rat plasma (Figure 11, A) and 10 ng/mL in rat urine (Figure 11, B). The standard curves of OJT007 in plasma and urine were linear in the concentration range of 5–1000 ng/mL (Figure 12, A) and 10-1000 ng/mL (Figure 12, B), respectively.
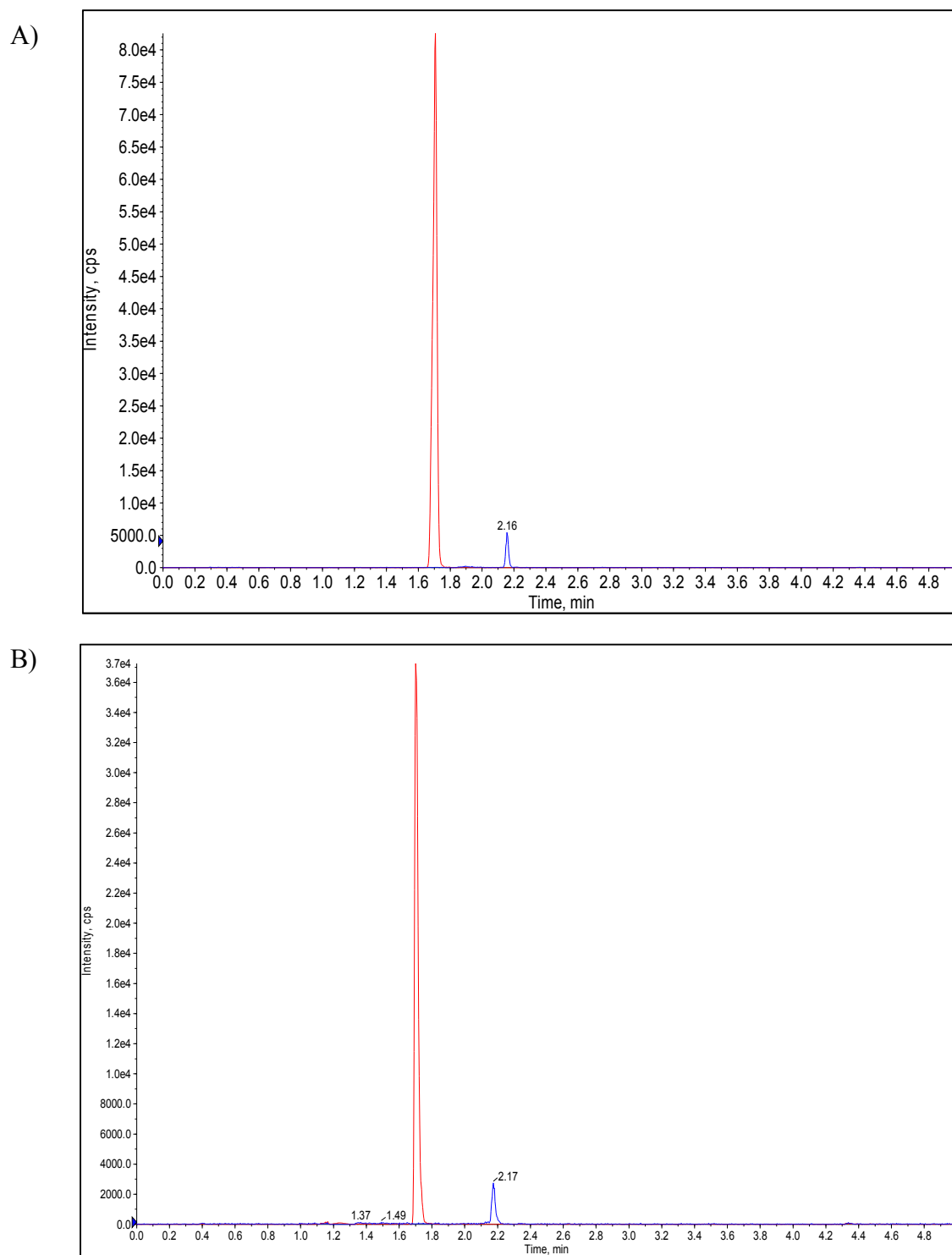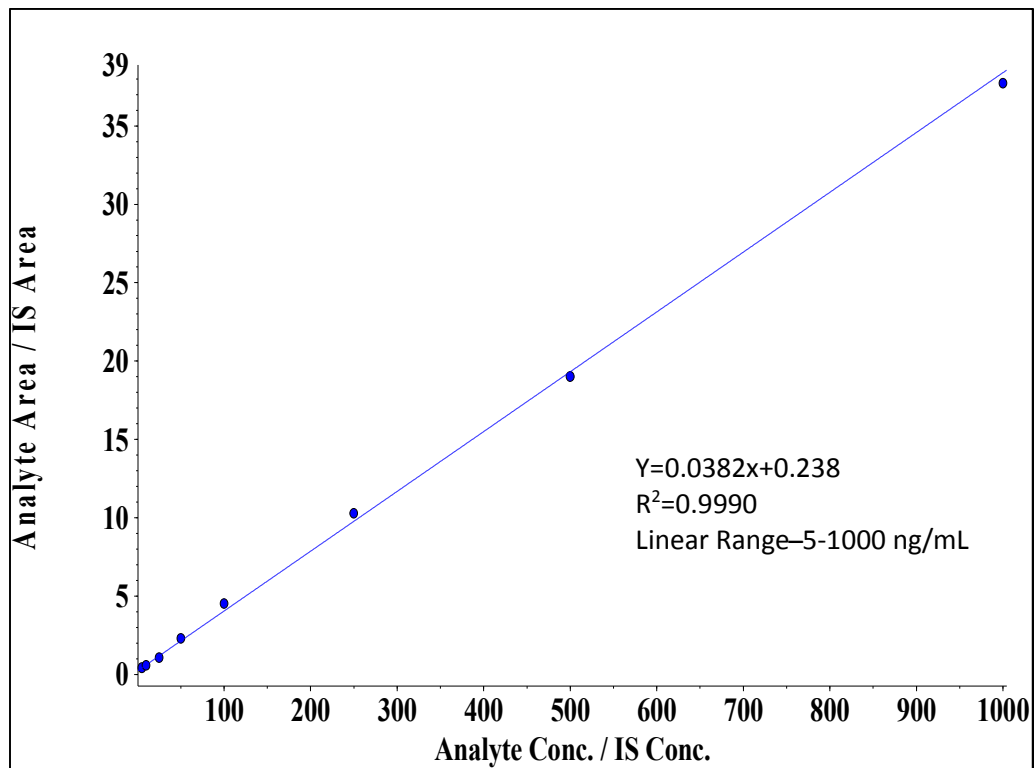
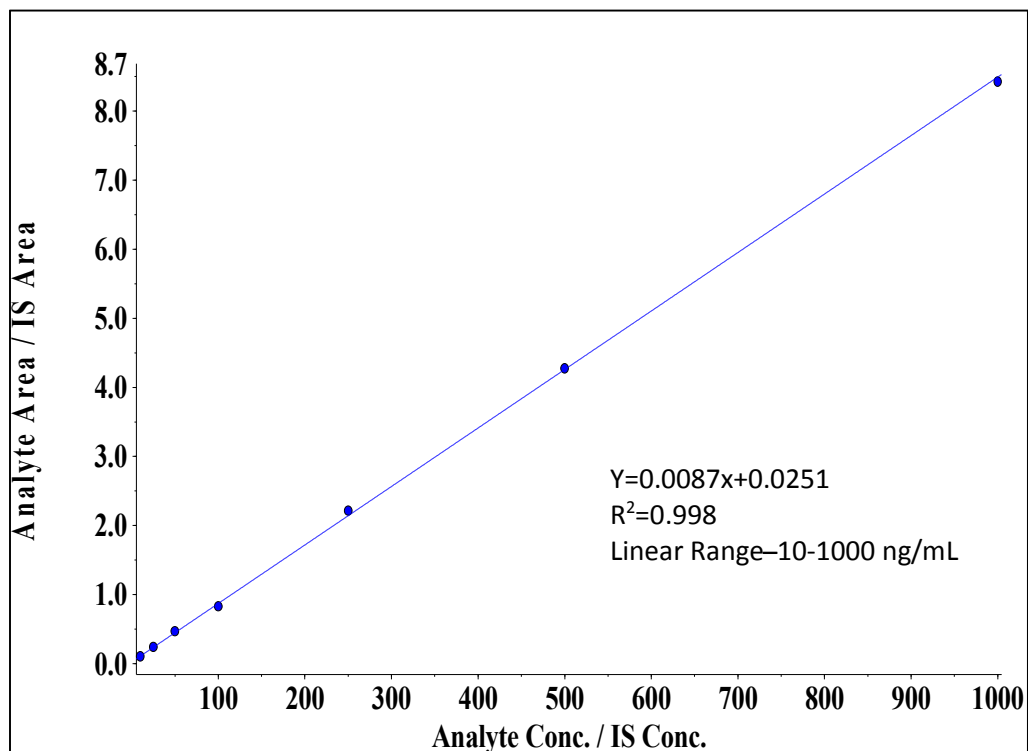**Figure 11:** *Representative LLOQ chromatograms in A) rat plasma and B) rat urine*

A)

B)

Figure 12: *Representative standard curves in A) blank rat plasma and B) blank rat urine*

4.2.2 Selectivity and Specificity

Selectivity or specificity identifies the ability of the assay to quantify the analyte in the presence of interferences present in the matrix. The acceptance criterion for specificity and selectivity is that the peak area ratio in the blank samples should be less than 20% of the peak areas of LLOQ samples. No significant interfering peak from endogenous matrix was found at OJT007 and IS retention time, neither in plasma (Figure 13, A) nor in urine (Figure 13, B), indicating good selectivity and specificity.

4.2.3. Accuracy and Precision

The intra- and inter-day accuracy, presented as the percentage of relative error, RE%; and precision, presented as the percentage coefficient of variation, CV%, are summarized in Table 6. In rat plasma, the intraday coefficient of variation ranged from 1.96 to 8.28%, and the percentage of relative error ranged from 3.40 to 10.1% in plasma. The inter-day coefficient of variation ranged from 3.99 to 11.5%, and the percentage of relative error ranged from 5.45 to 9.69% in plasma.

In rat urine, the intra-day coefficient of variation ranged from 0.96% to 6.49%, and the percentage relative error ranged from 0.09% to 8.60%. The inter-day precision in coefficient of variation ranged from 5.72% to 8.18%, while the inter-day accuracy ranged from 2.22% to 7.91%. The precision and accuracy were within the acceptable limit of ≤20% for LLOQ and ≤15% for the high, medium, and low QC, as established by the FDA Bioanalysis guidance both in plasma and urine. This data indicates that the developed LC-MS/MS method is accurate and precise for the quantification of OJT007 in
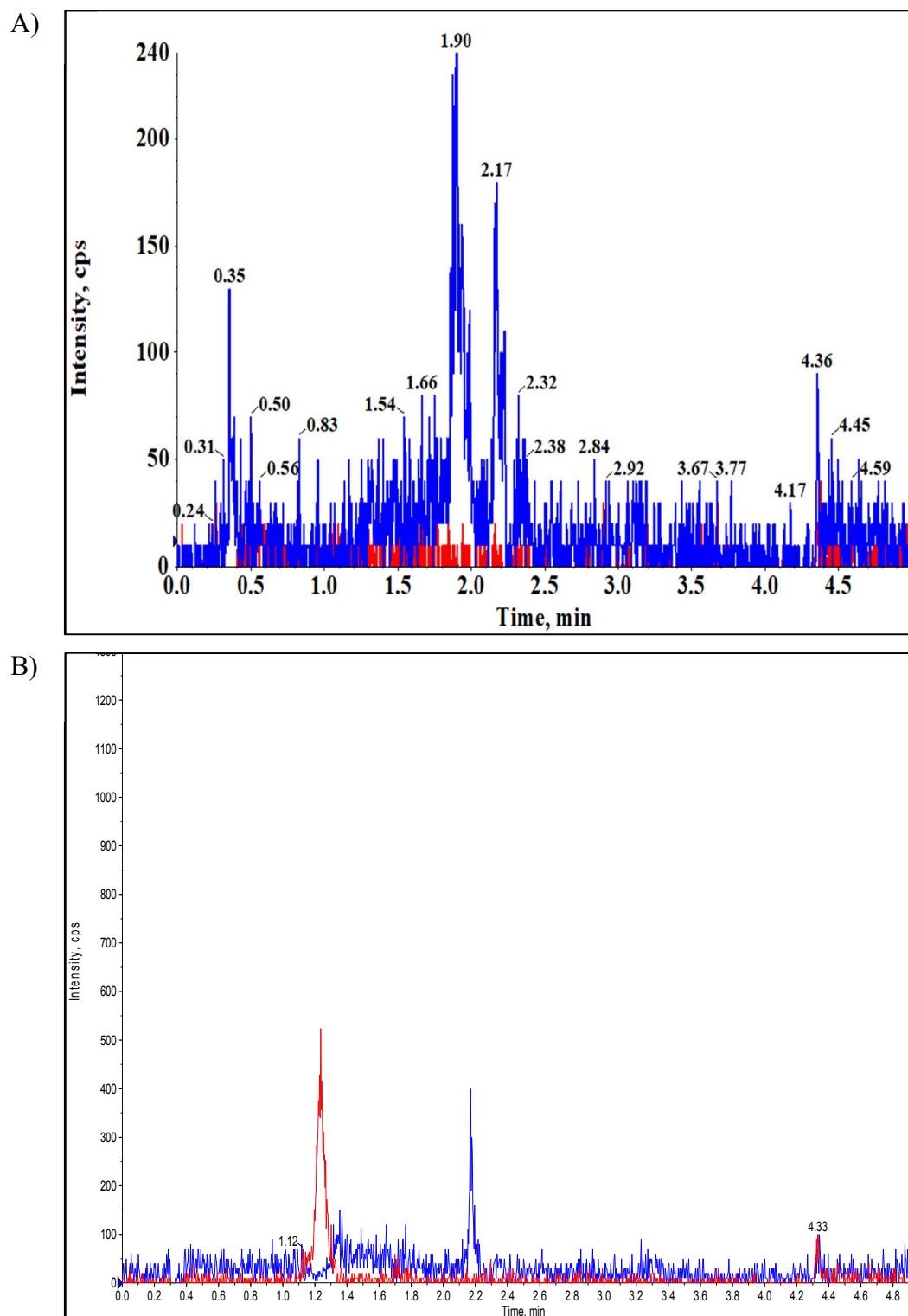
Figure 13: *Representative blank chromatograms in A) Blank rat plasma and B) Blank rat urine*

Table 6. *Intra and Inter-day Accuracy and Precision of the LC-MS/MS Assay.*

Biological Matrix	QC	Nominal Concentration (ng/mL)	Intra-day (n=6)		Inter-day (n=6)	
			Accuracy (RE, %) *	Precision (CV, %) *	Accuracy (RE, %) *	Precision (CV, %) *
Plasma	LLOQ	5	5.60	8.28	9.69	11.5
	Low	15	10.1	3.49	5.78	7.29
	Medium	75	2.88	1.96	5.52	4.58
	High	750	3.40	3.03	5.45	3.99
Urine	LLOQ	10	7.33	0.96	7.91	8.18
	Low	15	4.11	3.69	3.00	6.34
	Medium	75	0.094	3.63	3.71	6.74
	High	750	8.60	6.49	2.22	5.72

Accuracy and precision values ≤ 20% for LLOQ and ≤15% for QCs is considered acceptable according to the US FDA Guidance on Bioanalytical Method Validation

rat plasma and urine over a concentration range of 5–1000 ng/mL and 10-1000ng/mL, respectively.

4.2.4. Extraction Recovery and Matrix Effect

The extraction recovery of OJT007, expressed as the percentage recovered (Table 7), was calculated as a ratio of the response obtained from a sample of the biological matrix with OJT007 before protein precipitation to the response from sample spiked after protein precipitation. In blank rat plasma, the mean extraction recovery for OJT007 was 95.8% at the low QC (15 ng/mL), 98.3% at the medium QC (75 ng/mL), and 91.2% at the high QC concentration (750 ng/mL). Likewise, in blank rat urine, the mean extraction recovery for OJT007 was 85% at the low QC (15 ng/mL), 87% at the medium QC (75 ng/mL), and 86.1 % at the high QC concentration (750 ng/mL). This data indicates that the OJT007 extraction method from plasma and urine by protein precipitation with acetonitrile is appropriate**.**

The matrix effect indicates potential ion enhancement or suppression caused by co-eluting matrix components during LC-MS/MS analysis. A positive matrix factor value signifies an enhancement of the analyte signal, while a negative value indicates analyte signal suppression. No significant matrix effect is considered to have taken place if the matrix factor is within ±15%. Table 7 shows the average matrix factors for low, medium, and high QC concentrations of OJT007 in plasma and urine. This data suggests that the sample preparation method successfully removes the matrix components responsible for variability in the analyte signal intensity. Furthermore, this data suggests that the chromatographic conditions effectively prevented ion suppression or enhancement.

Table 7. *Extraction Recovery Rates and Matrix Factors of the LC-MS/MS Method for the Analysis of OJT007 in Rat Plasma and Urine.*

Biological Matrix	Nominal Concentration(ng/mL)	Extraction Recovery (mean ± SD, %)	Matrix Effect (mean ± SD, %)
Plasma	15	95.81± 1.54	3.79± 0.53
	75	98.26± 1.74	8.73± 1.71
	750	91.17± 2.38	3.40± 1.36
Urine	15	85.00± 6.84	8.73±1.89
	75	87.00± 5.18	14.90±5.28
	750	86.10± 7.94	12.64±2.45

**[n = 3; mean (± SD)]*.

4.2.5 Stability

4.2.5.1 Stability in Plasma

Stability studies were conducted to evaluate the stability of the analyte under the expected storage and handling conditions. The stability study results in rat plasma—expressed as the mean remaining percentage of the nominal concentration—are summarized in table 8.

The data in table 8 suggests that OJT007 was stable for up to 4 h in rat plasma at room temperature, this effectively eliminates any concern regarding analyte degradation during sample preparation. The long-term stability samples at low, medium, and high QC concentrations were within 10% of the nominal concentration, demonstrating that pharmacokinetic samples could be stored at −80 °C for up to 14 days without degrading the integrity of the sample. The mean recovery of OJT007 from rat plasma following three freeze–thaw cycles was 95.1%, 98.3%, and 96.1% at low, medium, and high QC samples, respectively, suggesting that repeatedly freeze–thawing the plasma samples did not influence the OJT007's stability. The autosampler stability was expressed as the mean recovery OJT007 from the extracted plasma placed on the autosampler for up to 24 h at 15 °C. The data demonstrate that OJT007 is stable in processed samples during analysis conditions for up to 24 h.

4.2.5.2 Stability in Urine

Stability studies were conducted to evaluate the stability of the analyte under the expected storage and handling conditions. The stability study results in rat urine—

Table 8: *Stability of OJT007 in Rat Plasma/Urine Samples for LC-MS/MS Analysis*

Stability Test	Nominal Concentration (ng/ml)	Mean Recovery% ± SD
Short-Term Stability (4 hr, RT)	15	102.44±4.44
	75	97.11±3.34
	750	91.42±3.91
Long-Term Stability (14 days, -80ºC)	15	96.00±4.37
	75	93.78±1.39
	750	94.67±3.93
Auto-Sampler Stability (24 hr)	15	89.56±7.70
	75	97.20±8.72
	750	101.6±1.85
Freeze Thaw (-80ºc to RT)	15	95.11±0.77
	75	98.33±0.40
	750	96.10±1.07

* [n = 3; (mean ± SD)]

expressed as the mean remaining percentage of the nominal concentration—are summarized in table 9.

The data in table 9 suggests that OJT007 was stable for up to 4 h in rat urine at room temperature; however, the decreased mean recovery suggests the drug should be processed in less than 4 hours upon removal from the freezer to avoid analyte degradation during sample preparation. The long-term stability samples at low, medium, and high QC concentrations were within 10% of the nominal concentration, demonstrating that pharmacokinetic samples could be stored at −80 °C for up to 14 days without degrading the integrity of the sample. The mean recovery of OJT007 from rat urine following three freeze–thaw cycles was 88.1%, 86.7% and 85.6% at low, medium, and high QC samples, respectively, suggesting that repeatedly freeze–thawing the plasma samples did not significantly influence OJT007's stability. The autosampler stability was expressed as the mean recovery OJT007 from the extracted urine placed on the autosampler for up to 24 h at 15 °C. The data demonstrate that OJT007 is stable in processed samples during analysis conditions for up to 24 h.

4.2.6 Dilution Integrity

The dilution integrity was assessed by determining the accuracy and precision of the samples diluted with blank plasma. The accuracy (RE%) was less than 7.35%, and the precision (CV%) was less than 8.91% (Table 10). The data suggest that the concentration of OJT007 in plasma samples of greater concentrations than the ULOQ can be accurately and precisely quantified following up to 50 times dilution with blank plasma before the analysis

Table 9: *Stability of OJT007 in Rat Urine Samples for LC-MS/MS Analysis*

Stability Test	Nominal Concentration (ng/ml)	Mean Recovery% ± SD
Short-Term Stability (4 hr, RT)	15	86.74±20.58
	75	90.11± 5.49
	750	88.09± 2.16
Long-Term Stability (14 days, -80ºC)	15	101.36±4.77
	75	95.04±23.35
	750	95.99±7.21
Auto-Sampler Stability (24 hr)	15	89.73 ±8.63
	75	92.48 ± 3.54
	750	93.29 ± 3.12
Freeze Thaw (-80ºc to RT)	15	88.08± 5.62
	75	86.69± 11.38
	750	85.62± 11.43

* [n = 3; (mean ± SD)]

Table 10. *Dilution Integrity Accuracy and Precision of OJT007 in Rat Plasma*

Biological Sample	Nominal Concentration (ng/ml)	Dilution Factor	Accuracy (RE%) (n=6)	Precision (CV%) (n=6)
Plasma	5000	5	7.35	5.67
		10	6.87	3.66
		20	3.77	8.91
		50	7.03	4.95

4.3 Preformulation

4.3.1 Solubility in Common Solvents

The solubility of OJT007 was evaluated in various common solvents. The solubility of OJT007 in water, ethanol, PEG 400, labrasol, DMSO, Tween 80 was determined by the shake flask method. Solubility in general increased with the hydrophobicity of the solvent, so it is possible that hydrophobic interactions govern the solubility of the drug. The results presented in figure 14 reveal that OJT007 has poor solubility in compounds with a high dielectric constant, as exemplified by the solubility of <0.5 mg/ml in water and 1.08mg/ml in ethanol. The dielectric constant is an index of solvent polarity. Nonetheless, polarity alone doesn't explain the poor solubility of OJT007 in water as OJT007 is very soluble in DMSO (>20mg/ml). DMSO is a polar aprotic solvent, which means it does not act as a proton donor. Thus, it is possible that this characteristic prevents OJT007 from being highly soluble in ethanol or water.

4.3.2 pH solubility

The aqueous solubility of OJT007 was assessed at various pH using standard buffer solutions of pH 1.2-7, representing the range of pH encountered through the GI tract. The dissolution media were sampled after 24 hours and quantified via UPLC for OJT007 dissolved. The pH solubility data is presented in figure 15.

OJT007 is more soluble at acidic pH. OT007 is an ionizable drug in aqueous solution because it contains a basic and acidic functional group. It can exist either as an uncharged or charged form. The drug in solution with a pH below its basic pKa (3.3) will get converted into the ionized form, making it a more soluble moiety.
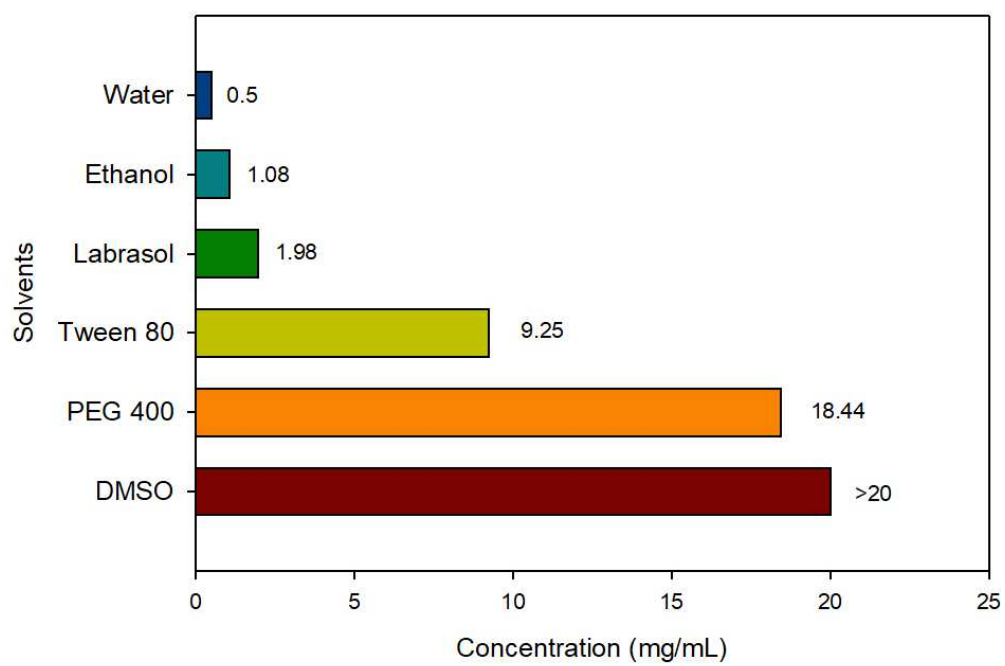
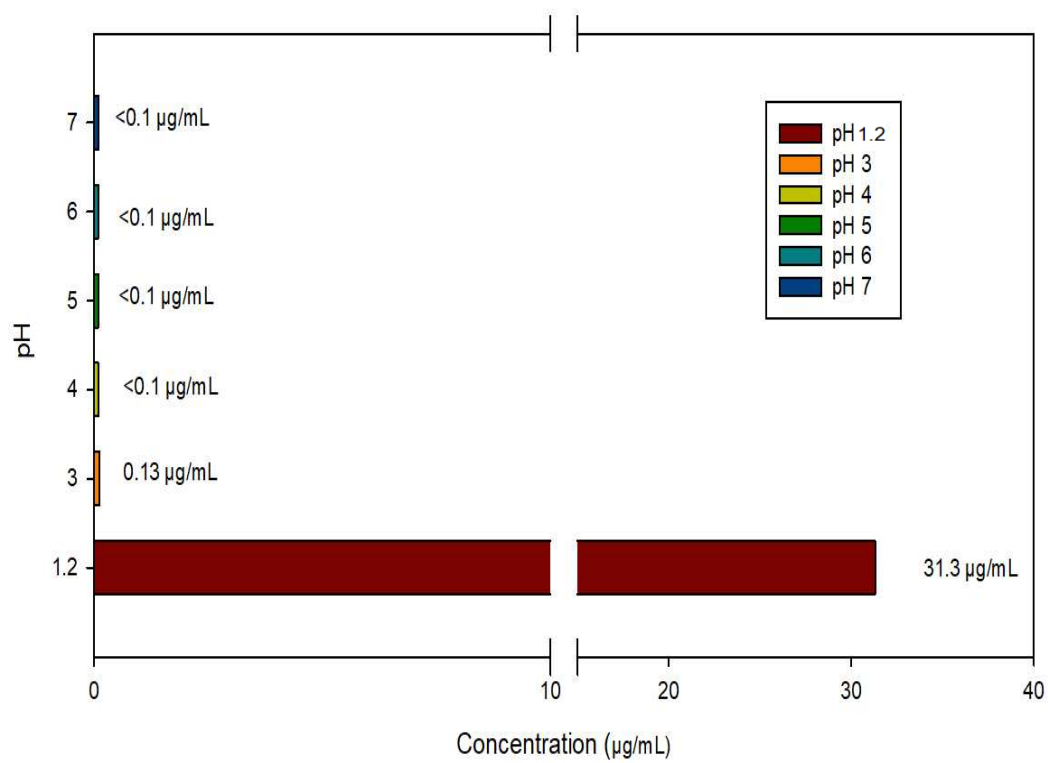**Figure 14**. *OJT007 solubility in various solvents at room temperature*

Figure 15: *OJT007 pH solubility*

4.3.3   Solution State pH Stability

Orally administered drug encounters through GI tract a varied pH environment. As such, we decided to evaluate the effect of varying pH conditions on the drug by incubating OJT007 respectively in buffers of various pH prepared according to United States Pharmacopeia (USP) guidelines. Figure 16 panel A shows a representative chromatogram of OJT007 at a wavelength of 254 nm. After incubation under acidic conditions, two new peaks eluting at 1.732 and 2.292 minutes were observed at that same wavelength (Figure 16, panel B).

Figure 17 depicts the stability of OJT007 under different pH. Degradation was rapid at pH 1.2-3, and by 0.5 hours 50% or less remained of the drug.   Likewise, by 2 hours 20% or less remained of the drug for pH 1.2-5. Therefore, there is a clear relation between pH and drug stability: the lower the pH, the higher the degradation. These results suggest that OJT007 is likely to be unstable on stomach pH and special formulation considerations must be accounted.

We hypothesize that this is caused due to OJT007 being a Schiff base. OJT007 contains an imine functional group that could be prone to acid-catalyzed hydrolysis (Scior & Garces-Eisele, 2006). Figure 18 shows the proposed degradation pathway in OJT007 based on the drug structure. In the hydrazone cleavage catalyzed by acidic pH, a proton attacks the imino nitrogen atom leading to the hydrolysis of the imino-carbon bond. The result of this hydrolysis is an aldehyde and a hydrazine.
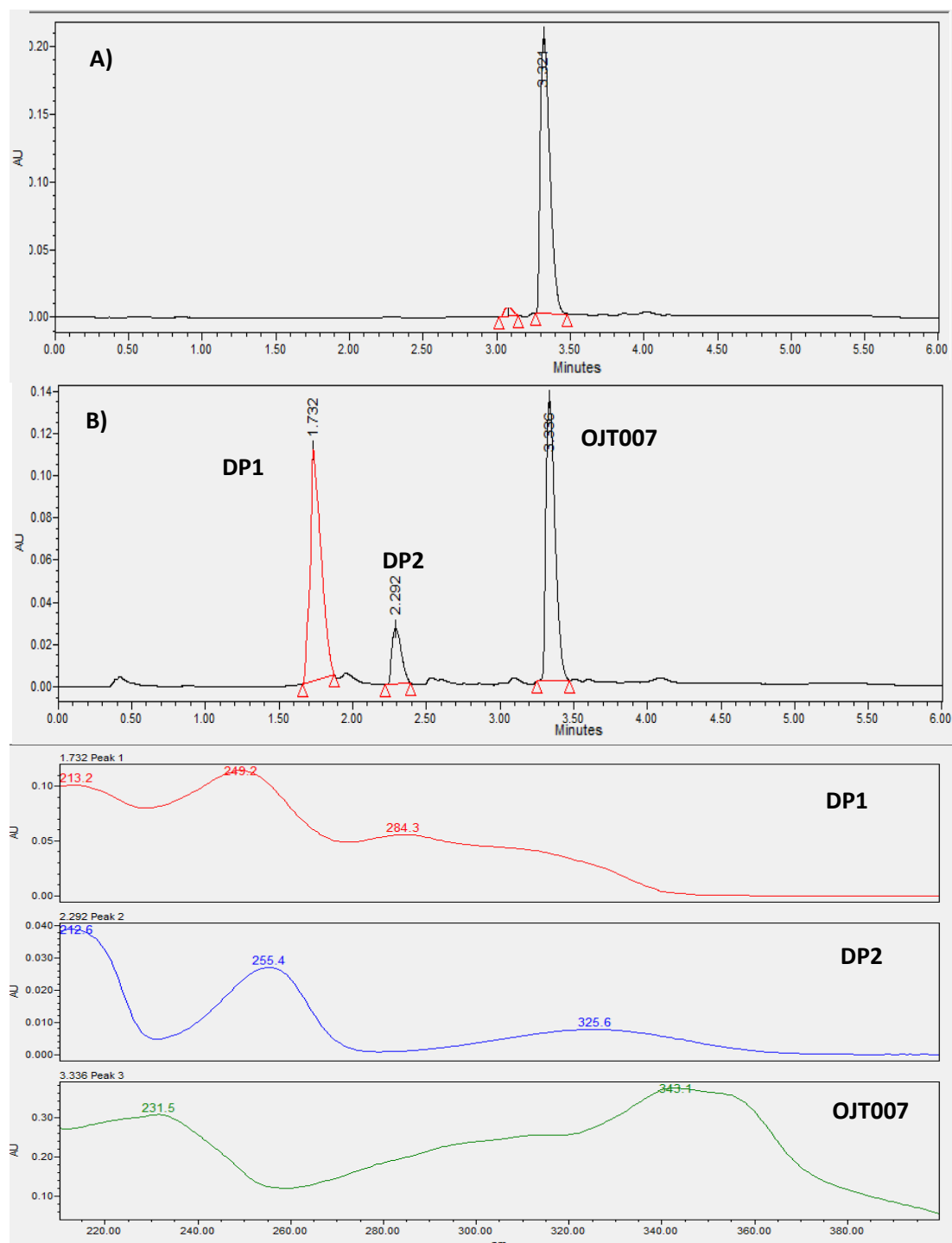
Figure 16: *A) Representative chromatogram for OJT007 at 254 nm. B) Representative chromatogram and Spectra for OJT007 at 254 nm after 1 hour incubation at pH 1.2*
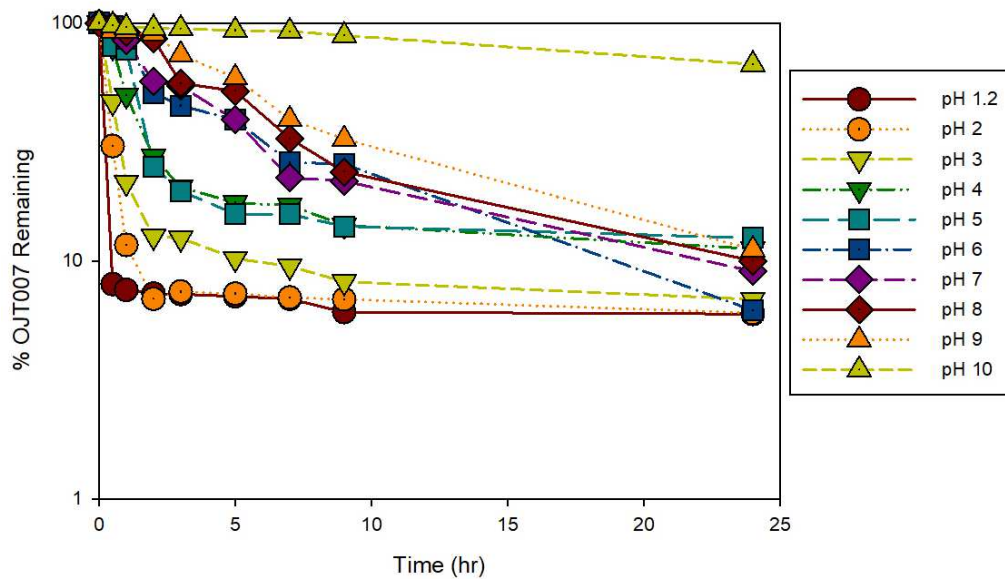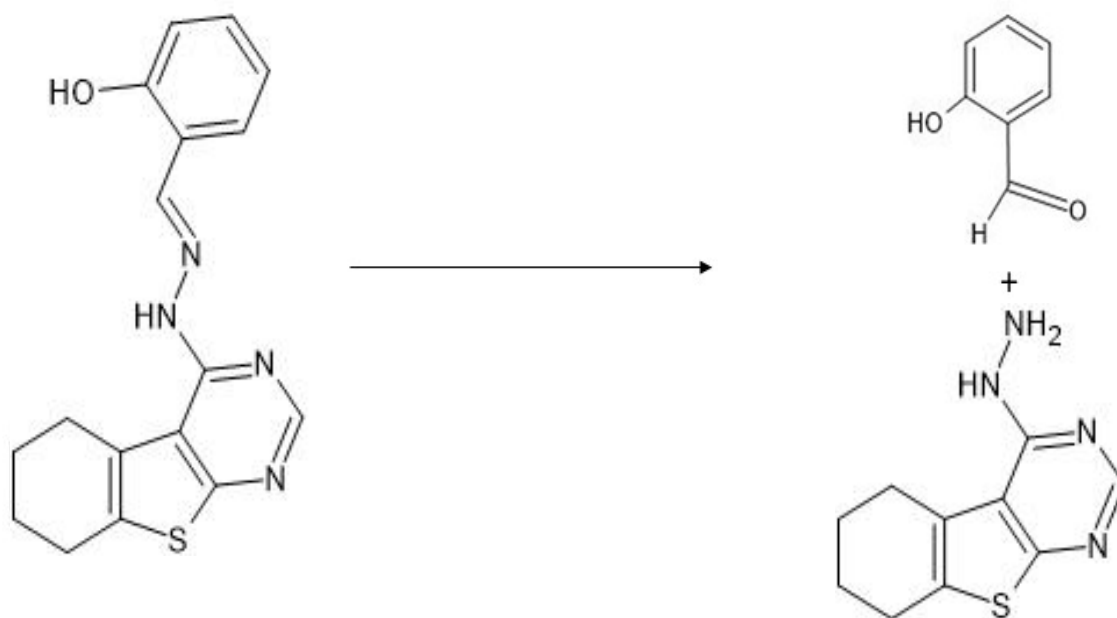
Figure 17*: Stability of OJT007 at pH 1.2-10.*

Figure 18: *Proposed degradation mechanism: Hydrazone hydrolysis of OJT007.*

4.3.4 PKa measurement

The pKa values for OJT007 were measured using the UV-metric method with the SiriusT3 and compared to the pKa values calculated by ACD/ChemSketch. For the UV-metric method to be successful, the ionizable groups must be located near a chromophore such that changes in protonation state will modulate the UV absorbance spectra. For OJT007, three pKa values were calculated by ACD/ChemSketch 8.7 (acid), 5.8 (base) and -3.3 (base). This latter pKa is outside the operating range in the SiriusT3. The Sirius T3 measured 10 (acid) and 3.3 (base).

4.3.5 Cosolvent formulation

The ideal vehicle for intravenous dosing is normal saline. Nonetheless, using saline alone was not an option for this project due to OJT007 low water solubility. The low solubility of OJT007 can be improved by incorporating it into a water-miscible cosolvent in which it has a good solubility. An important consideration during the formulation of OJT007 was preparing a formulation with a reasonable concentration to ensure that during drug administration, animals were not dosed more than 5 mL/Kg (IV Bolus) or 10 mL/Kg (PO). Furthermore, a cosolvent system suitable for intravenous administration must resist precipitation of the drug upon dilution with intravenous (IV) fluids or blood.

Various co-solvent systems with varying compositions and ratios of solvents were prepared and evaluated with OJT007 concentrations ranging from 1 – 10 mg/mL. Based on the solubility data, DMSO, PEG 400, Tween 80, and labrasol were selected as potential cosolvents for the formulation. The robustness of each system was tested by

diluting with different ratios of normal saline or water to evaluate OJT007 precipitation within 12 hours. The optimal cosolvent formulation was found to be PEG 400 57%, Tween 80 29%, DMSO 14%. This formulation is to be diluted with normal saline or water to a final concentration of 2.5 mg/mL

4.4 Plasma Protein Binding (PPB)

The plasma protein binding of OJT007 was evaluated at different concentrations using the ultrafiltration method. The fraction of OJT007 bound to plasma protein binding had a mean value of 99.11±1.18%. Binding to plasma proteins is affected by the chemical structure of the drug, the pKa of the substance, and the pH of plasma. Possibly, OJT007 binds preferentially to alpha-1 acid glycoprotein, given its basic nature.

OJT007 high PPB values may have implications on the drug disposition. PPB plays a crucial role in the pharmacokinetics and pharmacodynamics of drugs. Free drug hypothesis states that only unbound drug is available at the site of action for pharmacological activity (Bohnert & Gan, 2013). Drug molecules in vivo are bound reversibly to proteins in plasma (and in tissues), or they are unbound. Free drug molecules diffuse across the membranes to interact with the intended therapeutic target or other sites other than the therapeutic target, which could cause toxicity. Thus, PPB influences the distribution of a drug from blood to tissues and from tissues to site of action.

High plasma protein binding may predispose OJT007 to drug-drug interactions when co-administered with other high plasma protein-bound drugs due to drug displacement. Drug-drug interactions may have clinical implications in terms of efficacy and exposure

for drugs with narrow therapeutic index intravenously administered and for high extraction ratio intravenously administered drugs (Benet & Hoener, 2002). Following intravenous administration, total drug clearance is independent of plasma protein binding for high extraction drugs (CL= Q_H). Although average total drug concentrations and AUC are unaffected by changes in protein binding (AUC$_{IV}$= Dose/ Q_H), unbound drug concentrations are proportional to changes in plasma protein binding. (AUC$_{Unbound\ IV}$ = f_U x AUC$_{IV}$)(Benet & Hoener, 2002; Smith et al., 2010).

4.5 Metabolism of OJT007 in CYP and UGT reaction systems

CYP450 is a superfamily of enzymes that is responsible for the metabolism of most marketed drugs, and UDP-glucuronosyltransferases (UGT), is an enzyme family that conjugates the sugar molecule UDPGA to alcohols, acids, and basic amines. Both UGTs and CYPs represent more than 80% of the metabolic pathways of drugs (B. Wu et al., 2011); Thus, we evaluated CYP and UGT mediated metabolism of OJT007.

4.5.1 CYP Mediated Metabolism

Before incubation, a single peak eluting at 3.269 minutes corresponding to OJT007 was observed in UPLC analysis (Figure 19, A). After incubation, three additional peaks were observed at retention times of 2.041, 2.583, and 2.946 minutes in UPLC analysis (Figure 19, B). The UV spectra of these additional peaks were similar to that of OJT007, suggesting that the skeleton of these metabolites is similar to that of OJT007 (Figure 19, C).

`**Table 11.** *Plasma Protein binding of OJT007 in Rat Plasma*

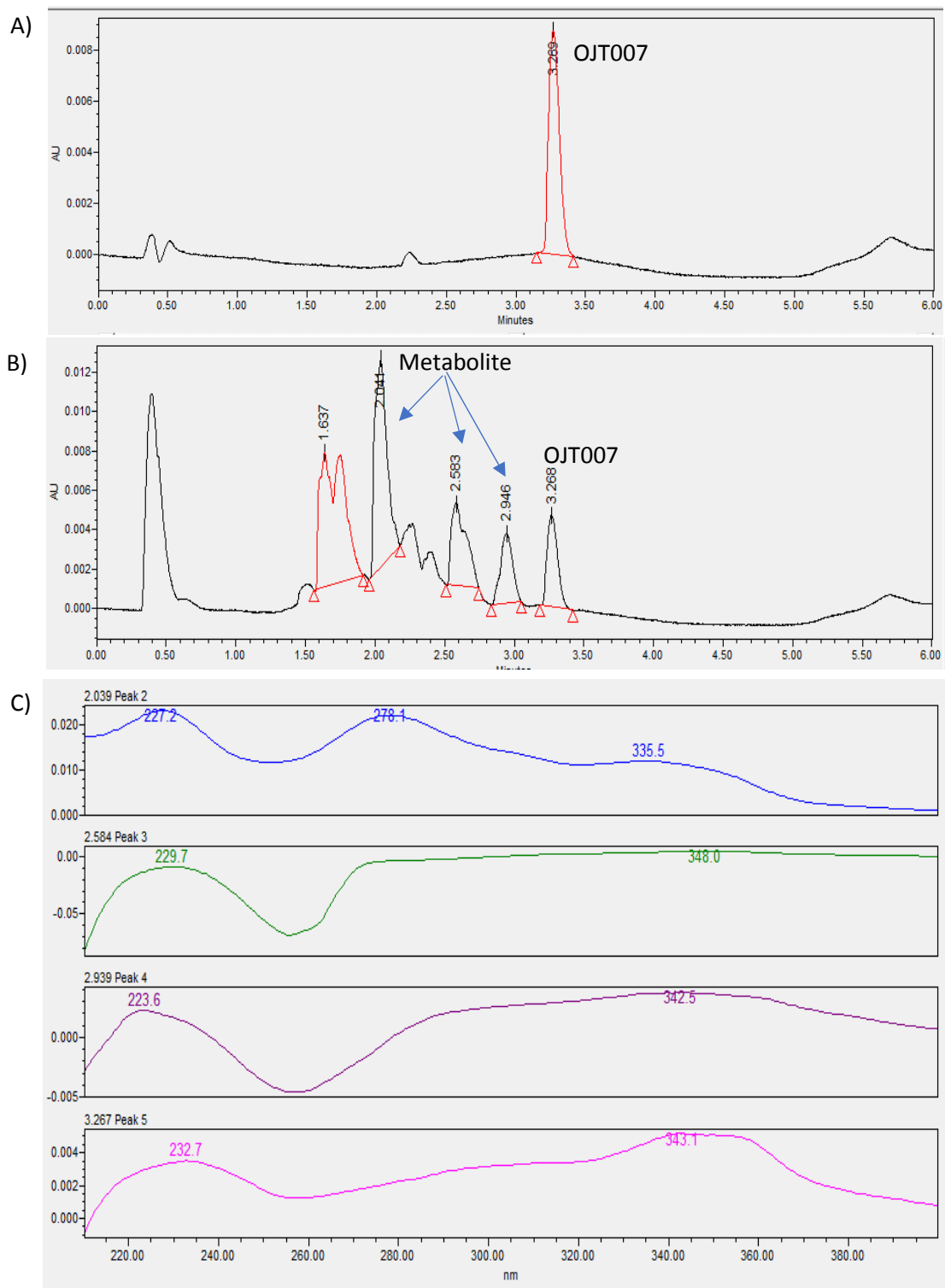| Concentration (µg/mL)	Bound Fraction (%) ± SD (n=3)
50	99.73±0.30
75	99.84±0.50
100	97.75±1.83

Figure 19: *A) Representative chromatogram of OJT007 B) Representative chromatogram of OJT007 and oxidation metabolites. B) UV spectra of OJT007 and oxidation metabolites*

4.5.1.1 Oxidation Metabolite Identification

LC-MS/MS Identification of Oxidation Metabolites

LC-MS/MS analysis was used to confirm the identity of the newly eluted peaks. Targeted metabolite identification takes advantage of the extensive understanding of metabolic enzymes and the metabolic pathways they could contribute. Hydroxylation reactions are very common in drugs containing aromatic rings or aliphatics (saturated or unsaturated in their chemical structure (Zhu et al., 2017). Q1MI scan (Figure 20, A-C) identified a pseudo-molecular ion at m/z 341, indicating hydroxylation at 1.66, 1.74 and 1.96 minutes.

In neutral loss scan, ions are scanned on Q1, fragmented in Q2, and then Q3 scans changes in mass which correspond to a set neutral loss. In other words, neutral loss scan displays the spectrum of all parent ions which lose a selected neutral loss fragment. From the product ion spectrum of OJT007 standard, the main product ion is m/z 205, corresponding to the loss of 120 Da. Thus, we performed a neutral loss scan for 120. This procedure (Figure 21) indicated the presence of OJT007 itself with an m/z of 325, plus one metabolite which eluted at 1.74 minutes with an m/z of 341. This finding confirmed that the peak eluting at 1.74 minutes corresponds to a mono-oxidative metabolite. In addition, this suggests that the oxidation occurs in the 5,6,7,8-Tetrahydro[1]benzothieno[2,3-d]pyrimidin-4-amine portion of the molecule.
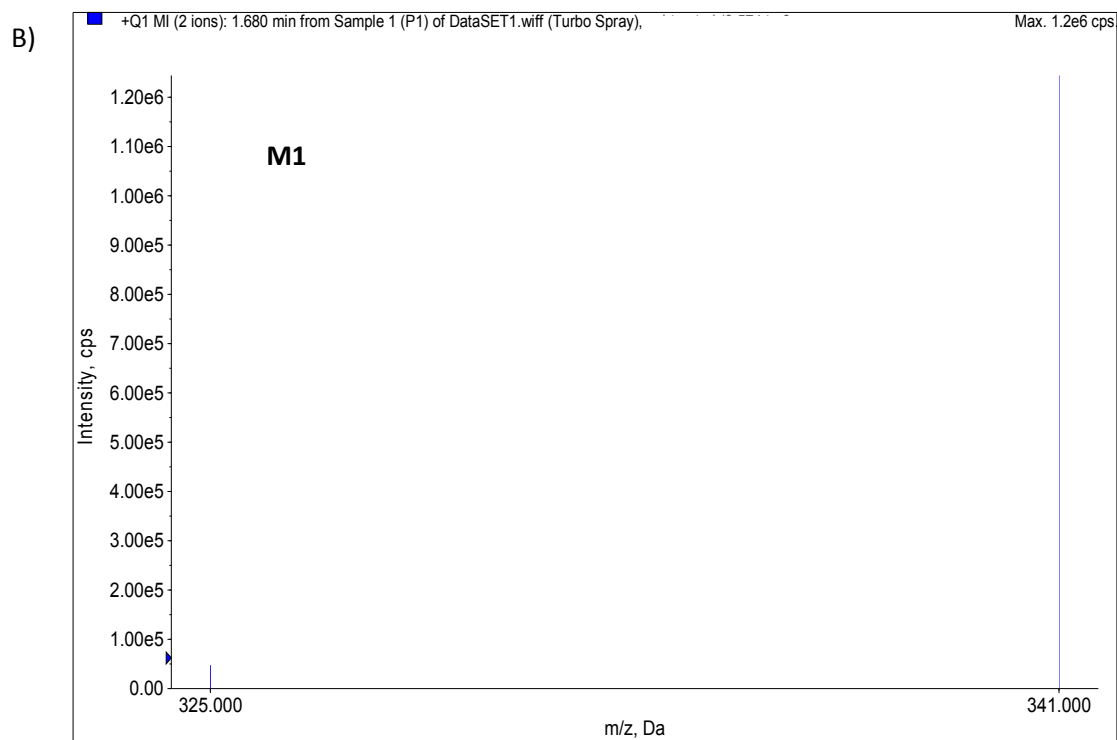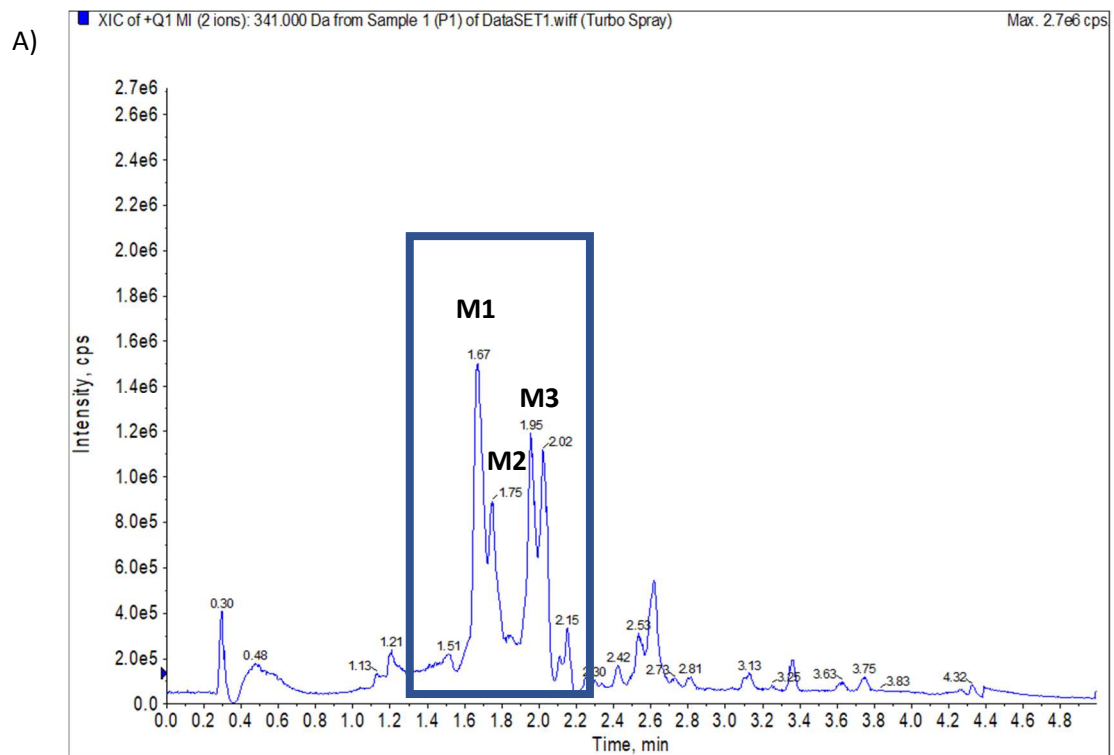
A NL scan (Figure 22) was then performed for 136 Da (120 plus 16) to screen for metabolites obtained by hydroxylation on the neutral fragment. Neutral loss scan evidenced three peaks eluting at 1.78, 1.96 and 2.17 minutes(Figure 22, A). NL spectra

for the peaks eluting at 1.78 (Figure 22, B), and 1.96 (Figure 22, C) showed ions with m/z 341, which is 16 Da higher than the addition ion of OJT007, confirming both peaks to belong to metabolites. The neutral loss scan suggests that oxidation for the metabolite eluting at 1.96 occurs in the phenol portion of the molecule. On the other hand, it is possible that the same neutral loss that gave rise to the peak at 2.16 (parent molecule), gave rise to the peak eluting at 1.78 minutes. Interestingly neutral loss scan did not show the presumed metabolite at 1.66 min, which could possibly indicate hydroxylation does not occur at the phenol ring.

Precursor ion scans yield as a result the spectrum of all parent ions which produce the same product ion in their spectrum. As such, a precursor scan for m/z 221 (m/z 205+16) was performed as this would indicate the presence of a metabolite hydroxylated in the 5,6,7,8-Tetrahydro[1]benzothieno[2,3-d]pyrimidin-4-amine portion (bottom half) of the molecule. Figure 23 shows a peak at 1.74 and abundant ions at m/z 341 suggesting hydroxylation occur in the bottom half of the molecule. In addition, this precursor ion scan confirms the observed neutral loss of 120.

As a final confirmation step, product ion analysis (figure 24, A-D) showed a pseudo-molecular ion for the metabolites at m/z 341 $[M+H]^+$, which is 16 Da higher than that of OJT007 (which is m/z 325), indicating hydroxylation. The spectra for the peak eluting at 1.66 (Figure 22, B) shows a major fragment at 221, which is 16 Da higher than the major fragment for OJT007. A similar major fragment at m/z 221 was observed for the peak eluting at 1.74 minutes. This fragmentation suggests that hydroxylation occur potentially in the bottom half of the molecule. The MS/MS spectra for the peak eluting at 1.96 (Figure 24, D) MS/MS spectra show a major fragment at m/z 205, which is similar

to the major fragment ion of OJT007. Likewise, the spectra for the peak eluting at 1.96

shown a fragment at 138, suggesting that hydroxylation potentially occur in phenol ring.

In MRM at m/z at m/z 341 → 221(Figure 25), the high intensity for the peaks eluting at

1.66 and 1.74 may further confirm hydroxylation occur on the bottom half of the

molecule. Based on these spectra, in figure 26 we have proposed possible metabolite

structures. The proposed structure for M1 and M2 comprehend a mono-hydroxylated

metabolite with hydroxylation occurring on the bottom half of the molecule while the

proposed structure for M3 corresponds to a mono-hydroxylated metabolite with oxidation

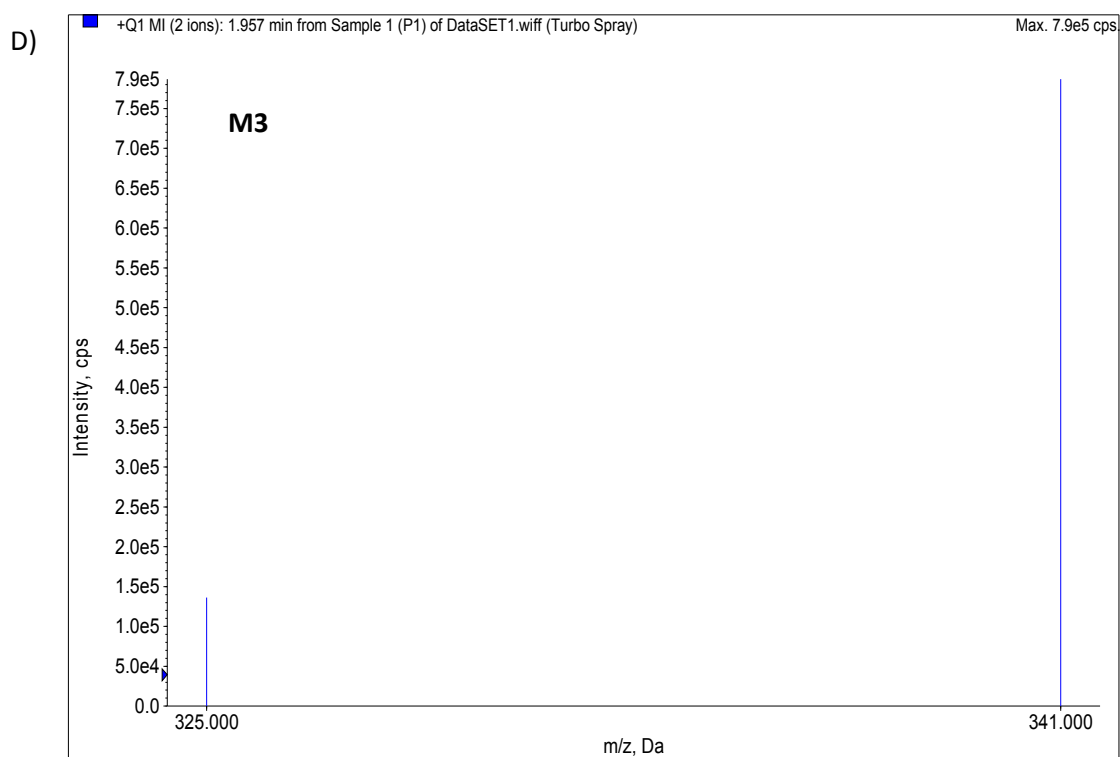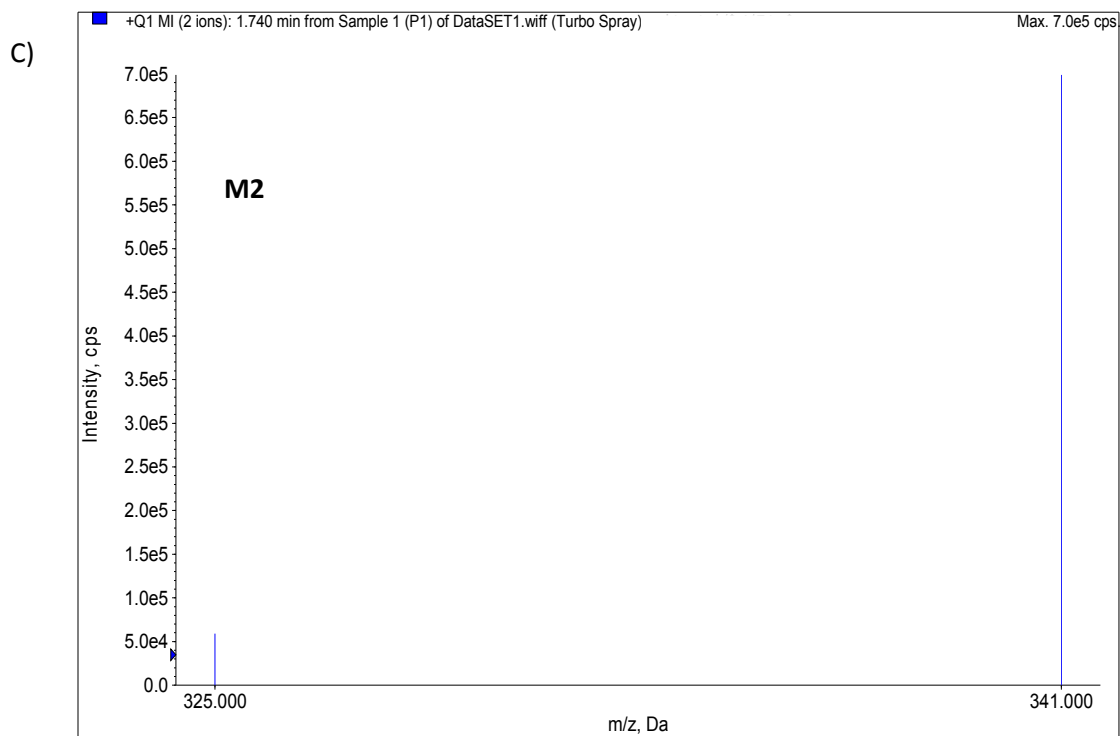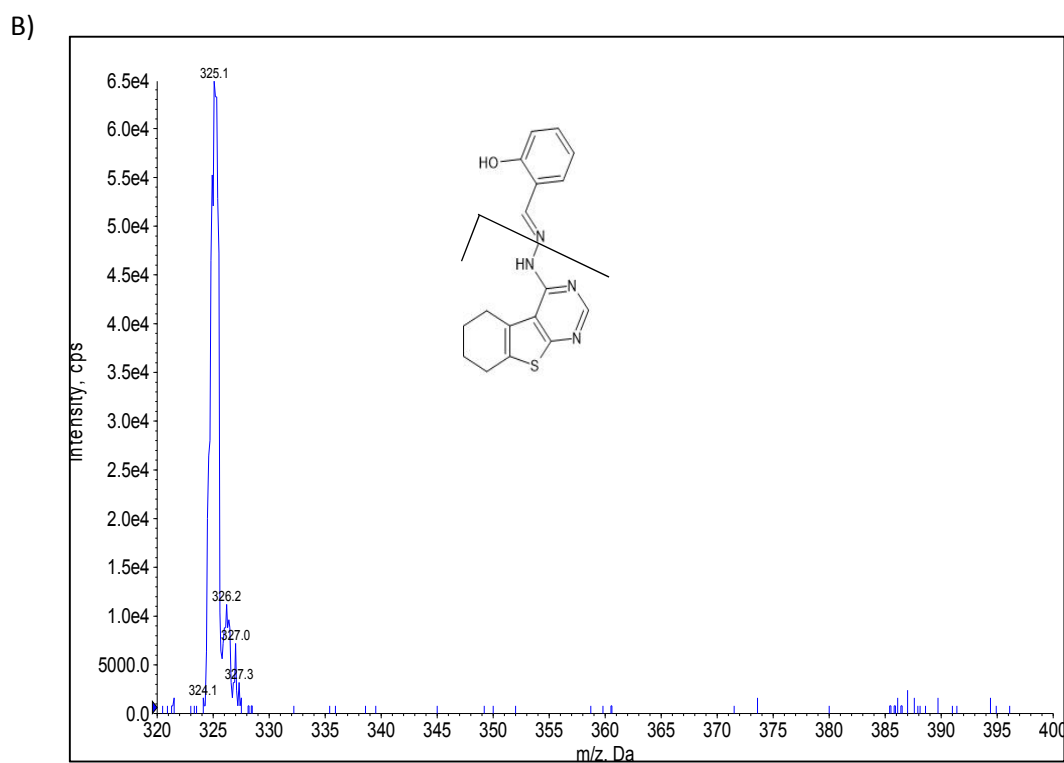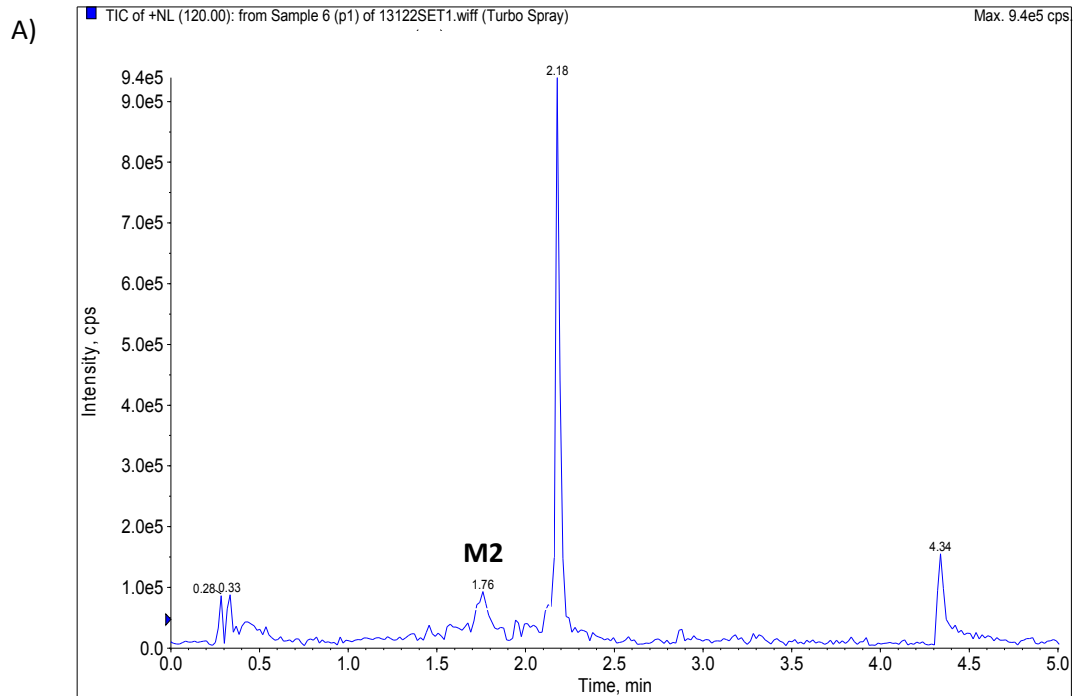occurring in the aromatic ring portion of the molecule.

A)

B)

C)

+Q1 MI (2 ions): 1.740 min from Sample 1 (P1) of DataSET1.wiff (Turbo Spray)   Max. 7.0e5 cps.

D)

+Q1 MI (2 ions): 1.957 min from Sample 1 (P1) of DataSET1.wiff (Turbo Spray)   Max. 7.9e5 cps.

Figure 20: *Q1MI Spectra for OJT007 oxidation metabolites A) 1.66 min B) 1.74 min and C) 1.96 min*
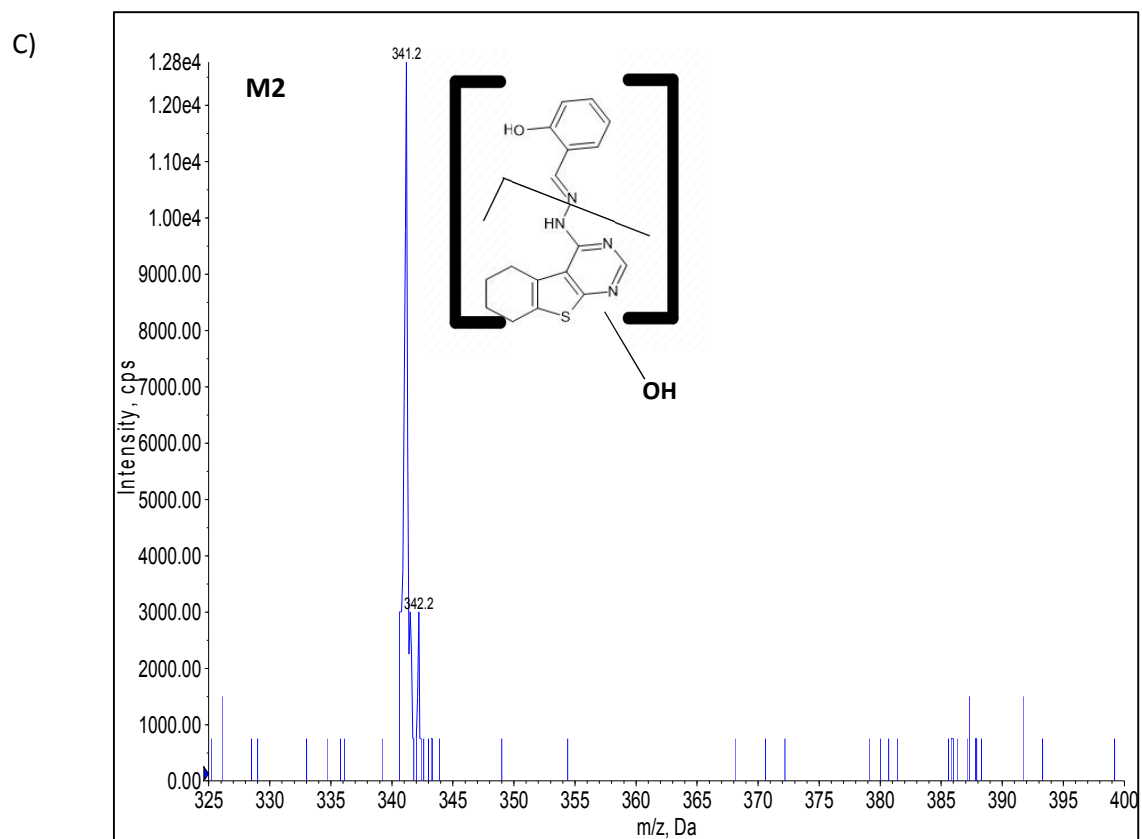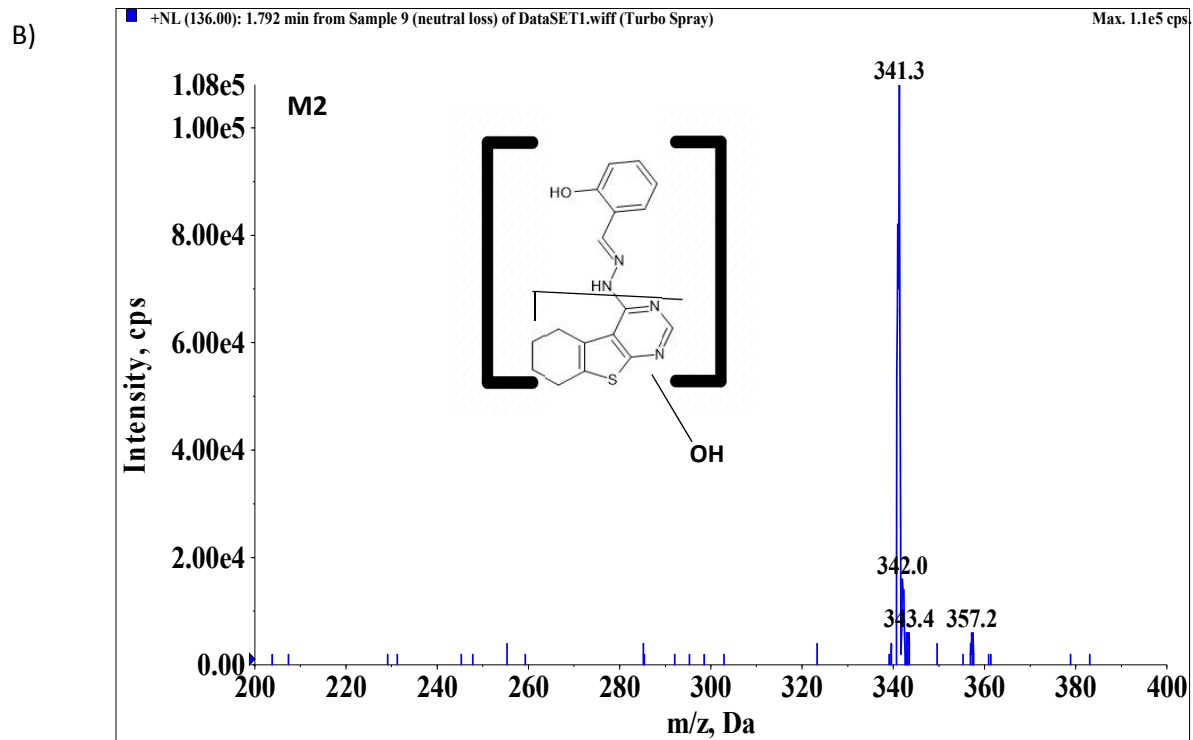
A)

B)

C)

Figure 21: *A) Neutral loss of 120 Da Chromatogram B) Spectra for OJT007. C)Spectra for M2*

A)

TIC of +NL (136.00): from Sample 9 (neutral loss) of DataSET1.wiff (Turbo Spray)   Max. 3.2e6 cps.

B)

+NL (136.00): 1.792 min from Sample 9 (neutral loss) of DataSET1.wiff (Turbo Spray)   Max. 1.1e5 cps.
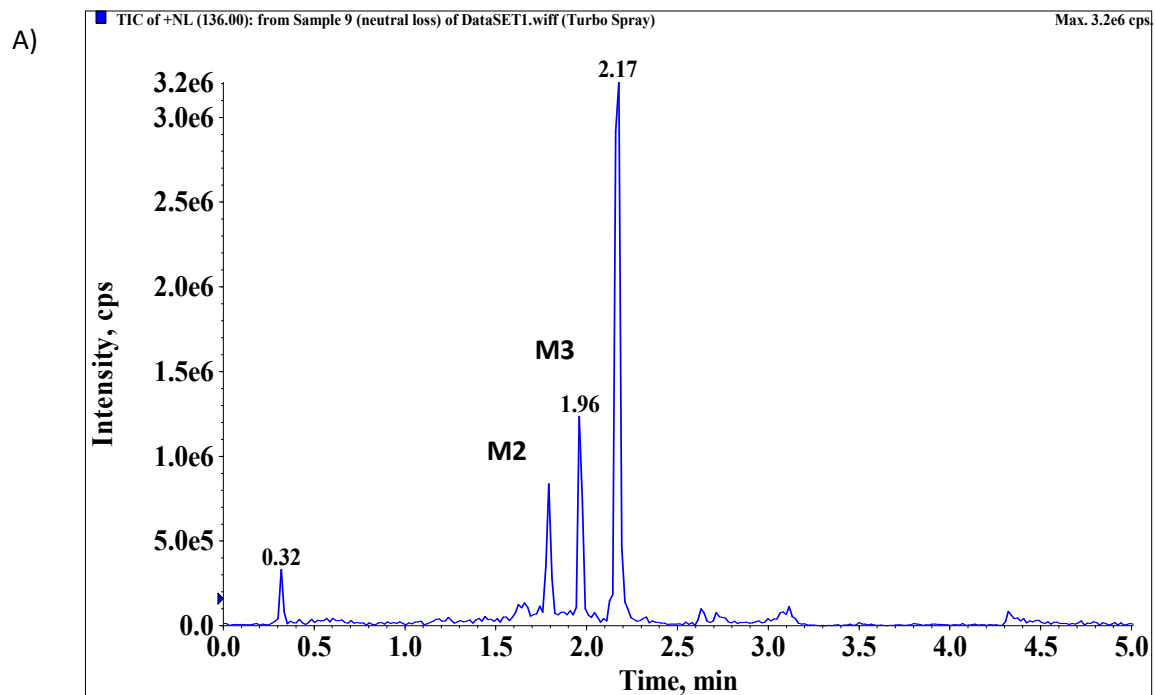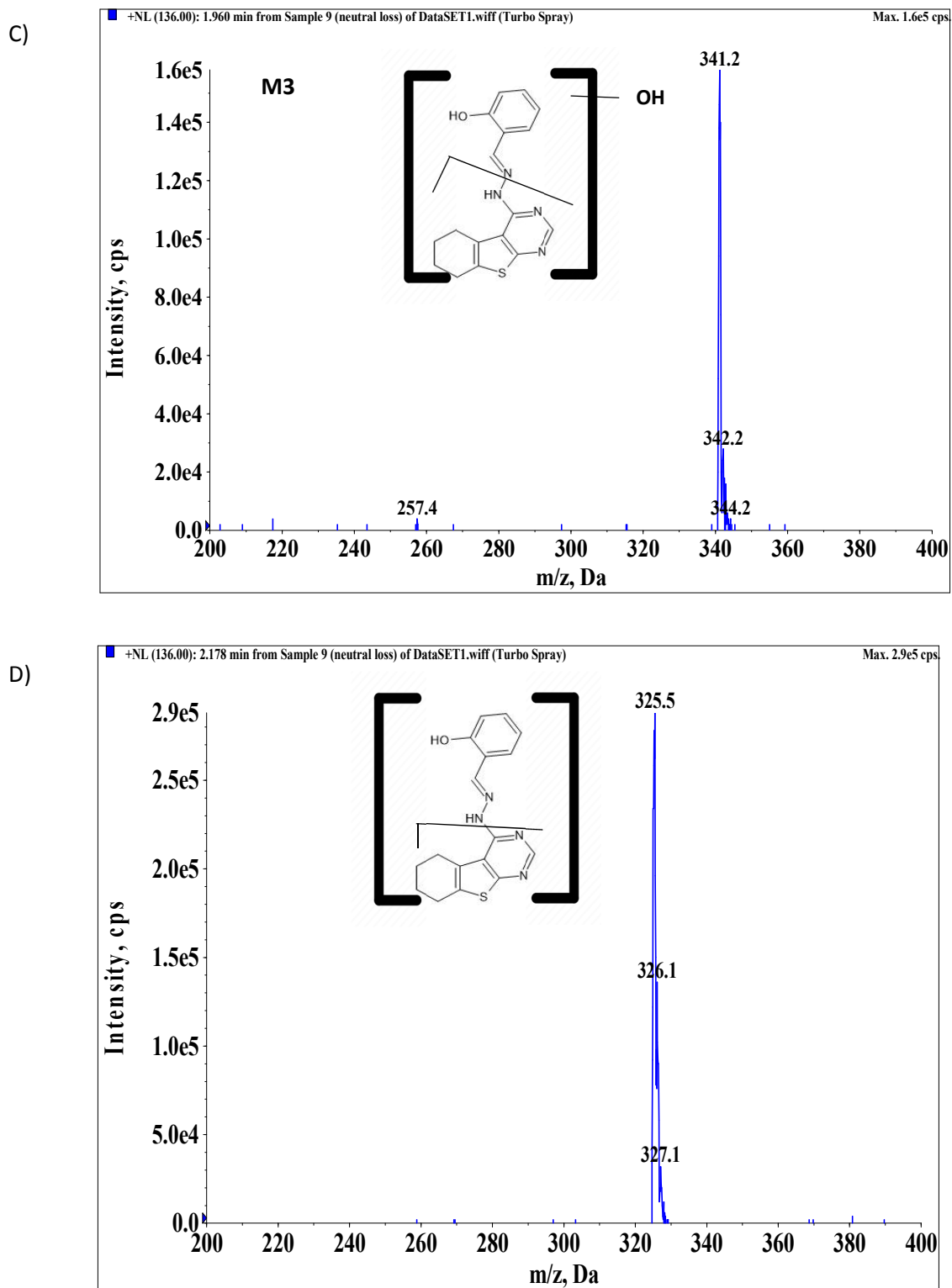
Figure 22: *Neutral loss of 136 A) chromatogram and Spectra at B) 1.74 minutes C) 1.96 minutes and D) 2.17 minutes*

A)

B)

Figure 23: *A) Precursor ion scan of 221 Da chromatogram. B) PI scan spectra for M2*
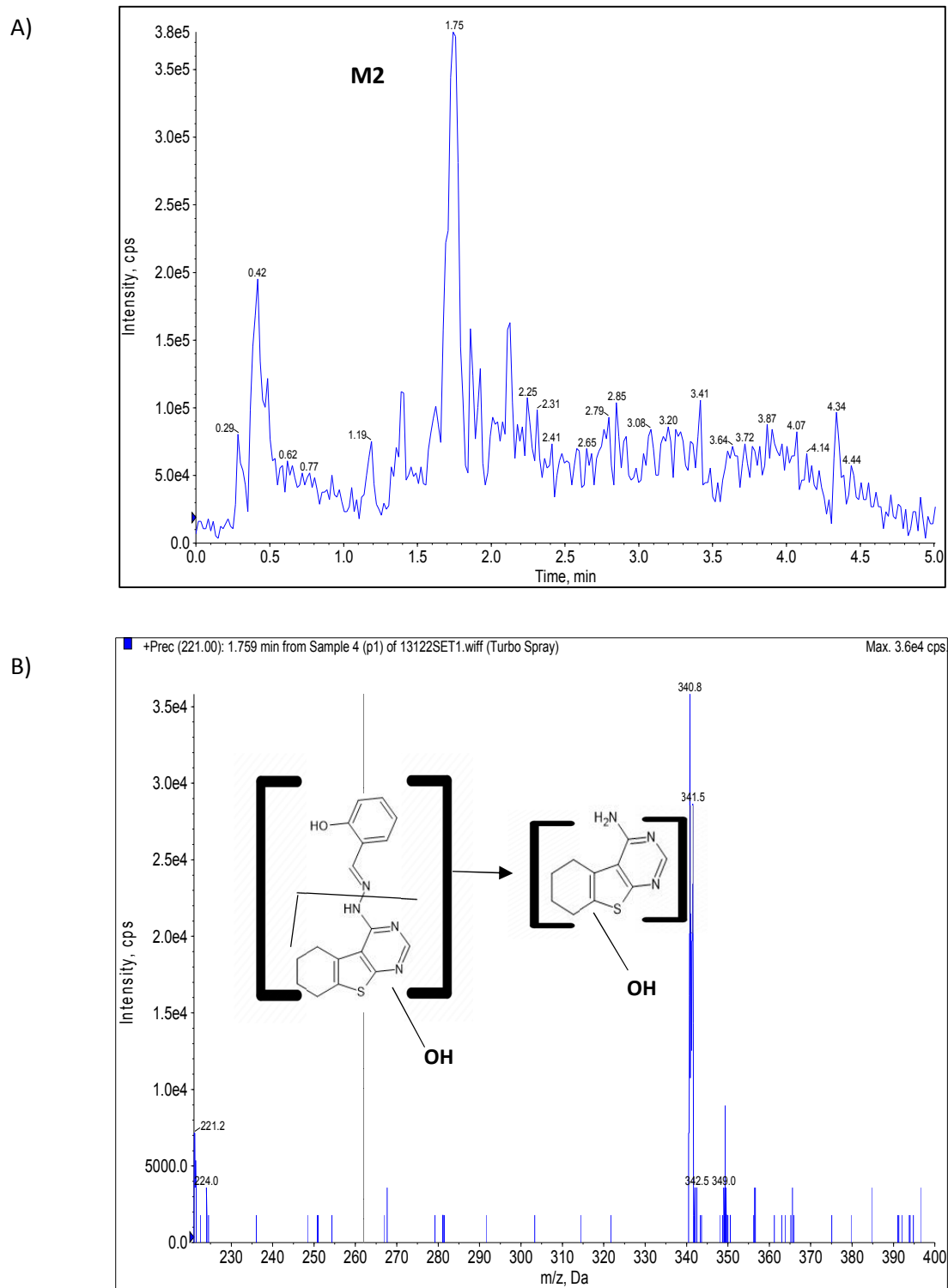
A)
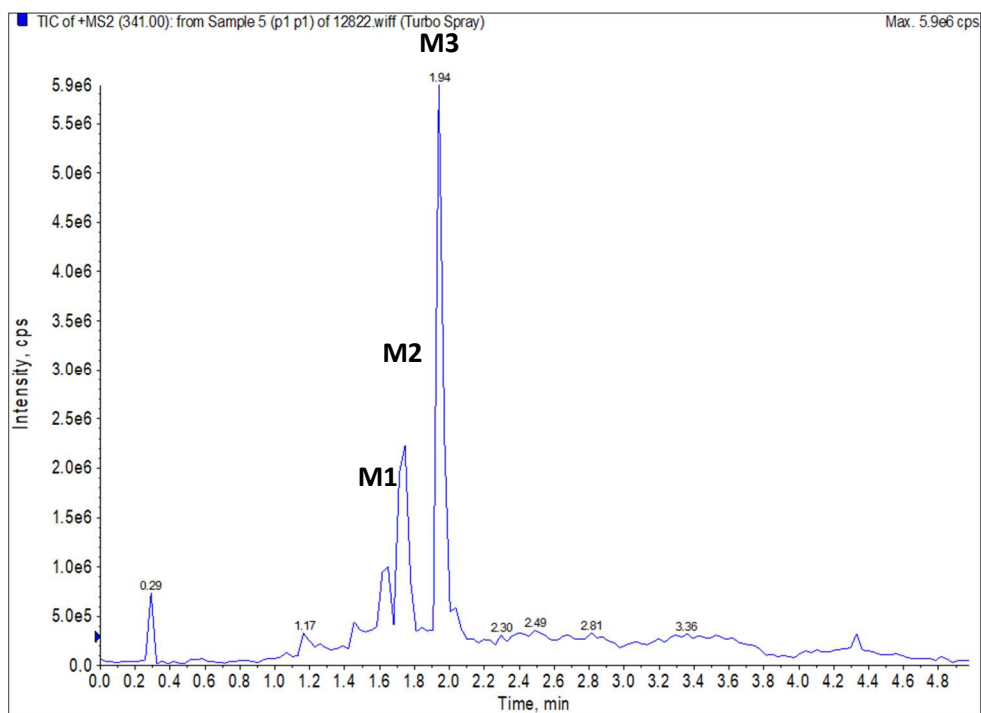
B)
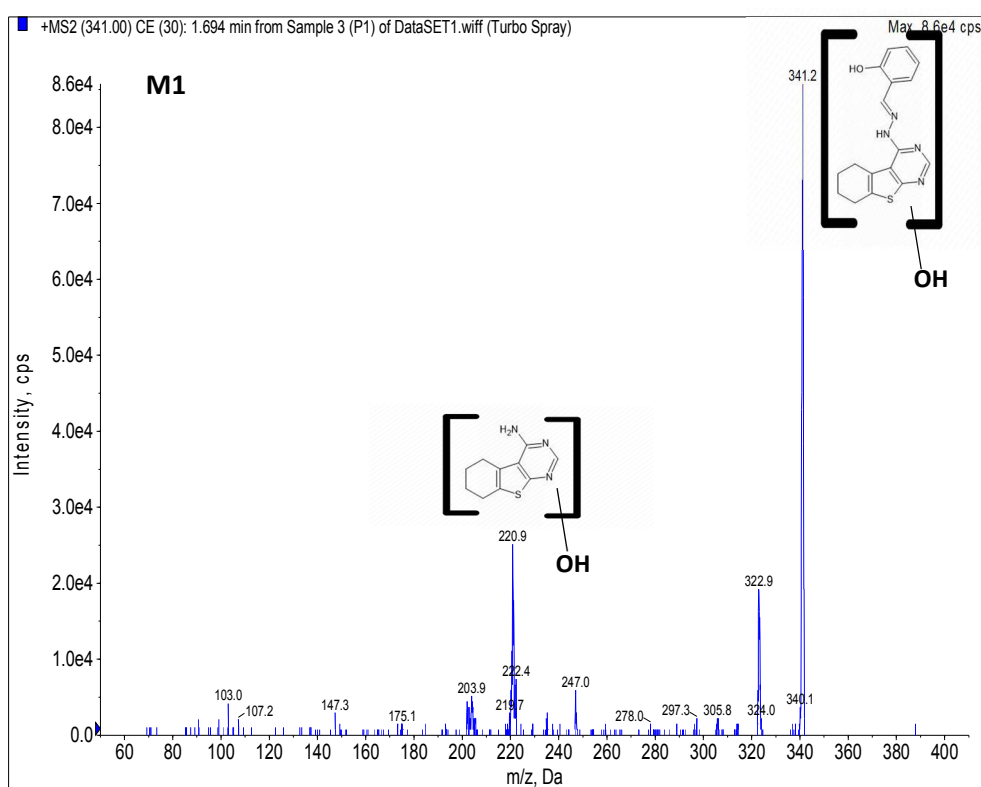
Figure 24: *A) MS/MS Chromatogram. B) MS/MS Spectra of M1. C) MS/MS Spectra of M2. D)MS/MS Spectra of M3.*

Figure 25: *Representative MRM chromatogram of OJT007 oxidation metabolites at m/z 341 → 221*

Figure 26: *Proposed Structure for M1, M2 and M3.*

4.5.1.2 Metabolic Stability of Oxidation Metabolites

In a typical microsomal stability assay, protein concentrations are kept below 2 mg protein/ml (to prevent nonspecific binding) with incubation times below 1 hour (to prevent loss of enzyme activity). In addition, measuring the dep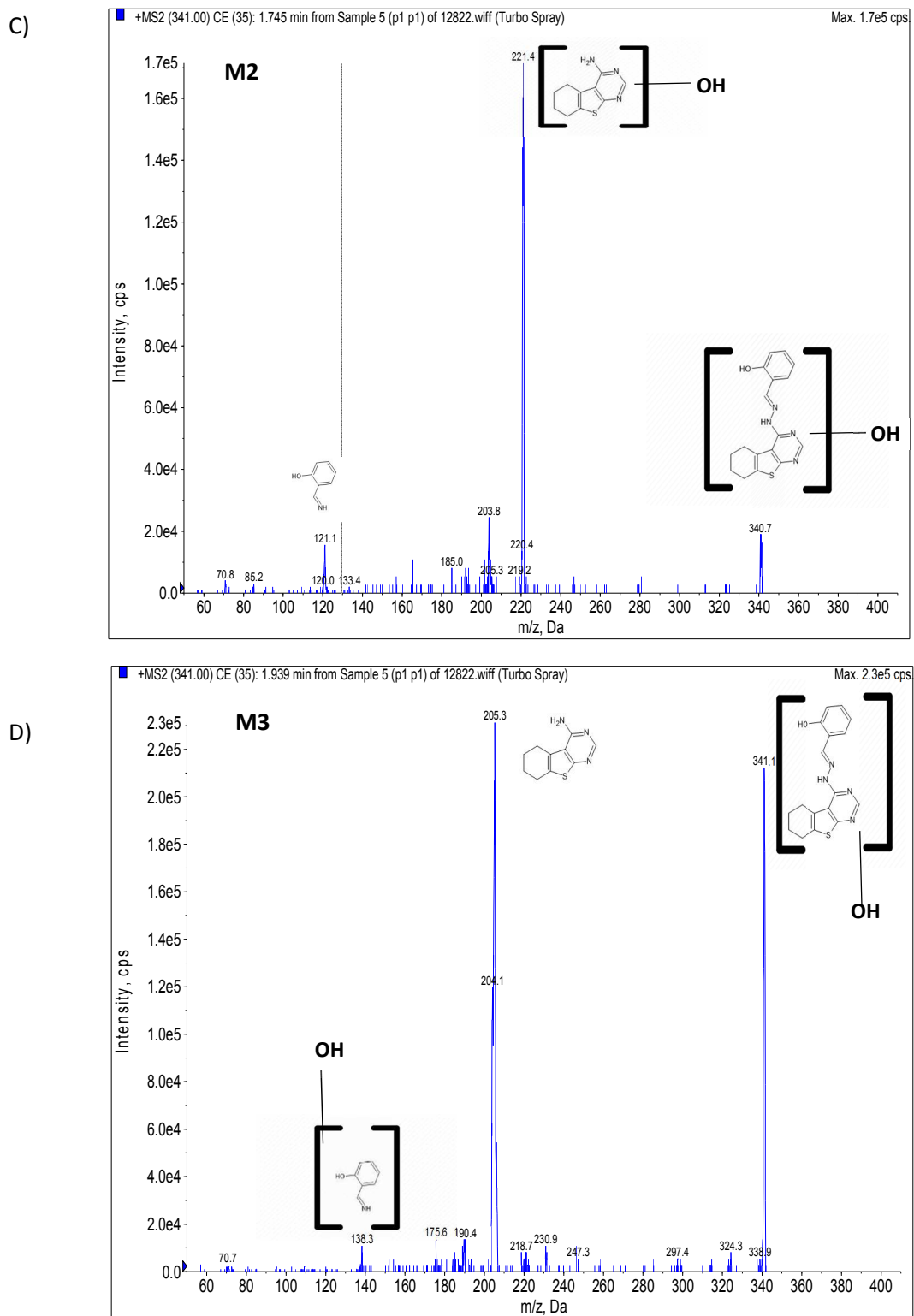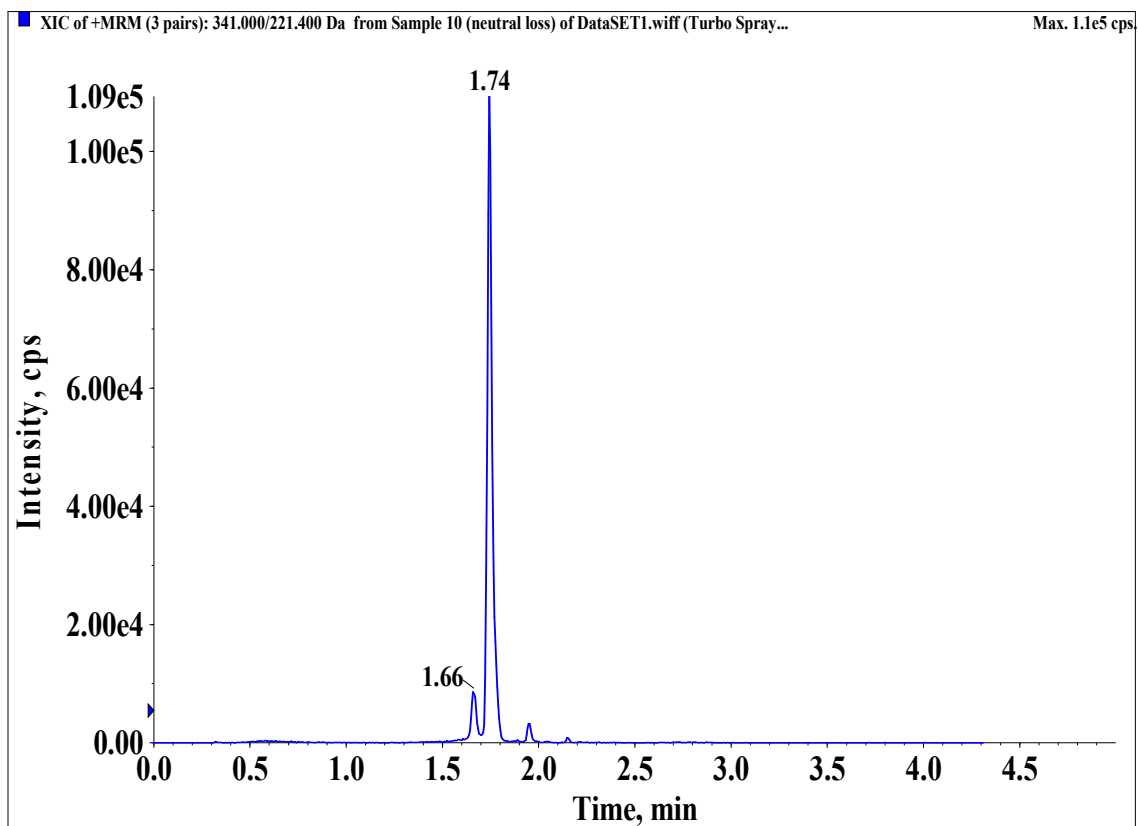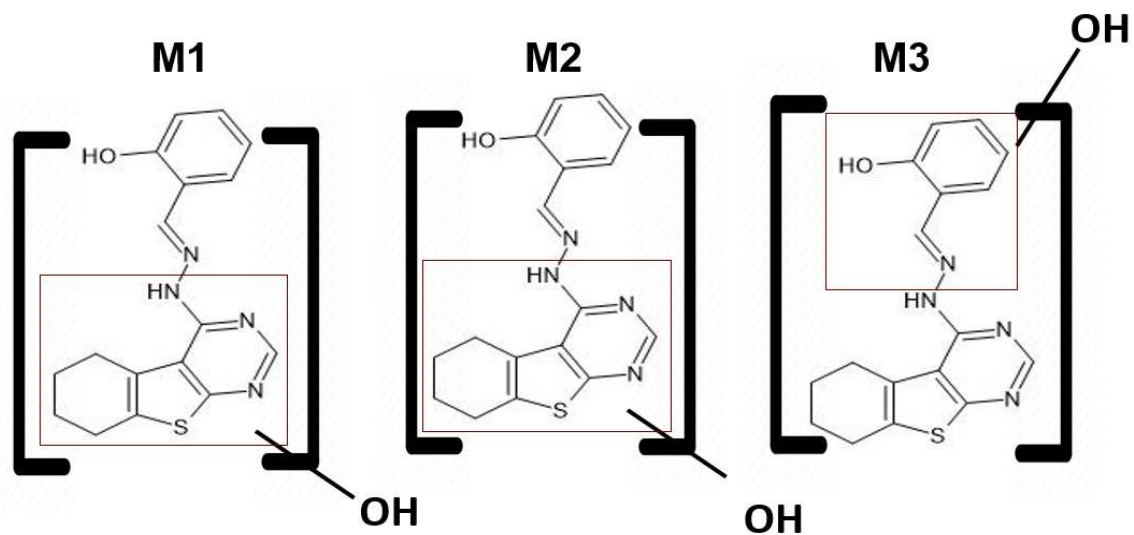letion of the parent drug entails at least 10-15% turnover to make a reliable measurement. This requirement is based on the bioanalytical method having accuracy and precision values within that range (Di & Obach, 2015).

In our study, OJT007 displayed no significant turnover of the parent drug with enzyme concentration below 10 mg protein/ml; thus, we used a high enzyme concentration. In figure 27 are shown the levels of OJT00 remaining after incubation with SD rat liver microsomes for different times. The biphasic profile is due to loss of enzyme activity due to long incubation time. Nonetheless, incubation for less than 1 hour yielded insufficient metabolism to conclude metabolic turnover. Furthermore, substrate depletion was observed in the incubation without cofactor; However, this may be attributed to the instability of OJT007 at pH of 7.4, which is consistent with our pH stability results.

For screening purposes, the metabolic half-life was determined using a single time point analysis (Di et al., 2004) based on first-order reaction kinetics. The equation for the calculation of half-life from % remaining of the parent at a given time is shown in equation 8.

The half-life for OJT007 is 1.28 hour making OJT007 a stable compound (Słoczyńska et al., 2019). The CYP metabolic screening results suggested that Phase I metabolism, though happening, may not be playing an important role in OJT007 metabolism.

4.5.2 UGT Mediated Metabolism

Rapid conjugation in the intestine and liver is primarily responsible for the poor oral bioavailability of phenolics. Glucuronidation of phenolics generally occurs at the nucleophilic –OH attached to the aromatic ring (O-glucuronidation). In an OJT007 molecule, there is one hydroxyl group that may serve as the glucuronidation site. Thus, we evaluated glucuronidation in OJT007.

Figure 28, panel A shows a representative chromatogram of OJT007 before microsomal incubation. After microsomal incubation, an additional peak was observed at 2.020 minutes (Figure 28, A). The UV spectra of this newly eluted peak were similar to that of OJT007 (Figure 28, B), suggesting that the skeleton of the additional peak was similar to that of OJT007. This newly eluted peak is tentatively identified as OJT007 glucuronide.
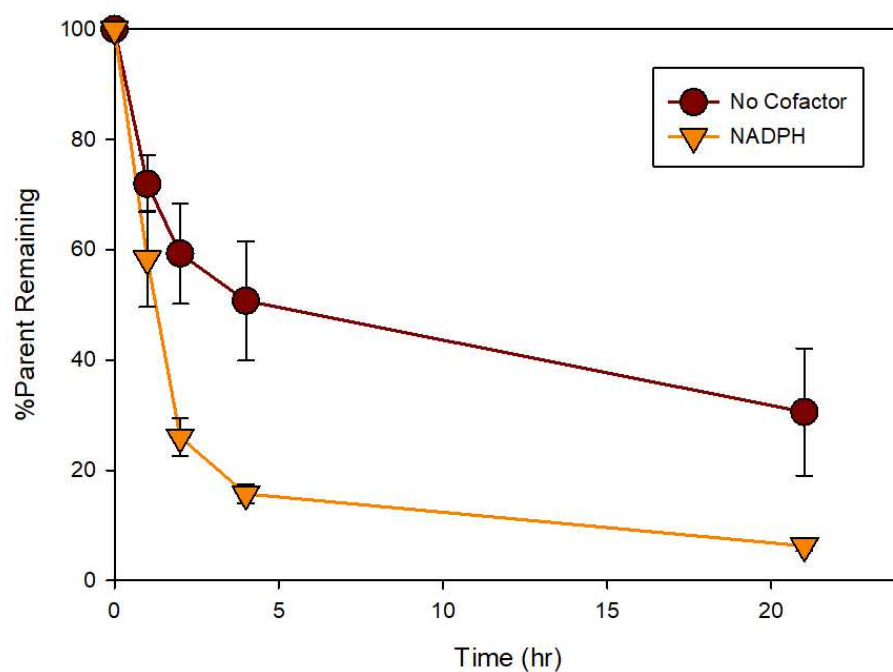
Figure 27: *Metabolic stability of OJT007. Levels of OJT007 remaining after incubation with SD rat liver microsomes for various times shown as % of starting amount at time 0*
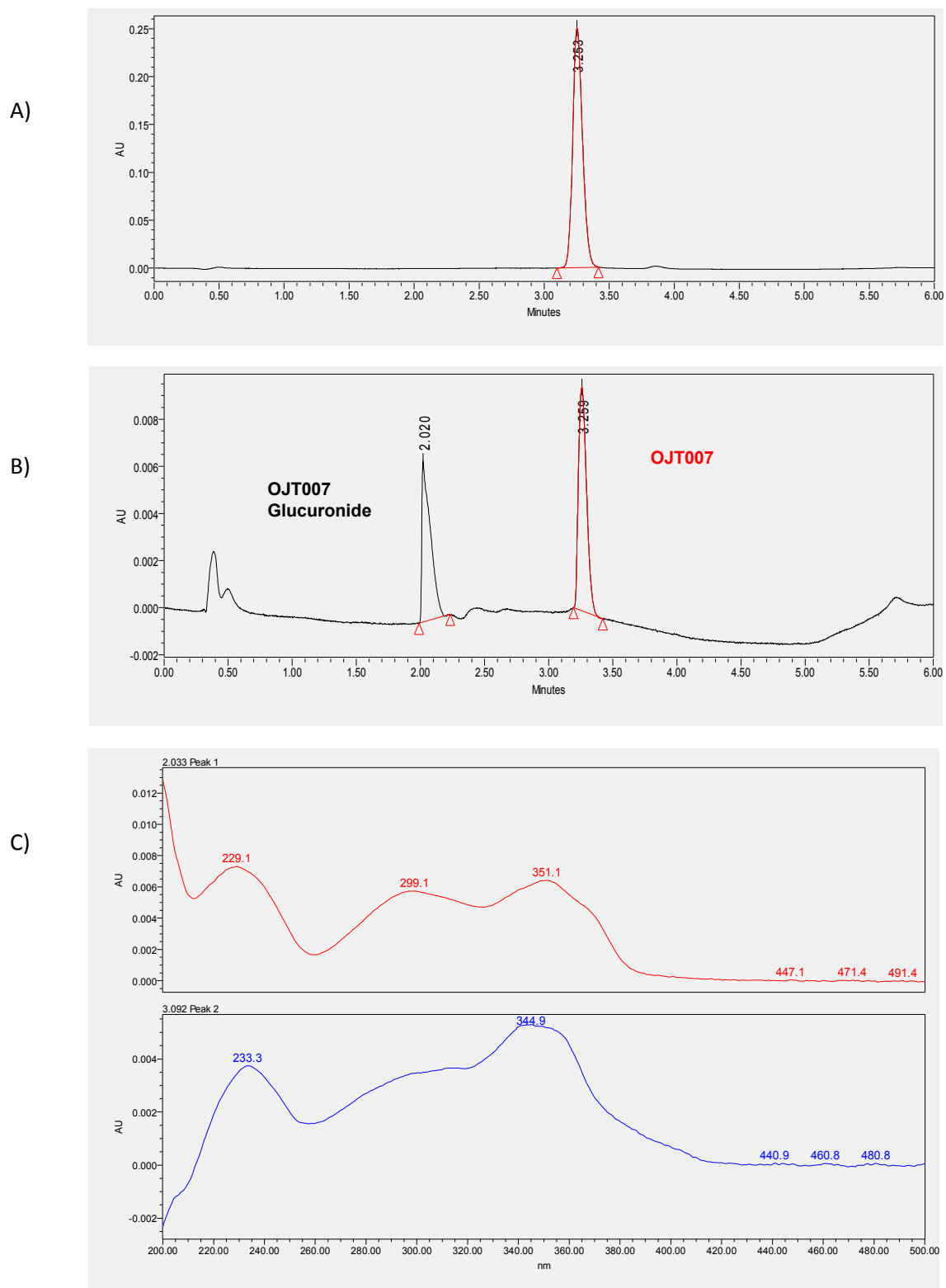
Figure 28: *A) Representative chromatogram of OJT007. B) Representative chromatogram of OJT007 and glucuronidation metabolite. B) UV spectra of OJT007 and glucuronide metabolite.*

4.5.2.1 Glucuronide Metabolite Identification

LC-MS/MS Identification of Glucuronide Metabolites

Q1 multiple ions (Q1MI), neutral loss (NL), product ion (MS/MS) scan and precursor ion scan (PI) in positive mode were used to identify the metabolite. In Q1MI scan, Q1 works in selected ion monitoring (SIM) by selecting a specific m/z value. Q1MI spectra (Figure 29) confirm the presence of the glucuronide metabolite as indicated by the presence of a pseudo-molecular ion at m/z 501.2, which is 176 Da higher than that of OJT007 at m/z 325.

In neutral loss (NL) scan, molecules which pass through Q1 and, after fragmentation in Q2 lose a neutral molecule of 176, are transmitted through Q3 for detection. Figure 27 shows the chromatogram and spectra obtained after a neutral loss 176. For the NL of 176 Da, the peak eluted at 1.37 minutes (Figure 30, A) had a precursor ion at m/z of 501 as shown in the spectra (Figure 30, B), which confirms the presence of a glucuronide.

The MS/MS spectra (Figure 31) show a pseudo-molecular ion of the conjugation metabolite at m/z 501.2. This is 176 Da higher than that of OJT007 at m/z 325, indicating the presence of glucuronic acid. Also, it showed major fragment ions at m/z 325, which is the mass of the addition ion of OJT007 at m/z 325. This spectra data confirms the newly eluted metabolite corresponds to a mono-glucuronidated OJT007.

Based on the NL scan results and the MS/MS spectra we performed a precursor ion scan with m/z 325 to further confirm the identity of the glucuronide.
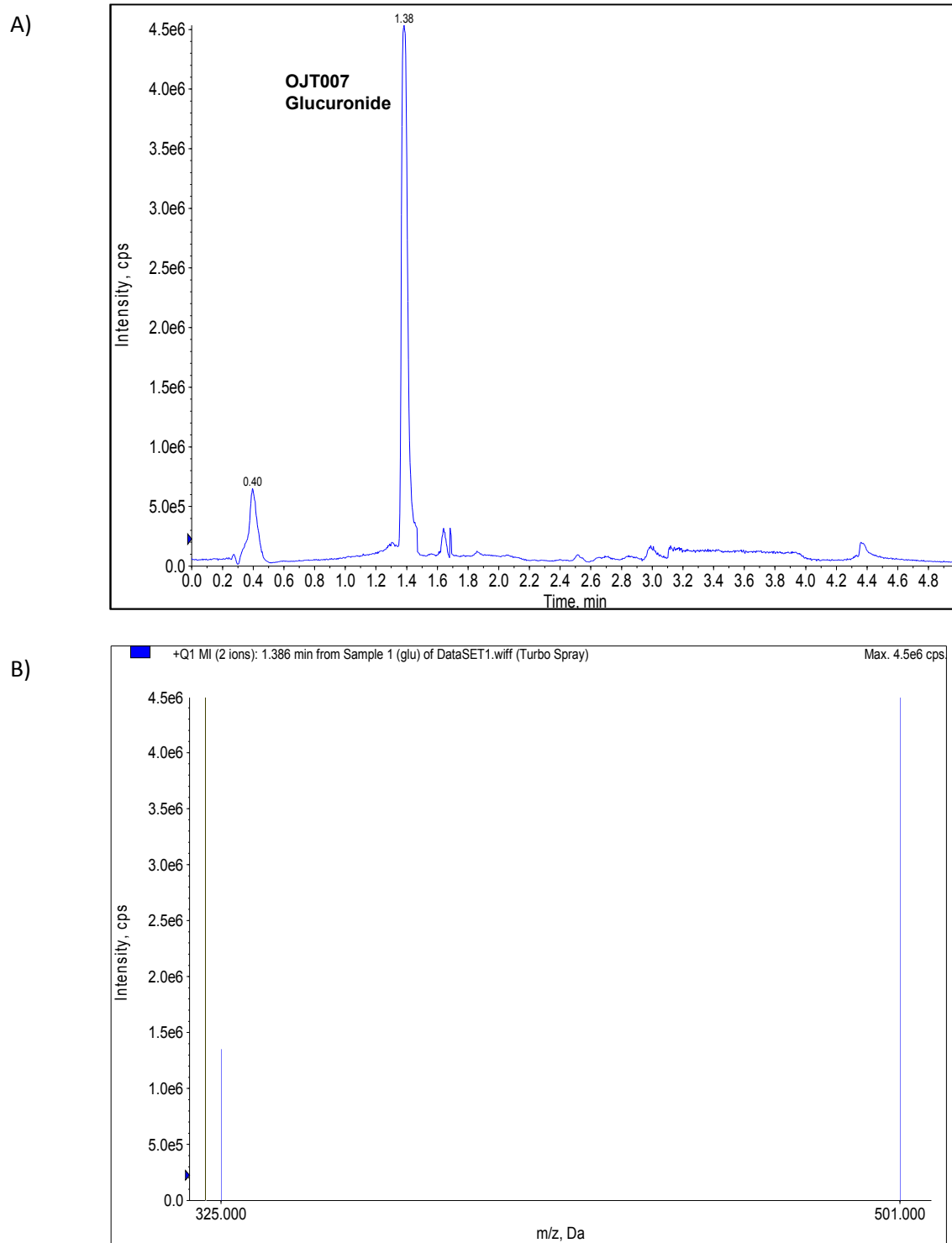
Figure 29: *A) Q1MI Chromatogram for m/z 501. B) Spectra for OJT007 glucuronide.*
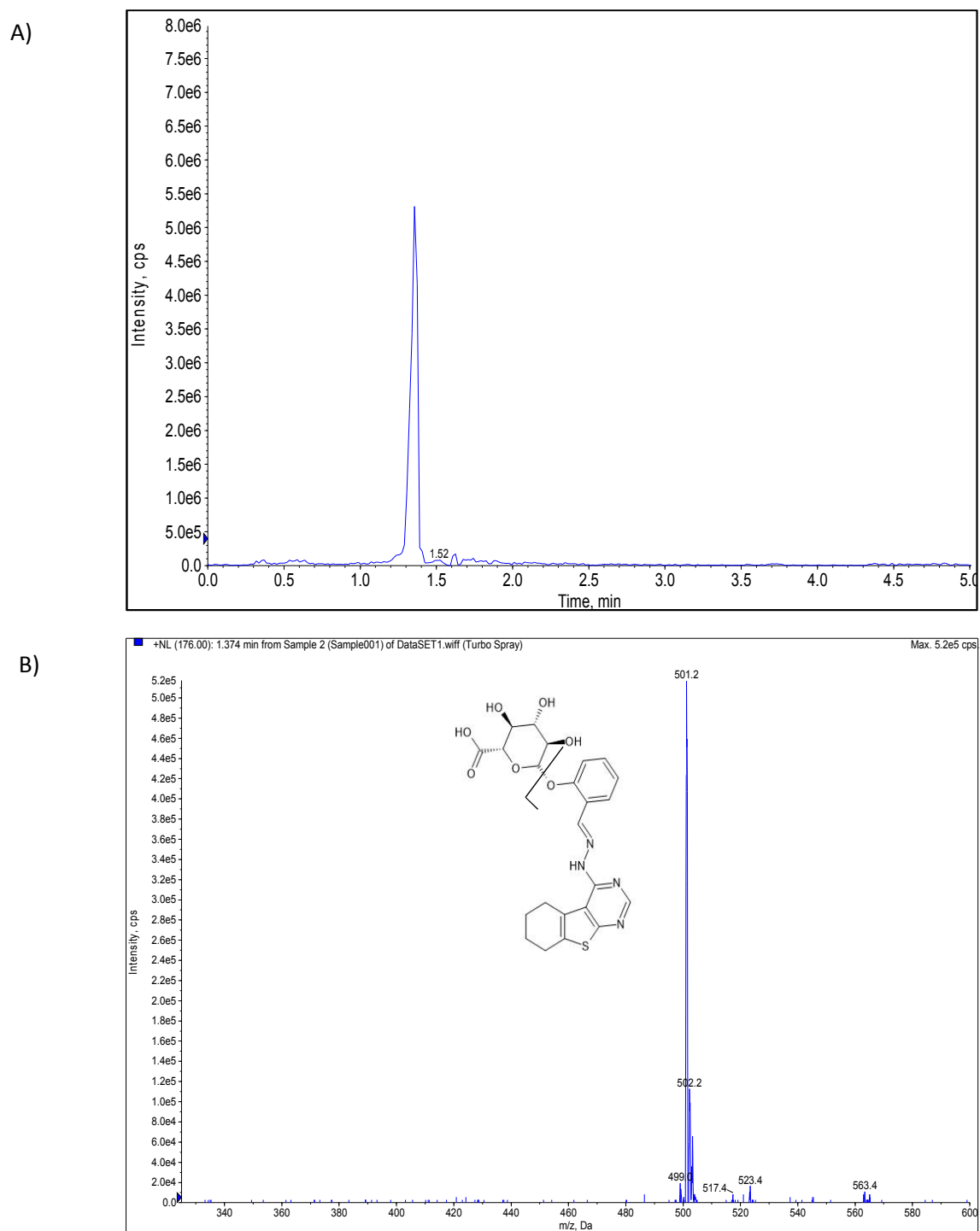
Figure 30. *A) Neutral loss at m/z 176 chromatogram. B) Spectra for OJT007 glucuronide.*
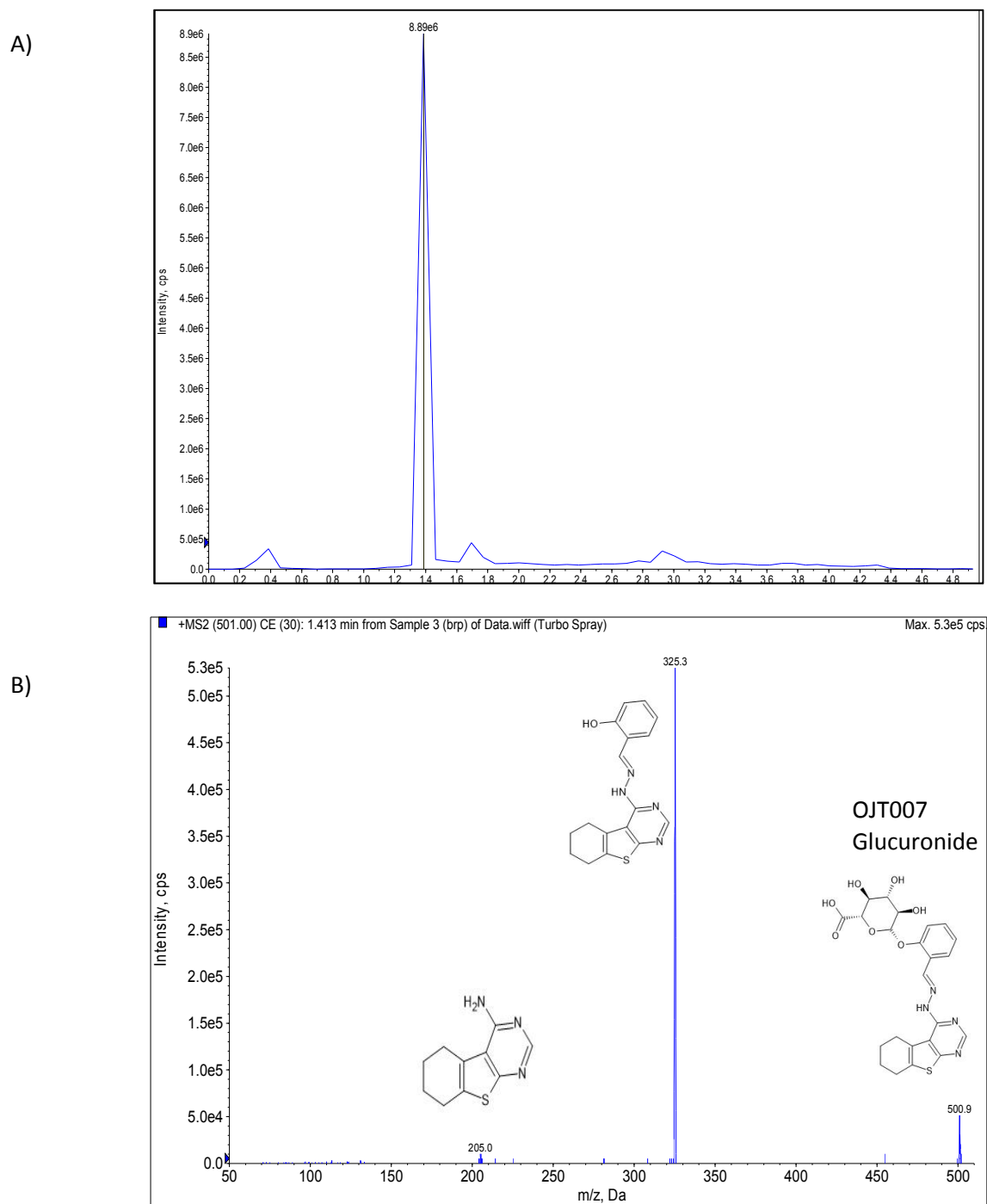
Figure 31. *A) MS/MS Chromatogram. B) MS/MS Spectra for m/z 501 OJT007 glucuronide*

Figure 32 confirms that the peak eluting at 1.40 minutes corresponds to OJT007 glucuronide with m/z 501.

Hydrolysis using β-glucuronidase

Figure 33 shows the hydrolysis of the OJT007 glucuronides, which were produced from the liver microsomes by β-glucuronidases. After incubating with β glucuronidases from E. Coli for two hours, the OJT007 concentrations increased at least 5-fold when compared with the control (Figure 33, A), whereas OJT007 glucuronide residuals dramatically decreased (Figure 33, B). This chemical data confirms that the newly eluted peak is OJT007 glucuronide.

4.6 Conversion Factors (K) of Extinction Coefficient

The glucuronidation reaction was performed at three different concentrations (2, 10, and 50 μM) to calculate average K values. The results showed that the K value for OJT007 glucuronide was 1.06. This conversion factor was used to calculate the concentration of OJT007 glucuronide using the standard curve for OJT007.

Figure 32. *(A) Precursor ion scan m/z 325 Chromatogram and (B) PI Spectra for OJT007 glucuronide*

A)

B)
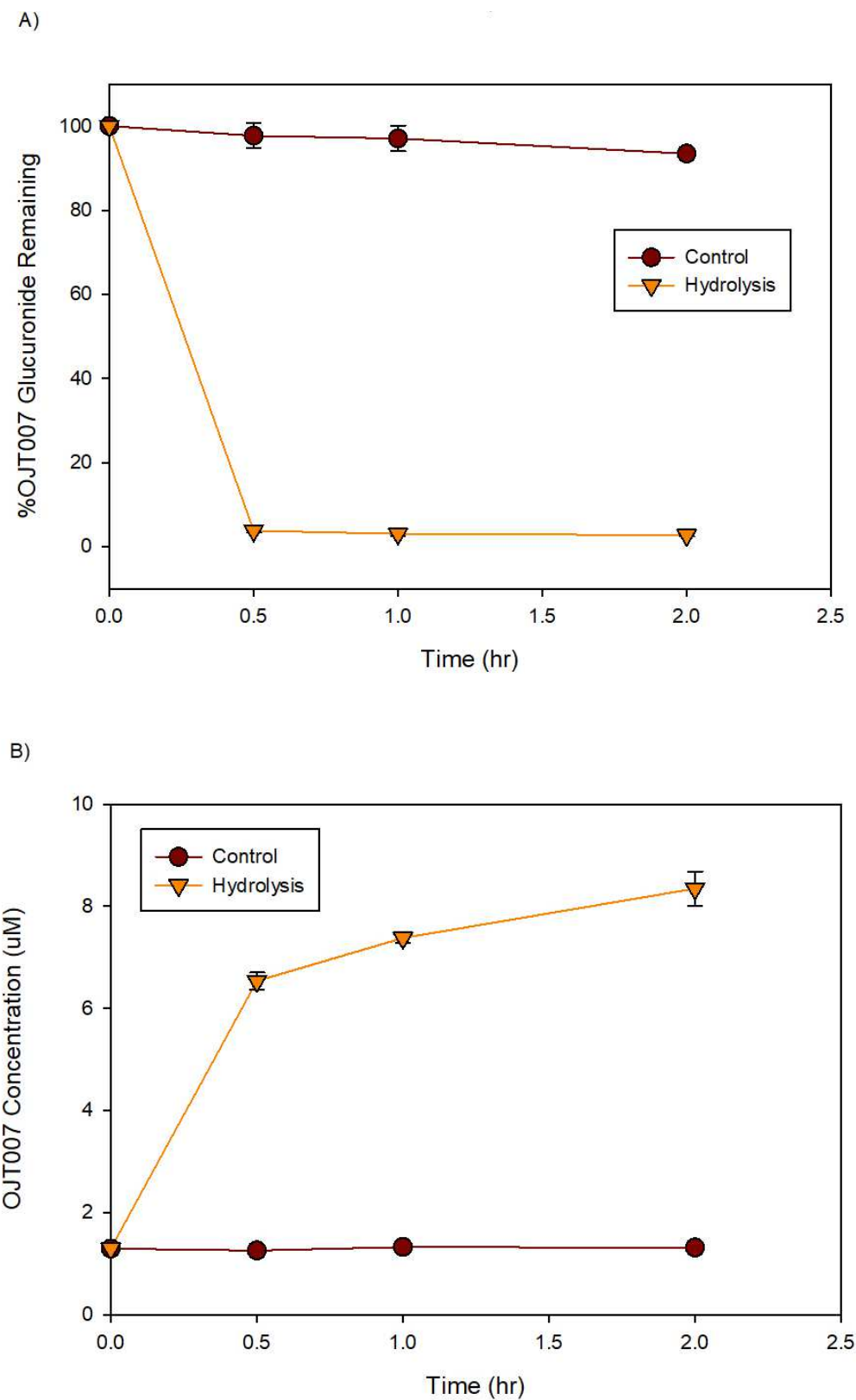
Figure 33. *Hydrolysis of OJT007 glucuronide generated by rat liver microsomes with E.Coli β-glucuronidase. Each data point indicated the mean ± SD.*

4.7   Glucuronidation rate of OJT007

Before a drug reaches the liver, it must first escape metabolism in the gut; thus, both intestinal and hepatic glucuronidation may contribute to in vivo disposition of oral OJT007. Therefore, the glucuronidation rates of OJT007 were determined using Rat Liver and intestine 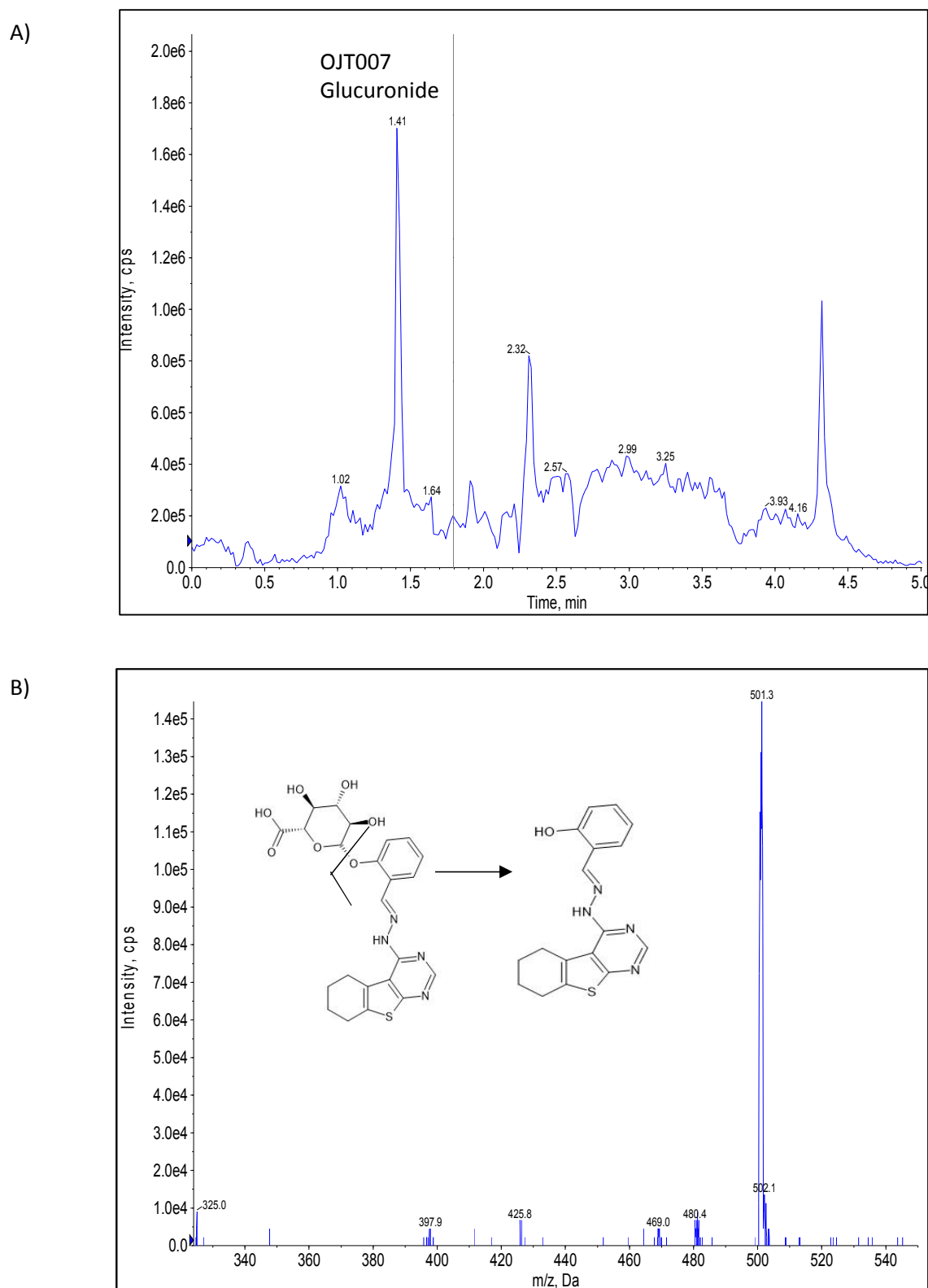microsomes. As shown in figure 34, the rate of formation is higher in liver microsomes than in intestine microsomes; However, rates are similar, suggesting that OJT007 would be glucuronidated by UGTs in the intestine as well. This has important implications on the in-vivo oral bioavailability for OJT007 because it is possible that absorbed OJT007 would be first metabolized in the intestine with smaller amounts reaching the liver to be further metabolized.

We also examined species-specific differences in the glucuronidation of OJT007 in human and rat liver microsomes. Although animals have UGTs orthologous to those in humans, these generally display different substrate specificity, tissue distribution, and efficiency of these enzymes. As shown in figure 35, the glucuronidation rate of OJT007 at substrate concentrations of 15 μM shows the species differences between HLMs and RLMs. This result is not surprising because each species has different UGT enzymes, and UGT enzymes from different species have different substrate specifics. Further studies are required to confirm this difference and to find a suitable in vivo model for future pharmacokinetic studies.
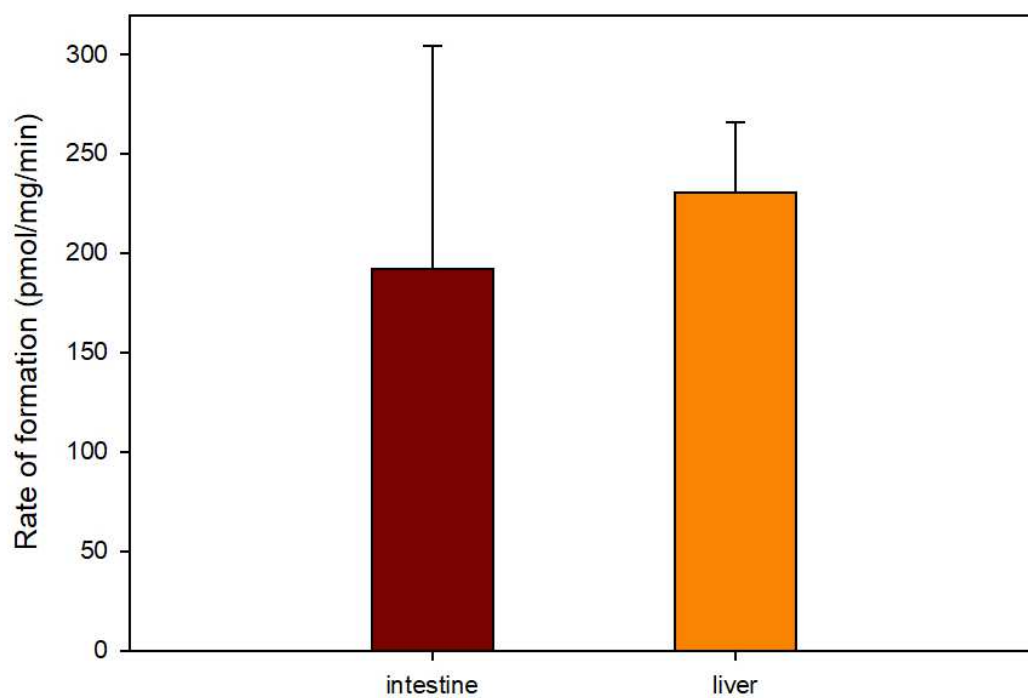
Figure 34. *Rate of formation of OJT007 glucuronide catalyzed by Rat liver and intestine microsomes at the substrate concentration of 15 μM (0.5 mg protein/ml). Each data point indicates the mean ± SD for triplicate samples*
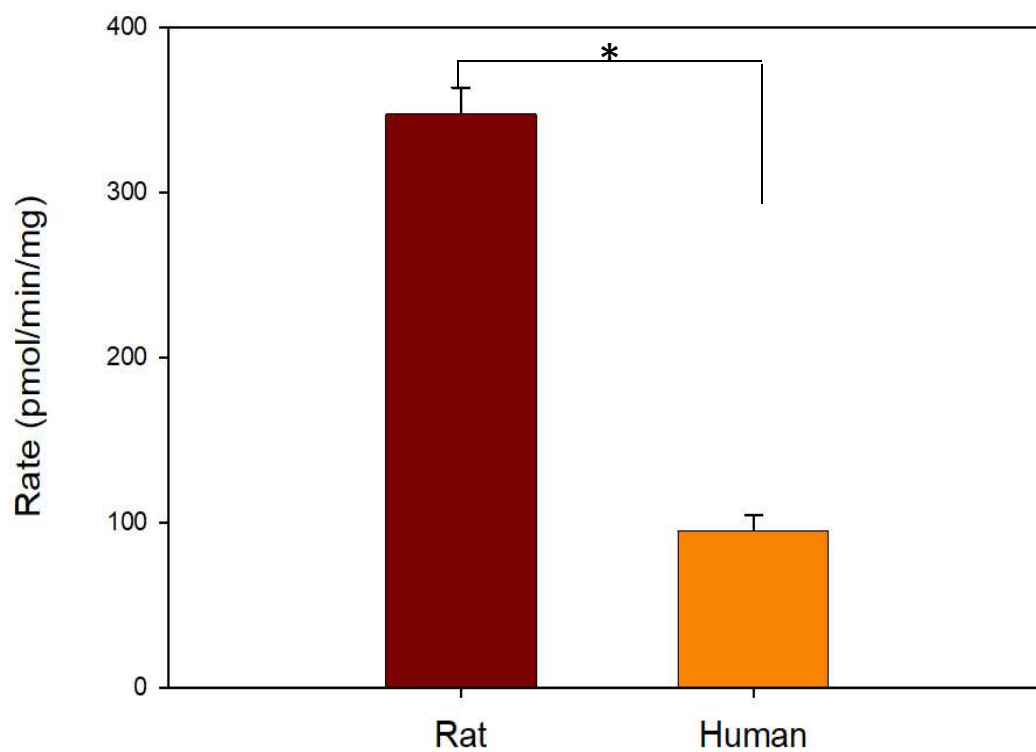
Figure 35. *Glucuronidation rates of OJT007 glucuronide catalyzed by liver microsomes Sprague Dawley and human liver microsomes at the substrate concentration 15μM (0.5 mg protein/ml). Each data point indicates the mean ± SD for triplicate samples. * Significant difference, p < 0.05*

4.8   Kinetics of OJT007 Glucuronidation

The OJT007 glucuronidation rate was determined by measuring the amount of metabolite formed in microsomes divided by the reaction time and protein concentrations. The substrate concentration evaluated ranged from $1.25-100$ μM, with a protein concentration of 0.035 mg of protein/mL and an incubation time of 60 minutes. The most appropriate model was selected based on the visual inspection of the Eadie-Hofstee plot (Figure 36). Quantitative analysis showed that the substrate concentration-glucuronidation velocity curves followed Michaelis-Menten Kinetics (Figure 36). The Maximal metabolic rate and the Michaelis Menten constants were 1.125 nmol/min/mg and 10.73 μM.

The rate of OJT007 glucuronidation was rapid via liver microsomes with an intrinsic clearance value similar to those of isoflavones, a class of compounds with limited oral bioavailability due to extensive metabolism (Chen et al., 2005). It is possible that extensive glucuronidation may have implications in the in vivo oral bioavailability of OJT007.

4.9 Prediction of In Vivo Clearance

To predict the in vivo clearance, the microsomal protein per gram of liver value was used as a scaling factor to calculate the intrinsic clearance in vivo from the in vitro intrinsic clearance. In addition, the in vivo hepatic clearance was estimated using the well-stirred hepatic clearance model (Obach, 1999) The calculated in vivo intrinsic clearance and hepatic clearances were 210.6 ml/min/mg and 43.61 ml/min/Kg, respectively. The estimated hepatic clearance closely approaches liver blood flow in rats

Figure 36. *Apparent enzyme kinetics of OJT007 glucuronidation*
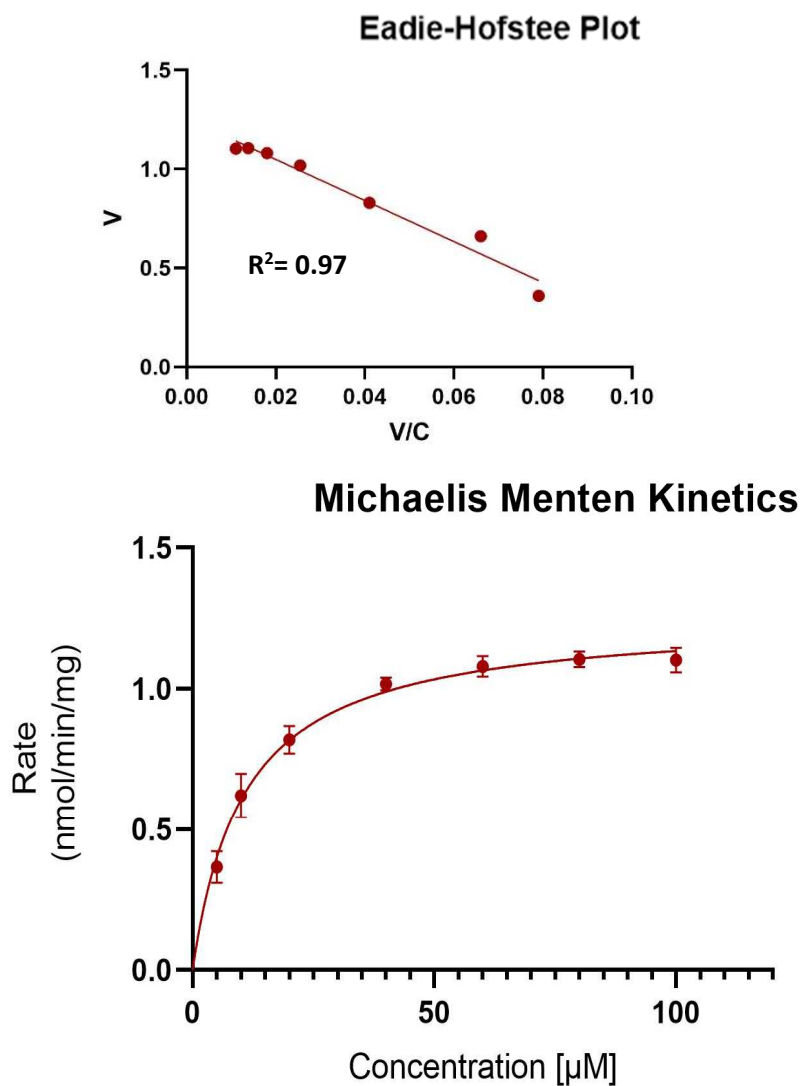
Apparent Enzyme Kinetics	
Vmax (nmol/min/mg)	1.125
Km (μM)	10.73
In vitro Cl_{int} (μL/min/mg)	116.96

(55mL/min/Kg) (Davies & Morris, 1993), which would make OJT007 a moderate to high extraction ratio drug.

4.10 Pharmacokinetic Studies

4.10.1 Oral Bioavailability

Intravenous Pharmacokinetics

In this study, a group of adult male Sprague-Dawley rats (n=5) received a single dose of 5 mg/Kg IV bolus dose of OJT007. The dose amount was selected based on a pilot study using one SD rat which received a single dose of 10 mg/Kg. From the pilot study, it was found that at 10 mg/Kg, the rat was lethargic; Thus, the dose was decreased by half. At 5 mg/Kg, no animal distress was observed, and adequate plasma concentrations were achieved.

Serial blood samples (100 µL) were collected before dose and at 0.033, 0.083, 0.25, 0.5, 1, 1.5, 2, 4, 6, 8, 10 and 24 hours. The sampled blood volume per time point was 100 µL to ensure blood draws from the animal were less than 10% of total blood volume. The sampling times were selected to ensure an appropriate characterization of the profile based on the pilot study. An important consideration in sampling time points is to ensure collecting at least three consecutive points in the elimination phase for the half-life calculation and 3-5 time points per phase. The OJT007 plasma concentration was quantified using LC-MS/MS. Urine samples were collected up to 24 hours post-dose, and the amount of OJT007 excreted unchanged was quantified by LC-MS/MS.

Non-compartmental and compartmental analysis using Phoenix WinNonlin was used to generate the pharmacokinetic parameters describing the in vivo disposition of

OJT007 after IV administration. The fitness of the pharmacokinetic model was determined using in-built diagnostics of WinNonlin software, Akaike Information Criterion (AIC), by plotting the predicted curve as a function of time with the observed concentrations overlaid on the plot indicating a close correlation of the values and the reported variability in the parameter values (Coefficient of variation, standard deviation). The standard deviation and coefficient of variation estimated for each parameter provide an estimate of how well the data is described by the parameters of the specified model. A large CV% (>20%) would indicate an improper model. Discrimination between models is driven by the minimization of the weighted squared residuals (WSS). Basically, the model with the lowest value of WSS and AIC is considered a better model.(Rudek et al., 2014). Based on these criteria, a two-compartment model was selected as the best fit.

The 2-compartment model used to estimate the in vivo PK parameters of OJT007 is described by the following equation:

$$C_t = Ae^{-\alpha t} + Be^{-\beta t} \tag{21}$$

Where A and B are the coefficients of the alpha and beta phases, respectively. α and β are the elimination rate constants in the distribution and elimination phases, and C_t is the plasma concentration of OJT007 at time t. Weighting of $1/Y^2$ was applied to compartmental analysis.

Table 12 shows the plasma concentrations observed after IV bolus administration of OJT007. Figures 37 and 38 show the plots generated for 2-compartmental and non-compartmental analysis, respectively. On the other hand, table 13 provides the mean PK

parameter estimates from both analyses. From figure 33, it is shown that the data fits a 2-compartment model adequately.

OJT007 displayed a biexponential disposition after intravenous administration, with a rapid distribution to the tissue compartment within the first 2 hours, followed by a slow elimination. The initial concentration after IV administration had a mean value of 3601 ng/ml, which is 30 times above the reported in vitro EC_{50} values of 162.2 ng/mL for OJT007 (Rodriguez et al., 2020).

The half-life of the distribution phase ($T_{1/2\alpha}$) was estimated to be 0.19 hr., while the half-life of the terminal (elimination) phase had a mean value of 2 hours. The mean volume of distribution at steady state (V_{ss}) was 7.77 ± 3.57 L/hr/Kg while a lower volume of distribution at steady state was calculated using compartmental analysis. This volume of distribution was greater than the total body water in rats (Davies & Morris, 1993), possibly due to drug partition into tissues. OJT007 is an amphoteric drug; however, at physiological pH, it is unionized. Thus, tissue binding would be directly related to drug lipophilicity (Smith et al., 2015).

Table 12. *Plasma Concentration in ng/mL After Intravenous Dose of 5 mg/Kg OJT007 to Rats*

	Rat A	Rat B	Rat D	Rat E	Rat F
Loading Solution Concentration (mg/mL)	1	1	2.5	2.5	2.5
Animal Weight (Kg)	0.357	0.350	0.328	0.332	0.327
Dosing Volume (mL)	1.79	1.7	0.66	0.67	0.65
0.033333	3750	2195	2160	2350	2340
0.083333	2970	1140	1480	1110	1240
0.25	1910	965	1040	677	865
0.5	1770	575	772	646	610
1	918	351	595	415	535
1.5	639	266	354.5	348	320.5
2	423	229	292	331	308
4	200	95.9	126	159	165
6	96.5	52.2	60.3	67.7	63.5
8	44.3	16.3	41.7	42.7	40.2
10	31.6	7.59	18.8	24.7	22
24	23.9	<5	7.43	9.99	9.54

A)

B)

C)

D)

E)
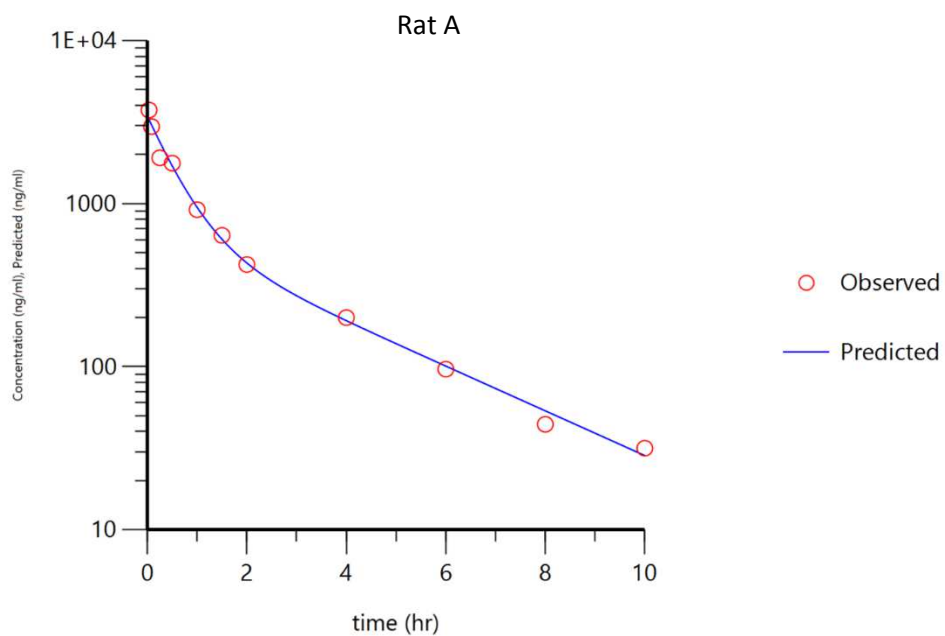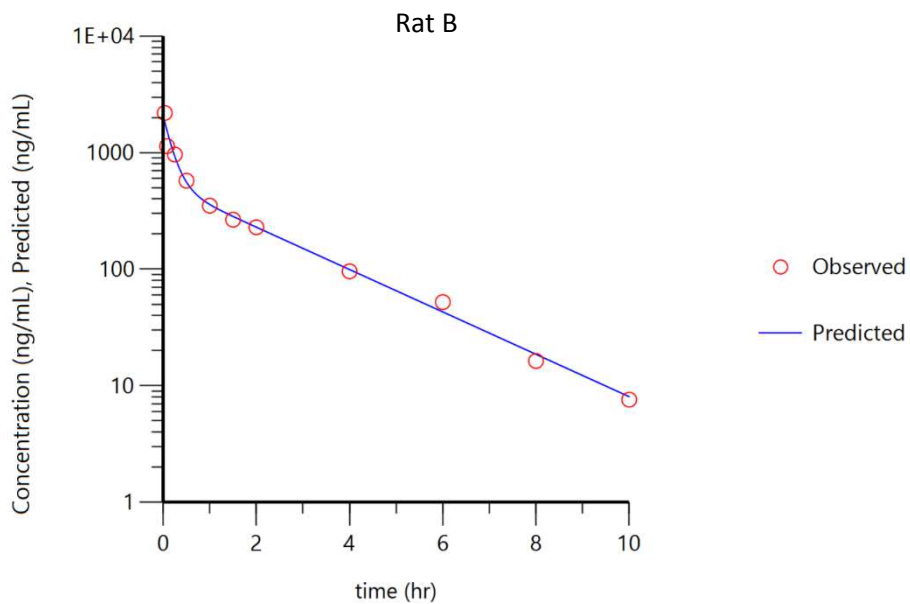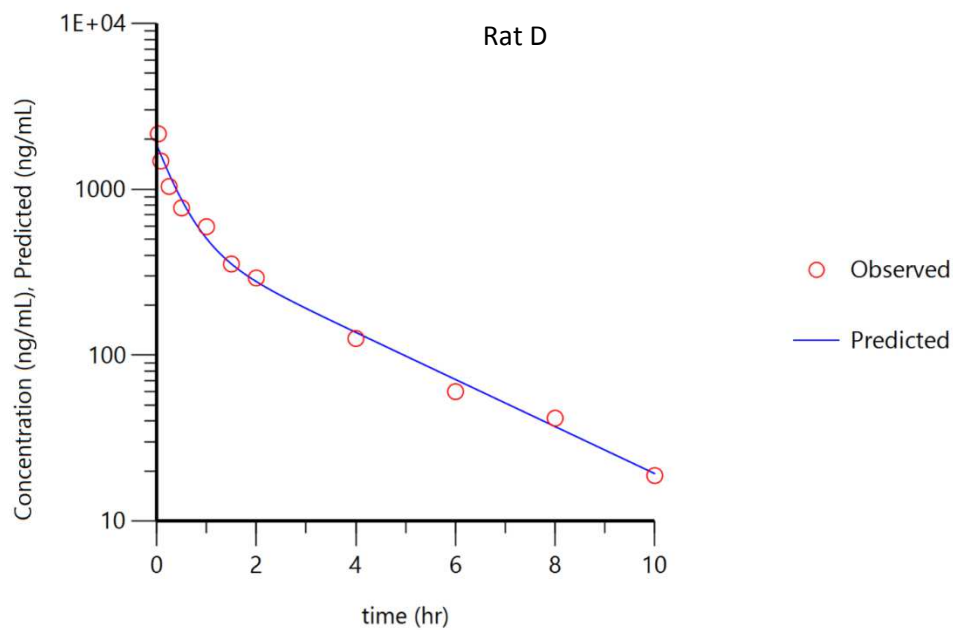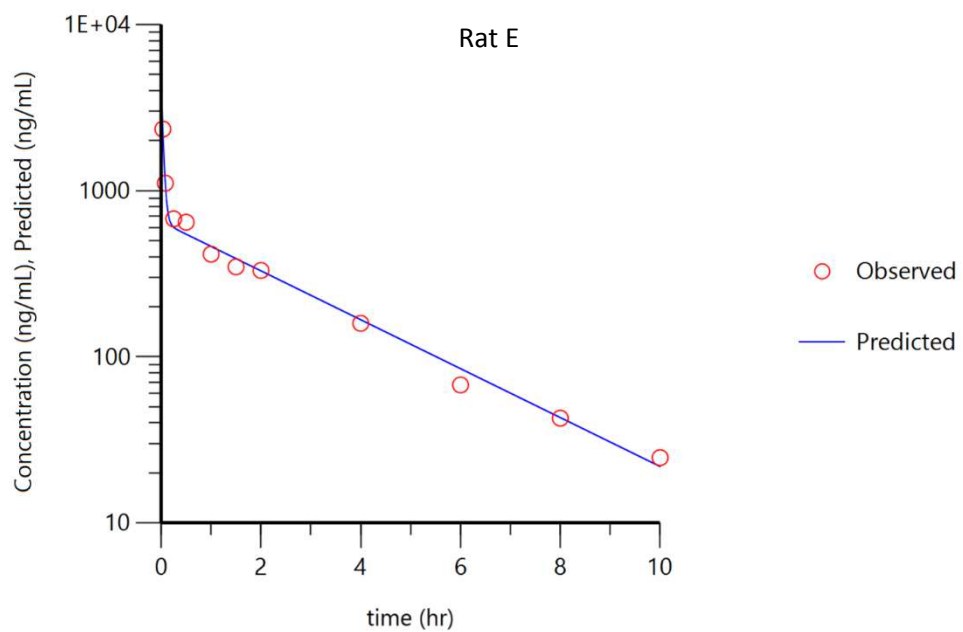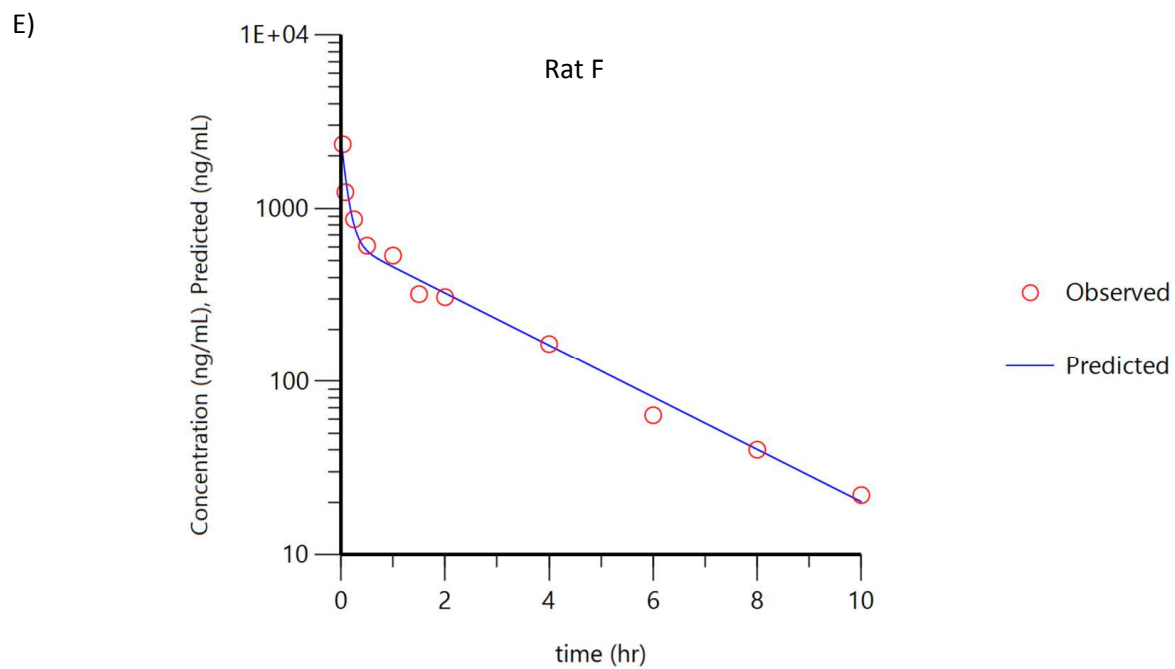
Figure 37. *Individual plots (A-E) of OJT007 after IV bolus dose of 5 mg/kg using 2-compartmental analysis*

A)

Rat A

Rsq=0.9857 Rsq_adjusted=0.981 HL_Lambda_z=2.0704
5 points used in calculation
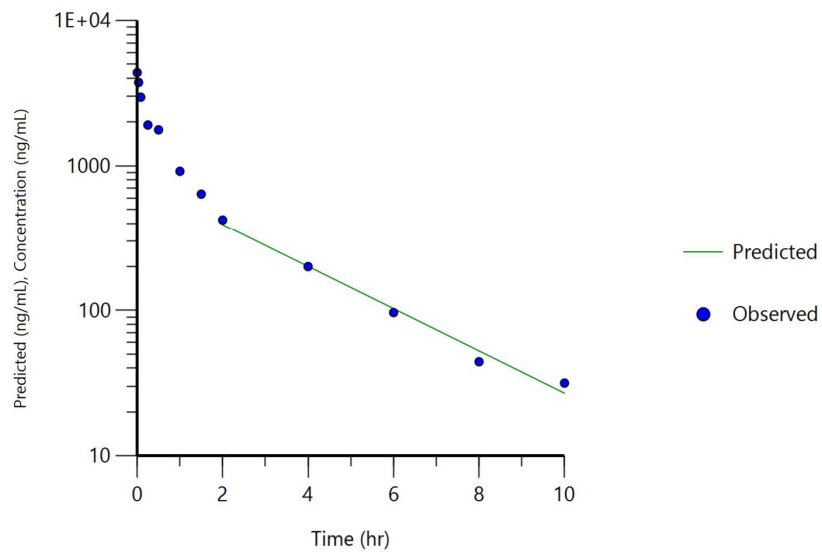
B)

Rat B

Rsq=0.9953 Rsq_adjusted=0.9943 HL_Lambda_z=1.6392
7 points used in calculation

Rat D

C)
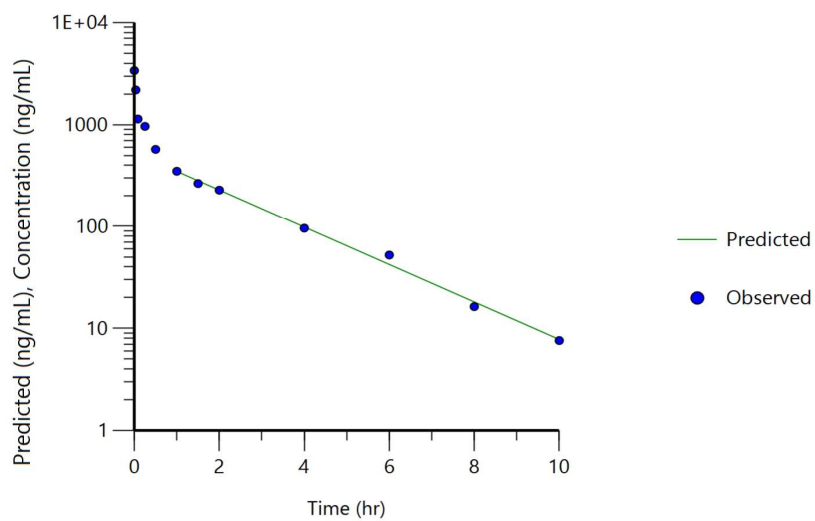
Rsq=0.9895 Rsq_adjusted=0.9868 HL_Lambda_z=2.0489
6 points used in calculation
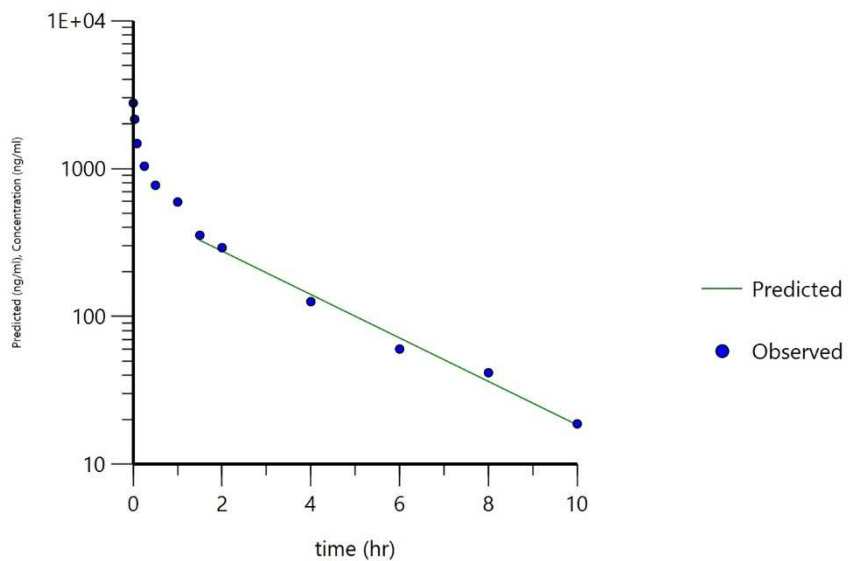
Rat E

D)

Rsq=0.9976 Rsq_adjusted=0.9951 HL_Lambda_z=2.7498
3 points used in calculation

E)
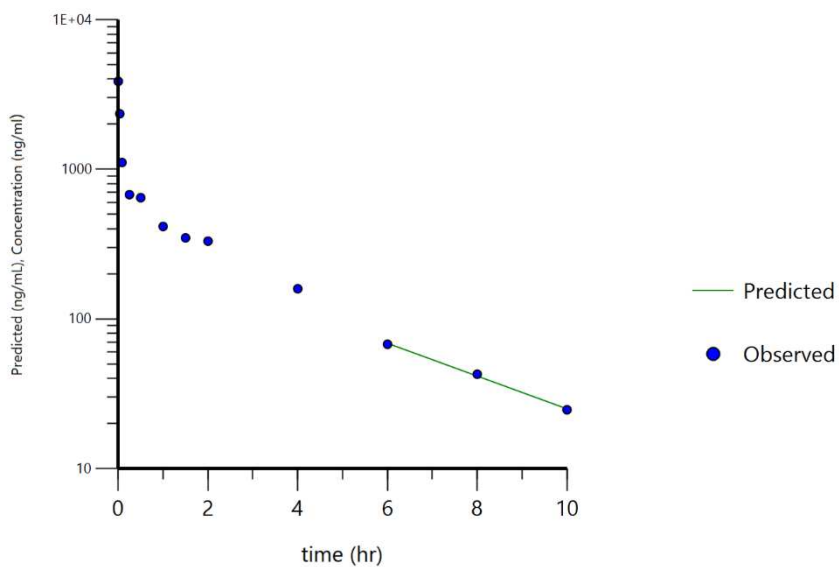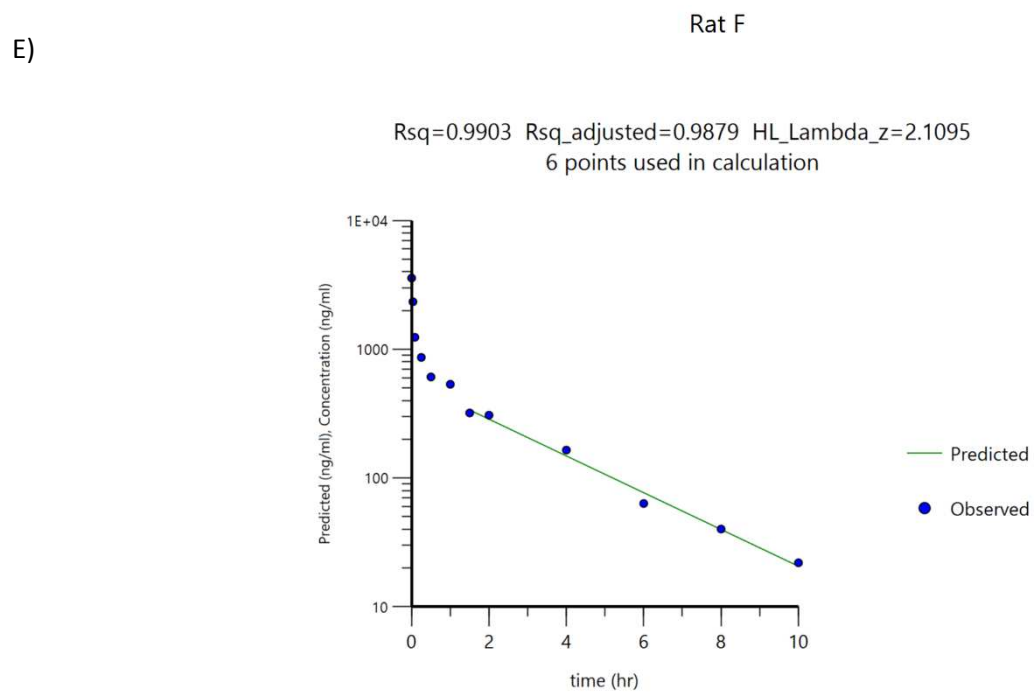
Figure 38. *Individual plots (A-E) of OJT007 after IV bolus dose of 5 mg/kg using Non compartmental analysis*

Table 13. *Mean Pharmacokinetic Parameters of OJT007 Following an IV bolus Dose of 5 mg/Kg*

PK Parameters (Units)	Mean ± SD	Mean ± SD
	NCA	2-Compartment
Route of Administration	IV	IV
N	5	5
Dose	5 mg/kg	5 mg/kg
C_{max} (ng/mL)	-	2919 ±1142.7
C_0 (ng/mL)	3601 ±591.72	-
$T_{1//2\alpha}$ (hr)	-	0.19 ± 0.15
$T_{1/2\beta}$ (hr)	-	2.00 ± 0.21
$AUC_{0-\infty}$ (hr.ng/mL)	2061.31 ± 240.8	2310.2 ± 791.4
$t_{1/2}$ (hr)	2.12 ± 0.40	-
Cl (mL/hr/kg)	2278.3 ± 609.9	2333.5 ± 640.7
V_z (mL/kg)	6898.9 ± 1902.5	-
V_2 (mL/kg)	-	3533 ± 1567
V_{ss} (ml/kg)	7773.1 ± 3565	5446.1 ± 1528
MRT (hr)	2.25 ± 0.33	2.33 ± 0.33

The mean systemic clearance (CL) was 2.3 L/h/kg, which accounts for about 68% hepatic blood flow (Davies & Morris, 1993). Since the systemic clearance of a drug after intravenous administration reflects hepatic elimination, we can calculate the hepatic extraction ratio by taking the ratio of systemic clearance to liver blood flow (Benet, 2010; M. Rowland, 1972). The extraction ratio (ER) for OJT007 is 0.69, which would make OJT007 a moderate to high extraction ratio drug (Benet & Zia-Amirhosseini, 1995). A good correlation was observed between the predicted hepatic clearance obtained from the in vitro studies (2.61 L/hr/Kg) and the observed in vivo clearance in rats.

The mean area under the plasma concentration–time curve extrapolated to infinity ($AUC_{0 \to \infty}$) were 2.06 mg.h/L (NCA) and 2.31 mg.h/L (2-Compartment). The mean percentage of the dose excreted unchanged in urine after 24 hours was 0.39%, suggesting extensive metabolism, which would be consistent with our in vitro studies.

OJT007 glucuronide was detected in vivo after IV administration. For instance, excretion of the glucuronide in urine was detected at 24 hours. Likewise, the glucuronide was detected in plasma. Figure 39 shows a representative plasma chromatogram at 1 hour after IV administration. The glucuronide metabolite elutes at 1.42 minutes, while at 2.17 minutes is shown the OJT007 parent peak. On the other hand, the oxidation metabolites identified in vitro were not found in rat plasma and urine samples. It is possible that the oxidation metabolites undergo glucuronidation as well; thus, oxidation metabolites were not detected. Nonetheless, our in vitro studies suggested oxidation was not a very significant pathway.
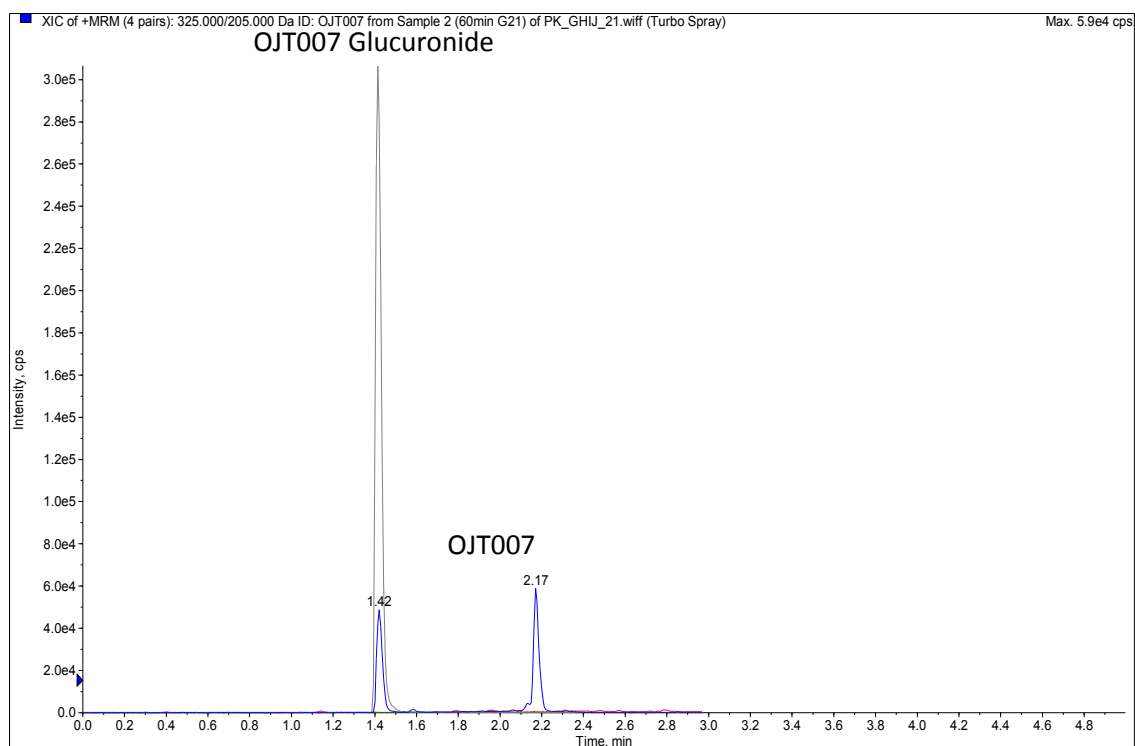
Figure 39. *Representative MRM chromatogram of rat plasma sample at 1 hour. Peak eluting at 1.46 minutes is OJT007 glucuronide.*

Oral Pharmacokinetics

The oral pharmacokinetics of OJT007 was evaluated by administering a dose of 10 mg/Kg OJT007 cosolvent formulation through oral gavage to the adult male SD rats. Serial blood samples (100 µL) were collected from each rat before dose and at 15, 30, 45, 60, 90 minutes, and 2, 3, 4, 6, 8, 10, and 24 hours post-dose. These sampling time points were selected to ensure an appropriate characterization of the pk profile. In other words, we were ensuring at least 3 points before the t_{max} and at least three points to describe the terminal phase. The plasma concentrations obtained after oral administration are summarized in table 14.

The pharmacokinetic parameters for OJT007 were computed using WinNonlin v8.3 via non-compartmental and compartmental analysis. The most suitable compartmental model and the most suitable weighting scheme were selected following the same criteria followed after IV administration.

The pharmacokinetics observed after intravenous administration suggested a two-compartment model described the disposition for OJT007; However, based on the above-described criteria, a one-compartment model and no lag time was selected for the compartmental analysis of the data. After oral administration, a drug following a two-compartment model would be described by the Loo-Riegelman method (Equation 22), while a drug following a one compartment model would be described by the Wagner-Nelson method (Equation 23)

$$C_t = Ae^{-\alpha t} + Be^{-\beta t} + Ce^{-K_a t} \tag{22}$$

$$\text{Where } A = \frac{D\,(Ka(K21-\alpha))}{V(\alpha-\beta)(\alpha-Ka)}$$

Table 14. *Plasma Concentration in ng/mL After Oral Dose of 10mg/Kg OJT007 to Rats*

Time (hr)	Rat A	Rat B	Rat D	Rat E	Rat F
Loading Solution Concentration (mg/mL)	1	1	2.5	2.5	2.5
Animal Weight (Kg)	0.292	0.355	0.300	0.309	0.309
Dosing Volume (mL)	2.9	3.6	1.2	1.23	1.24
0.25	10.2	6.42	27	31.4	17.5
0.5	29.2	18.72	62.1	58.2	36
0.75	40.2	29.9	62.8	88.5	67.9
1	48.7	42.9	67.8	96.7	68.9
1.5	86.4	96.9	68.9	98.1	67.9
2	81.2	60.6	65.1	96.6	63.9
3	72.6	52.9	61.4	96.7	62.7
4	49.4	38	51.7	71.2	56.1
6	26.6	26	45.1	66.7	28.1
8	12	10.1	16.6	24.6	14
10	5.98	8.2	14.6	12.7	6.94
24	<5	<5	<5	<5	<5

$$B = \frac{D \ (Ka(K21 - \beta))}{V(\alpha - \beta)(\beta - Ka)}$$

$$C = \frac{D \ (Ka(K21 - Ka))}{V(\beta - Ka)(\alpha - Ka)}$$

K21 is the micro rate constants out of compartment 2 in a two-compartment model. α and β represent disposition constants describing distribution and elimination in a two-compartment model

$$C_t = \frac{Dose.K_a}{V(K_a - K_e)} (e^{-k_a t} + Be^{-k_e t}) \tag{23}$$

Where K_a (absorption rate), K_e (elimination rate), and V is (volume of distribution)

In our study, seemingly, a term in the two compartment oral equation (equation 22) "vanished". A similar phenomenon has been discussed by others. (Nielsen-Kudsk et al., 2009; Ronfeld & Benet, 1977). The first-order absorption rate constant (K_a) determined in the oral animal studies is considerably lower than the α-values obtained after intravenous studies. As the K_a values are lower than K_{21} values obtained using a two-compartment value after IV administration ($K_{21} = 1.82$), the coefficient of the exponential becomes negative; thus, disposition is described by a one-compartment model. The pharmacokinetic parameters for OJT007 after oral administration are summarized in table 14. Figure 40 and 41 summarizes the plots generated after compartmental and non-compartmental analysis of OJT007. A high degree of agreement between elimination rates after the two routes of administration in SD rats was observed.

A maximum plasma concentration of 83.84 ng/mL attained at 1.4 hours was observed after oral administration. Although this concentration is below the EC_{50}, many in vitro assays overexpress the target protein to enhance assay sensitivity, which translates into

higher EC_{50}. In this case, efficacious drug concentrations can be significantly lower than the in vitro activity(Smith et al., 2010). Further studies are required to assess whether the current dosing regimen is efficacious. OJT007 has an oral absorption half-life of 0.98 ± 0.34 hours. The area under the curve, which indicates the extent of absorption or exposure, was found to be 451.01 ± 116.92.

The absolute oral bioavailability of OJT007 was calculated using the following equation:

$$F_{abs} = \frac{(AUC)_{PO} / (Dose)_{PO}}{(AUC)_{IV} / (Dose)_{IV}}$$

OJT007 has an oral bioavailability of $10.9 \pm 2.47\%$. To get an intuition behind the attenuation of oral bioavailability, we looked at the kinetic expression of bioavailability. Assuming that during GI transit drug does not degrade after oral administration, bioavailability is the product of three availability factors $F = F_{abs}$. F_G. F_H, where F_{abs} is the fraction of the administered drug that is absorbed into the gut wall. F_G is the fraction that gets through the gut wall unchanged, while F_H is the fraction that passes through the liver and into the systemic circulation unchanged.

In our intravenous studies, we found that the extraction ratio (ER) for OJT007 is 0.69. We can calculate the hepatic availability using Rowland's prediction of first-pass hepatic metabolism $F_H = 1 - ER$ (M. Rowland, 1972). Thus, the hepatic bioavailability of OJT007 is only 31%. This would mean the great majority of a dose would be metabolized in the liver on its first pass prior to reaching the systemic circulation. A bioavailability of 31% would be expected, assuming no drug degradation, complete absorption in the gut, and no

gut metabolism. However, since bioavailability is only 10.9%, a fraction of the dose may be lost due to degradation or an incomplete absorption in GI mucosa (F_{abs}) and/or gut wall metabolism (which in turn affect F_G).

Some authors argue that generally, the contribution of gut metabolism is negligible compared to liver metabolism; this would, in turn, simplify the kinetic expression of bioavailability to F= F_{abs}. F_H (Lin et al.,1999). Nonetheless, significant contributions of gut wall metabolism have been reported for several substrates (Jones et al., 2016; Takahashi et al., 2016). A contribution of gut wall metabolism would be consistent with our in vitro studies which suggested intestinal UGTs may play an important role in the metabolism of OJT007, and thus in the oral bioavailability. Further studies are warranted to confirm the contribution of F_{abs} and F_G to oral bioavailability experimentally.

The percentage OJT007 excreted unchanged in the urine at 24 hours after oral administration ranged from 0.034% to 0.794%, suggesting extensive metabolism. In our in vitro studies, we identified four possible metabolites: three oxidation metabolites and one glucuronide. Although OJT007 glucuronide was detected in urine and plasma samples, the oxidation metabolites identified in vitro were not detected in rat plasma or urine. Figure 42 shows a representative urine chromatogram for OJT007. OJT007 glucuronide elutes at 1.4 minutes, while OJT007 elutes at 2.16 minutes.

A)

Rat A

B)

Rat B

C)

Rat D

D)

Rat E
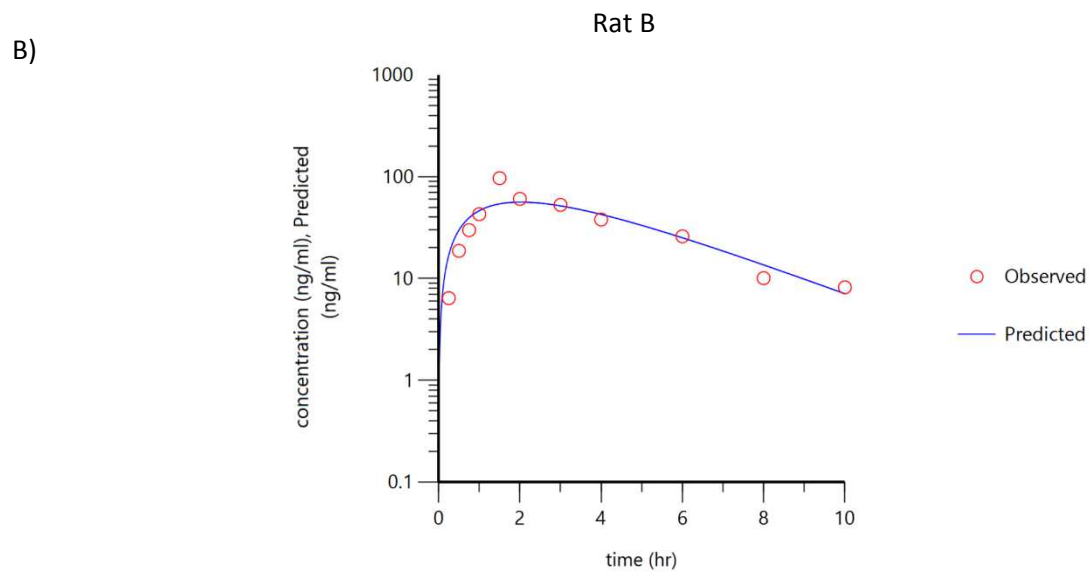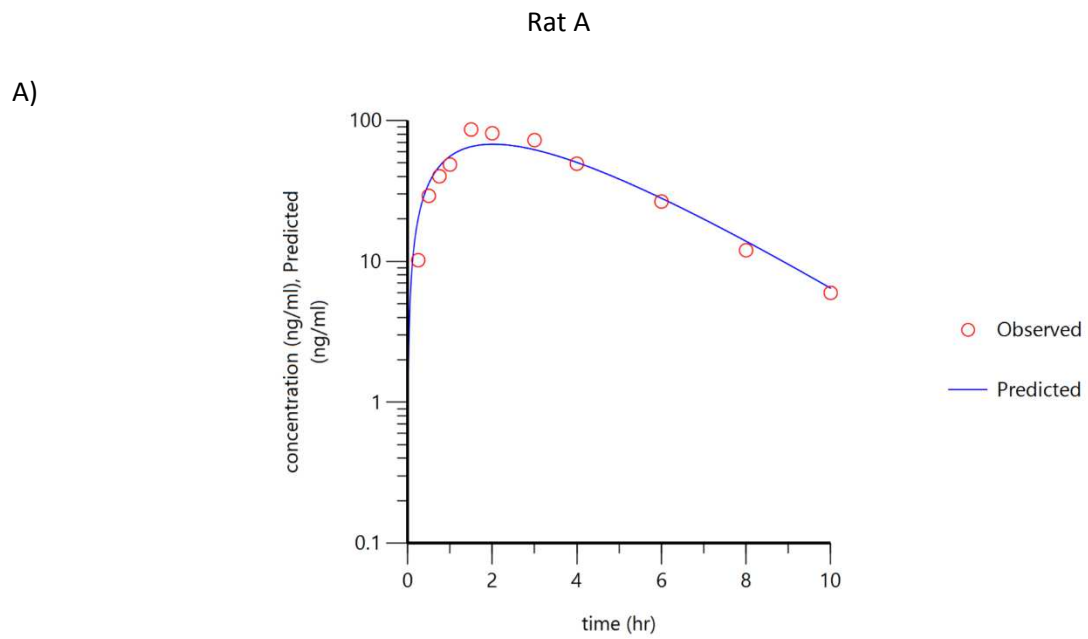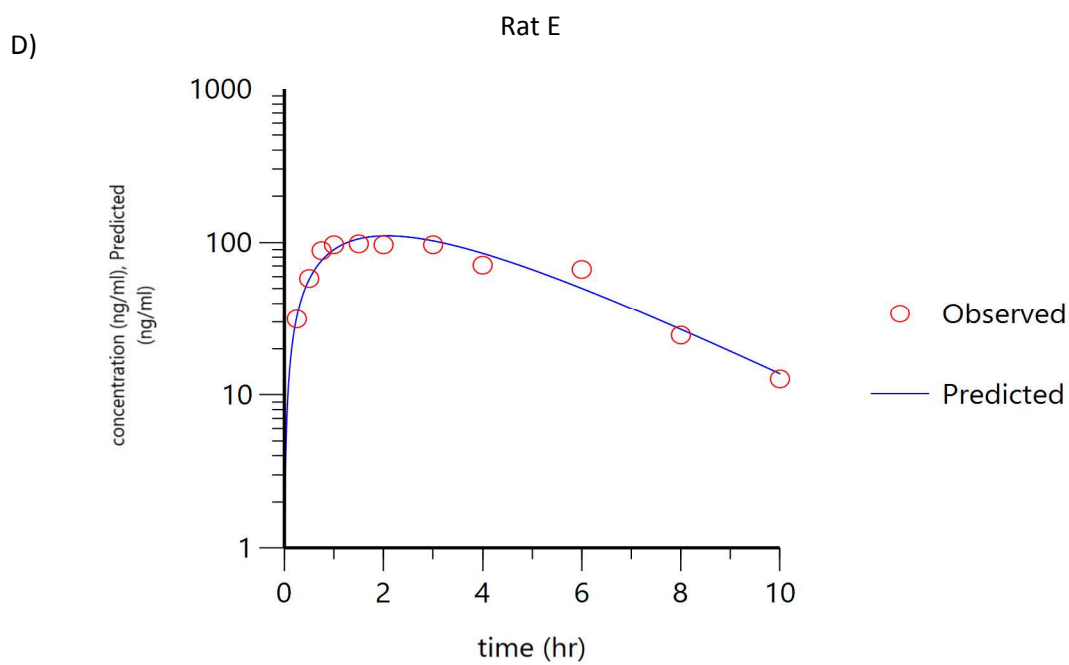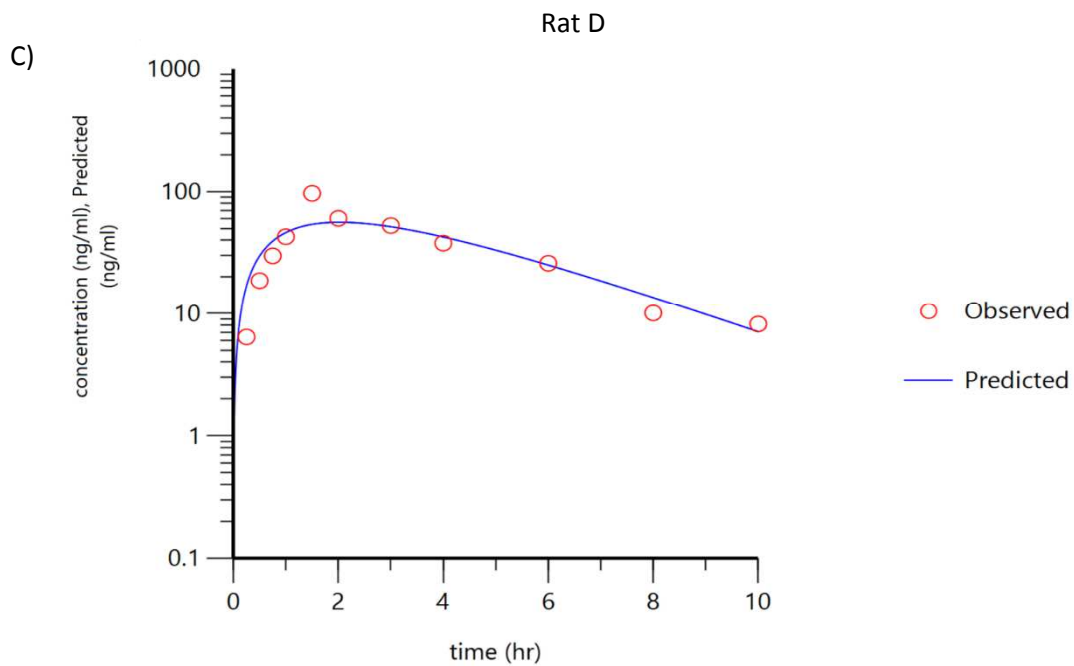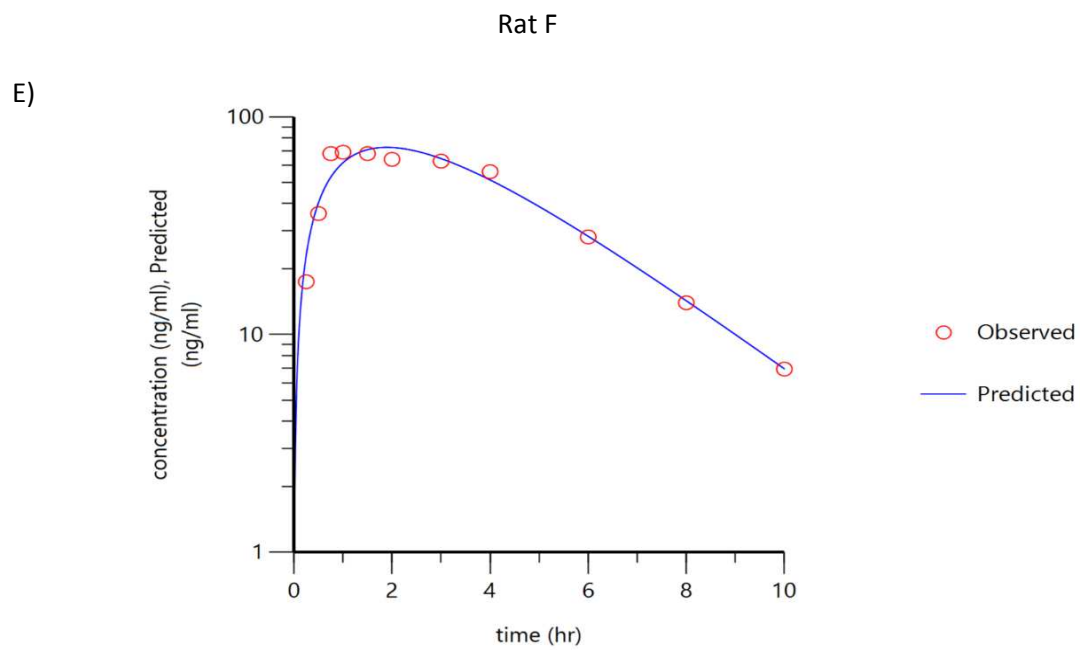
Figure 40. *Individual plots (A-E) of OJT007 after PO dose of 10 mg/kg using 1-compartmental analysis*

A)

Rat A

Rsq=0.9987 Rsq_adjusted=0.9983 HL_Lambda_z=1.9467
5 points used in calculation
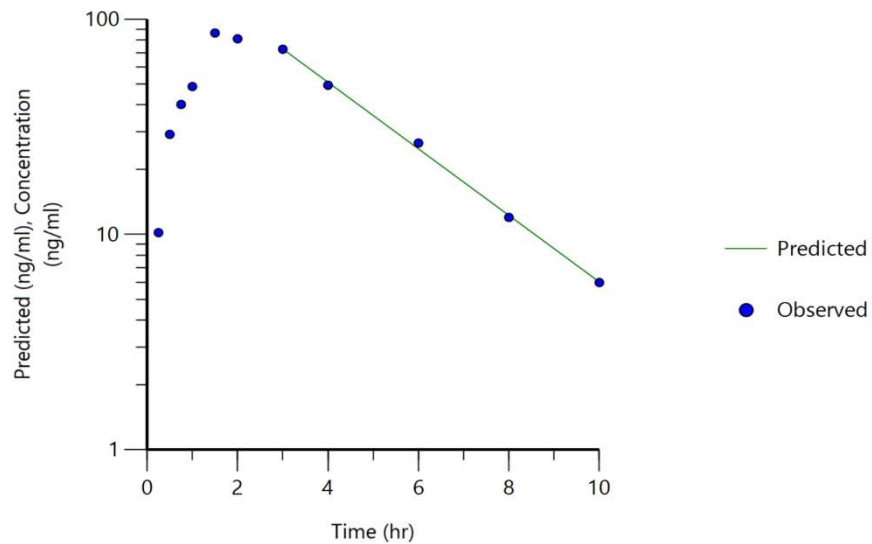
B)

Rat B

Rsq=0.9715 Rsq_adjusted=0.9643 HL_Lambda_z=2.5595
6 points used in calculation
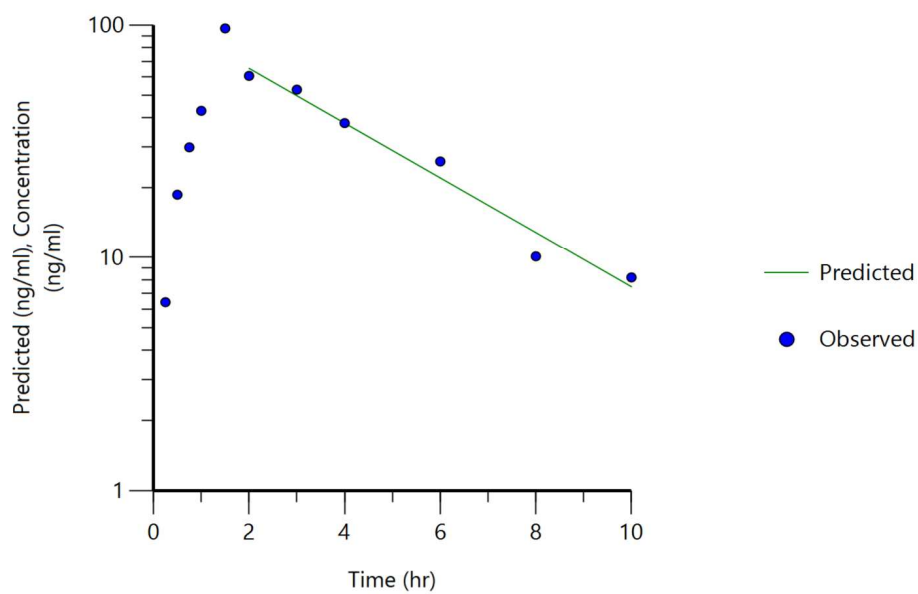
C)

Rat D

Rsq=0.9126 Rsq_adjusted=0.8908 HL_Lambda_z=3.3477
6 points used in calculation
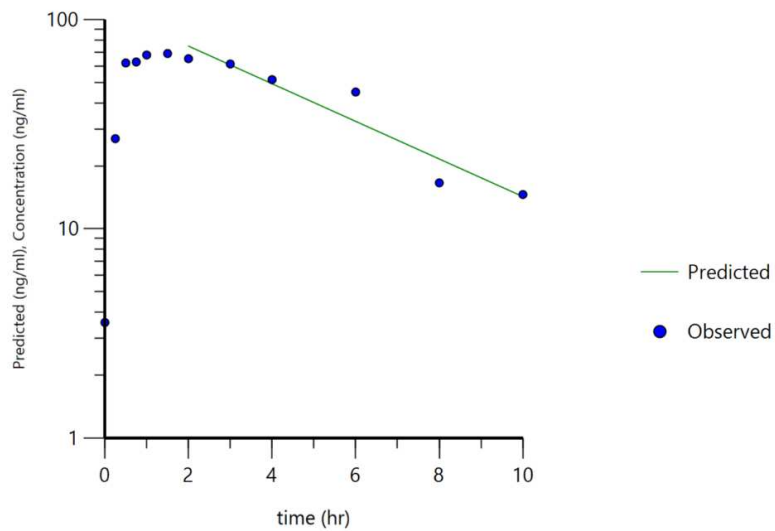
D)

Rat E

Rsq=0.9865 Rsq_adjusted=0.973 HL_Lambda_z=1.6716
3 points used in calculation

D)
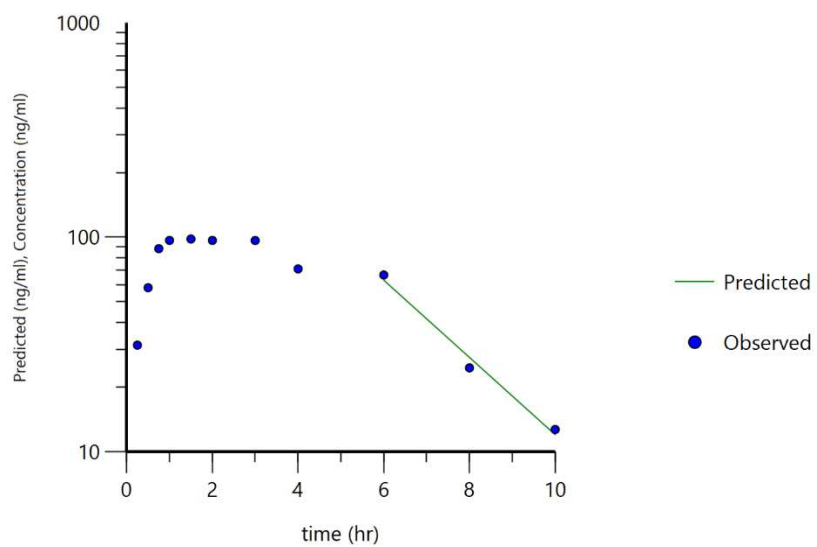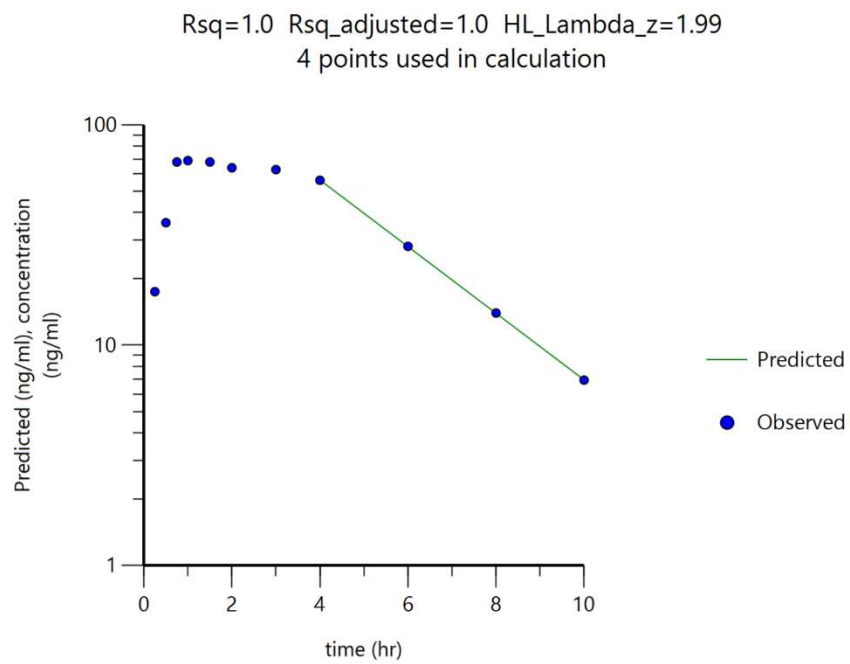
Figure 41. *Individual plots (A-E) of OJT007 after PO dose of 10 mg/kg using non compartmental analysis*

Table 15. *Mean Pharmacokinetic Parameters of OJT007 Following an Oral Dose of 10mg/Kg.*

PK Parameters (Units)	Mean ± SD	Mean ± SD
	NCA	1- Compartment
Route of Administration	Oral (n=5)	Oral (n=5)
N	5	5
Dose	10 mg/kg	10 mg/kg
C_{max} (ng/mL)	83.84 ± 14.38	76.4 ± 20.4
$T_{1//2ka}$ (hr)	-	0.98 ± 0.34
$T_{1/2}$ (hr)	2.35±0.62	2.10 ± 0.72
$AUC_{0-\infty}$ (hr.ng/mL)	451.01 ± 116.92	445.9 ± 126.4
Cl/F (L/hr/kg)	23.19 ± 5.23	23.73 ± 5.84
V_z/F (L/Kg)	78.60 ± 25.05	-
Vd/F(L/kg)	-	70.25 ± 22.99
tmax	1.4 ± 0.22	1.89±0.23
F%	10.9 ±2.47	
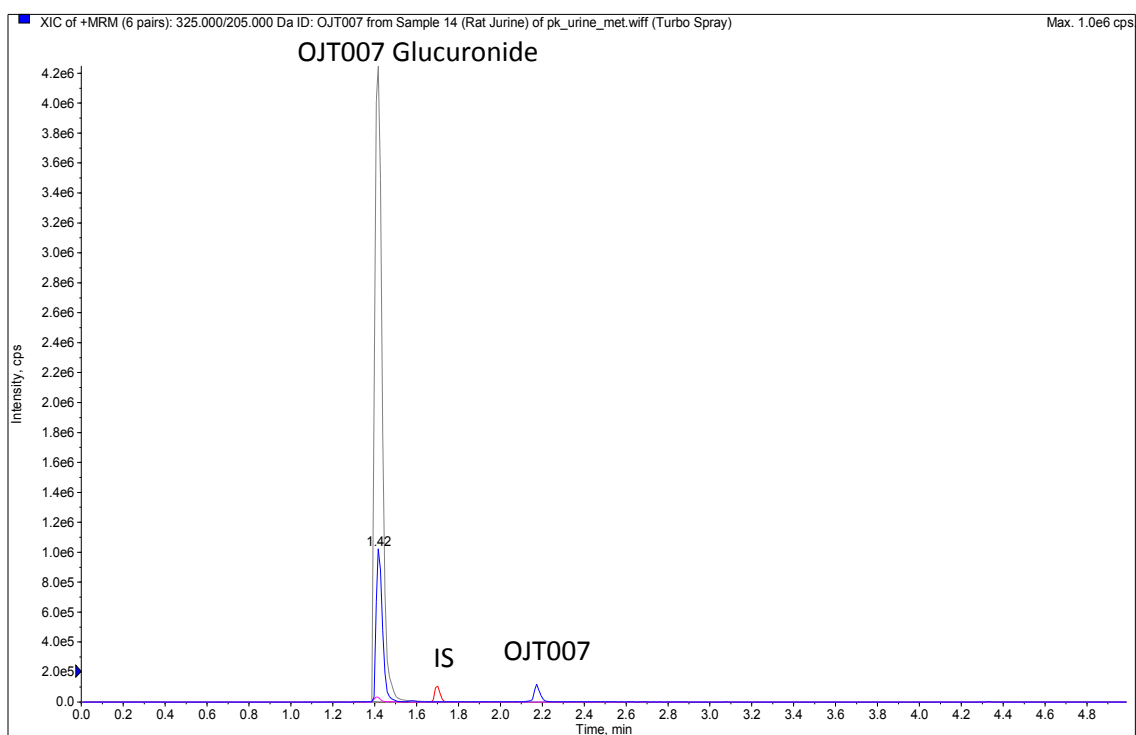
Figure 42. *Representative MRM chromatogram of rat plasma urine sample at 24 hours. Peak eluting at 1.4 minutes is OJT007 glucuronide.*

4.10.2 Drug Interaction Studies Following Co-administration of OJT007 and Rabeprazole

We conducted in vitro studies that indicated drug instability under acidic conditions. This raised the question of whether gastric degradation could contribute to drug loss prior to absorption in GI mucosa. Thus, to determine the effect of gastric fluids under fasting conditions on the absorption of OJT007, the AUC of rats treated with and without rabeprazole was assessed.

Determination of Gastric pH

The reported fasting gastric pH in rats ranges from 2.2-2.6 (Kosugi et al., 2015). Treatment with rabeprazole (10mg/Kg) increased the pH of the stomach fluid (6.5-7) 30 minutes following rabeprazole administration. The high pH on the stomach was maintained for at least 1 hour (pH 7-7.5). Two hours after rabeprazole administration, the stomach pH decreased to 4.5-5. These results demonstrate that treatment with rabeprazole can effectively increase the gastric pH in rats.

Evaluation of Pharmacokinetics in Rats Whose Gastric Acid Secretion was Controlled.

Figure 43 shows the mean OJT007 plasma concentration-time profile with and without rabeprazole pretreatment. Table 16 summarizes the pharmacokinetic parameters obtained with and without rabeprazole. We hypothesized that given the instability at acidic pH, the exposure would increase at raised pH. Contrary to our hypothesis, following pretreatment with rabeprazole, statistically significant reductions in Cmax (P = 0.022) and $AUC_{0-\infty}$ (P = 0.011) of approximately 50% were observed compared to

OJT007 alone. Interestingly, significant reductions in t_{max} ($p<0.05$) were observed. This data suggests that the mechanisms driving the poor oral bioavailability for OJT007 is not degradation in the GI tract and rather, more importantly, solubility and rapid metabolism.

High gastric pH has been shown to significantly decrease the absorption of basic drugs which have low solubility at high pH (Mitra & Kesisoglou, 2013). According to our in vitro studies, the solubility of OJT007 was low at high pH. Thus, it is possible that the increased pH caused by the PPI resulted in reduced drug solubility, and this at least in part decreased OJT007 exposure. Studies have determined that rabeprazole use does not affect gastric emptying of drugs nor the metabolism mediated by CYPs (Kosugi et al., 2015). Further studies are required to elucidate what mechanism drives the decreased exposure.
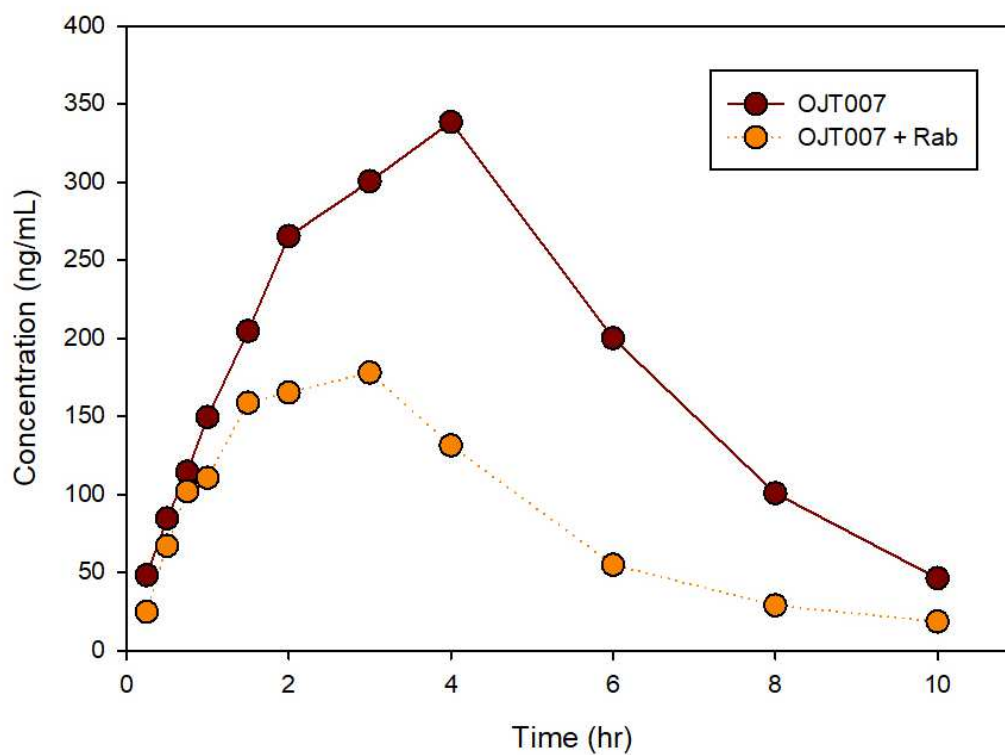
Figure 43. *Mean OJT007 plasma concentration-time profile with and without rabeprazole pretreatment.*

Table 16. *OJT007 Pharmacokinetics With and Without PH Modulator.*

PK Parameter	OJT007		OJT007+Rab		% Change
	Mean	SD	Mean	SD	
C_{max} (ng/mL)	418	149.32	184.3	65.94	44.10
AUC_{0-last} (ng.hr/mL)	1880.40	499.19	803.59	317.65	42.73
$AUC_{0-\infty}$ (ng.hr/mL)	1973.37	463.36	848.63	319.71	43.00
T_{max} (hr)	3.5	1.91	2.13	0.629	60.71

CHAPTER 5

SUMMARY AND CONCLUSION

OJT007 was identified as a methionine aminopeptidase inhibitor with potent activity against L. major, the causative agent of cutaneous leishmaniasis. Early assessment of the calculated physicochemical properties of OJT007 suggested that OJT007 would likely be orally active. In this work, preclinical studies were conducted to evaluate the feasibility of OJT007 becoming an oral chemotherapeutic for the treatment of cutaneous leishmaniasis.

Bioanalytical assays are essential throughout drug development. Certainly, preclinical development studies rely on accurate and precise quantification of the drug. Thus, our first aim was to develop and validate a sensitive, specific, and reproducible LC-MS/MS method for the quantification of OJT007 in plasma and urine. The method was accurate, precise, and linear in the concentration range of 5-1000 ng/mL and 10-1000 ng/mL for plasma and urine, respectively. This method was successfully applied to the biological samples obtained from the in-vivo studies. Furthermore, a UPLC-UV method was developed for the quantification of experiments conducted in buffers.

An important prerequisite for conducting animal studies is to have a suitable formulation of the drug. Therefore, we conducted pre-formulation studies to evaluate OJT007 basic physicochemical properties. These studies showed OJT007 is practically insoluble in water but soluble in DMSO and other common solvents.

168

Nonetheless, the solubility slightly increases under acidic conditions. On the other hand, our studies also highlighted the instability of OJT007 under acidic conditions, which raised the question of whether gastrointestinal conditions could potentially affect the exposure of orally administered OJT007. In addition, OJT007 is highly bound to plasma proteins. These properties were used for the development of a suitable formulation for in-vivo studies. A formulation comprised of 5% DMSO, 10% Tween 80, 20% PEG 400 and 65% Normal saline or water with a final concentration of 2.5 mg/mL OJT007 was found to be optimal for studies.

In vitro drug metabolism studies showed that CYP450 mediated metabolism was not a very important pathway for OJT007. On the other hand, OJT007 was rapidly glucuronidated in liver microsomes. Initial rates of glucuronidation were similar in the liver and intestine. The rapid glucuronidation of OJT007 may have important implications in the *in vivo* disposition and bioavailability of OJT007. Furthermore, in a comparison of initial rates of glucuronidation in human and rat liver microsome, it was found that glucuronidation was slower in human microsomes, suggesting that metabolism mediated by UGTs may be species-specific. Further studies are required to compare metabolism kinetics across different species to select a suitable animal model for toxicokinetic studies.

The oral bioavailability of OJT007 was evaluated in a crossover study design using rats as an animal model. Following intravenous administration, OJT007 has a biexponential disposition with a rapid distribution followed by a slower elimination. The volume of distribution for OJT007 was larger than total body water in rats, possibly due to partition into tissue. The mean systemic clearance of OJT007 approximated liver blood

flow. The extraction ratio of OJT007, calculated as the ratio of systemic clearance to liver blood, was 0.69, suggesting that OJT007 is a moderate to high extraction ratio drug. Likewise, less than 1% of the dose was recovered unchanged in urine, suggesting OJT007 is extensively metabolized.

Following a week washout period, the pharmacokinetics after oral administration of OJT007 were evaluated. OJT007 has an oral bioavailability of 10.92%. Likewise, less than 1% of the dose was recovered unchanged in urine. Assuming OJT007 to be completely absorbed and only metabolized by the liver, the expected oral bioavailability would be 31%. The lower-than-expected bioavailability would indicate that the drug is not completely absorbed and/or is metabolized in the gut. Our in vitro studies suggested an implication of intestinal UGTs in the metabolism of OJT007. Further studies are warranted to assess the gastrointestinal permeability of OJT007 to evaluate its potential role in bioavailability.

Since our in vitro stability studies showed a steep degradation for OJT007 under acidic conditions, we conducted an in-vivo study in which we controlled gastric secretion using the proton pump inhibitor rabeprazole. Contrary to our hypothesis, studies showed that increasing the gastric pH did not increase exposure but rather the opposite. Based on our solubility studies, it is possible that the increased pH decreased the solubility of the drug. For drugs to be absorbed, they must be in solution as a prerequisite. Thus, gastric acid pH did not negatively affect bioavailability. The results from our study suggest that low solubility and extensive metabolism may be major contributors to OJT007 low bioavailability.

In summary, bioanalytical assays were developed for the quantification of OJT007 in relevant biological matrices. A suitable formulation was developed for conducting animal studies. The in vitro metabolism of OJT007 was evaluated in liver microsomes. The pharmacokinetic profile of OJT007 in adult male SD rats was characterized. The effect of gastric secretion on exposure was evaluated. Essentially, our ADME evaluations demonstrated that exposure was limited by an interplay of extensive metabolism and low solubility. These studies will be invaluable to the further development of OJT007 as a drug for the oral treatment of cutaneous leishmaniasis.

REFERENCES

Abdel-Hamid, M. E. (2000). Comparative LC–MS and HPLC analyses of selected antiepileptics and beta-blocking drugs. *Il Farmaco*, *55*(2), 136–145. https://doi.org/10.1016/S0014-827X(00)00006-9

Ajavon, A. D., & Taft, D. R. (2010). Pharmacokinetics/ADME of Small Molecules. In *Preclinical Drug Development* (2nd ed.). CRC Press.

Akilov, O. E., Khachemoune, A., & Hasan, T. (2007). Clinical manifestations and classification of Old World cutaneous leishmaniasis. *International Journal of Dermatology*, *46*(2), 132–142. https://doi.org/10.1111/j.1365-4632.2007.03154.x

Barry, M. A., Koshelev, M. V., Sun, G. S., Grekin, S. J., Stager, C. E., Diwan, A. H., Wasko, C. A., Murray, K. O., & Woc-Colburn, L. (2014). Cutaneous Leishmaniasis in Cuban Immigrants to Texas who Traveled through the Darién Jungle, Panama. *The American Journal of Tropical Medicine and Hygiene*, *91*(2), 345–347. https://doi.org/10.4269/ajtmh.14-0124

Benet, L. Z. (2010). Clearance (née Rowland) concepts: A downdate and an update. *Journal of Pharmacokinetics and Pharmacodynamics*, *37*(6), 529–539. https://doi.org/10.1007/s10928-010-9187-8

Benet, L. Z., & Hoener, B.-A. (2002). Changes in plasma protein binding have little clinical relevance. *Clinical Pharmacology & Therapeutics*, *71*(3), 115–121. https://doi.org/10.1067/mcp.2002.121829

Benet, L. Z., & Zia-Amirhosseini, P. (1995). Basic Principles of Pharmacokinetics. *Toxicologic Pathology*, *23*(2), 115–123. https://doi.org/10.1177/019262339502300203

Bhat, S. Y., Dey, A., & Qureshi, I. A. (2018). Structural and functional highlights of methionine aminopeptidase 2 from Leishmania donovani. *International Journal of Biological Macromolecules*, *115*, 940–954. https://doi.org/10.1016/j.ijbiomac.2018.04.090

Bioanalytical Method Validation Guidance for Industry. (2018). 44.

Blanz, J., Williams, G., Dayer, J., Délémonté, T., Gertsch, W., Ramstein, P., Aichholz, R., Trunzer, M., & Pearson, D. (2017). Evaluation of relative MS response factors of drug metabolites for semi-quantitative assessment of chemical liabilities in drug discovery. *Journal of Mass Spectrometry*, *52*(4), 210–217. https://doi.org/10.1002/jms.3918

Bohnert, T., & Gan, L.-S. (2013). Plasma protein binding: From discovery to development. *Journal of Pharmaceutical Sciences*, *102*(9), 2953–2994. https://doi.org/10.1002/jps.23614

Bosselmann, S., & Williams, R. O. (2012). Route-Specific Challenges in the Delivery of Poorly Water-Soluble Drugs. In R. O. Williams III, A. B. Watts, & D. A. Miller (Eds.), *Formulating Poorly Water Soluble Drugs* (pp. 1–26). Springer. https://doi.org/10.1007/978-1-4614-1144-4_1

Bowers, W. F., Fulton, S., & Thompson, J. (1984). Ultrafiltration vs Equilibrium Dialysis for Determination of Free Fraction. *Clinical Pharmacokinetics*, *9*(1), 49–60. https://doi.org/10.2165/00003088-198400091-00007

Brian Houston, J. (1994). Utility of in vitro drug metabolism data in predicting in vivo metabolic clearance. *Biochemical Pharmacology*, *47*(9), 1469–1479. https://doi.org/10.1016/0006-2952(94)90520-7

Burza, S., Croft, S. L., & Boelaert, M. (2018). Leishmaniasis. *The Lancet*, *392*(10151), 951–970. https://doi.org/10.1016/S0140-6736(18)31204-2

Caldwell, G. W., & Yan, Z. (2014). Metabolic Assessment in Alamethicin Activated Liver Microsones: Co-activating CYPs and UGTs. In *Optimization in Drug Discovery*. Humana Press.

Chen, J., Wang, S., Jia, X., Bajimaya, S., Lin, H., Tam, V. H., & Hu, M. (2005). Disposition of Flavonoids Via Recycling: Comparison of Intestinal Versus Hepatic Disposition. *Drug Metabolism and Disposition*, *33*(12), 1777–1784. https://doi.org/10.1124/dmd.105.003673

Choi, B. K., Hercules, D. M., & Gusev, A. I. (2001). LC-MS/MS signal suppression effects in the analysis of pesticides in complex environmental matrices. *Fresenius' Journal of Analytical Chemistry*, *369*(3–4), 370–377. https://doi.org/10.1007/s002160000661

Correia, D., Macêdo, V. O., Carvalho, E. M., Barral, A., Magalhães, A. V., de Abreu, M. V., Orge, M. L., & Marsden, P. (1996). [Comparative study of meglumine antimoniate, pentamidine isethionate and aminosidine sulfate in the treatment of primary skin lesions caused by Leishmania (Viannia) braziliensis]. *Revista Da Sociedade Brasileira De Medicina Tropical*, *29*(5), 447–453. https://doi.org/10.1590/s0037-86821996000500007

Daly, K., De Lima, H., Kato, H., Sordillo, E. M., Convit, J., Reyes-Jaimes, O., Zerpa, O., & Paniz-Mondolfi, A. E. (2014). Intermediate cutaneous leishmaniasis caused by Leishmania (Viannia) braziliensis successfully treated with fluconazole. *Clinical*

and Experimental Dermatology, *39*(6), 708–712.

https://doi.org/10.1111/ced.12359

Davies, B., & Morris, T. (1993). Physiological Parameters in Laboratory Animals and

Humans. *Pharmaceutical Research*, *10*(7), 1093–1095.

https://doi.org/10.1023/A:1018943613122

Davis, M. E., & Brewster, M. E. (2004). Cyclodextrin-based pharmaceutics: Past, present

and future. *Nature Reviews Drug Discovery*, *3*(12), 1023–1035.

https://doi.org/10.1038/nrd1576

Deshpande, M. M., Kasture, V. S., & Chavan, M. M. and M. J. (2019). Bioanalytical

Method Development and Validation: A Review. In *Recent Advances in*

Analytical Chemistry. IntechOpen. https://doi.org/10.5772/intechopen.81620

DesJardins, C., Li, Z., & McConville, P. (n.d.). *CARRYOVER MITIGATION USING*

NEEDLE WASH SOLVENT CHEMISTRY AND AUTOSAMPLER FEATURES OF

A UPLC-MS SYSTEM. 1.

Di, L., Kerns, E. H., Gao, N., Li, S. Q., Huang, Y., Bourassa, J. L., & Huryn, D. M.

(2004). Experimental Design on Single-Time-Point High-Throughput Microsomal

Stability Assay. *Journal of Pharmaceutical Sciences*, *93*(6), 1537–1544.

https://doi.org/10.1002/jps.20076

Di, L., & Obach, R. S. (2015). Addressing the Challenges of Low Clearance in Drug

Research. *The AAPS Journal*, *17*(2), 352–357. https://doi.org/10.1208/s12248-

014-9691-7

Dorlo, T. P. C., Balasegaram, M., Beijnen, J. H., & de Vries, P. J. (2012). Miltefosine: A

review of its pharmacology and therapeutic efficacy in the treatment of

leishmaniasis. *Journal of Antimicrobial Chemotherapy*, *67*(11), 2576–2597. https://doi.org/10.1093/jac/dks275

Dorlo, T. P. C., van Thiel, P. P. A. M., Huitema, A. D. R., Keizer, R. J., de Vries, H. J. C., Beijnen, J. H., & de Vries, P. J. (2008). Pharmacokinetics of Miltefosine in Old World Cutaneous Leishmaniasis Patients. *Antimicrobial Agents and Chemotherapy*, *52*(8), 2855–2860. https://doi.org/10.1128/AAC.00014-08

El-On, J., Livshin, R., Even-Paz, Z. v. i., Hamburger, D., & Weinrauch, L. (1986). Topical Treatment of Cutaneous Leishmaniasis. *Journal of Investigative Dermatology*, *87*(2), 284–288. https://doi.org/10.1111/1523-1747.ep12696697

Eriksson, U. (2001). Comparison of effects of amphotericin B deoxycholate infused over 4 or 24 hours: Randomised controlled. *BMJ*, *322*(7286), 579–579. https://doi.org/10.1136/bmj.322.7286.579

Galvão, E. L., Rabello, A., & Cota, G. F. (2017). Efficacy of azole therapy for tegumentary leishmaniasis: A systematic review and meta-analysis. *PLOS ONE*, *12*(10), e0186117. https://doi.org/10.1371/journal.pone.0186117

Gao, S., Yang, Z., Yin, T., You, M., & Hu, M. (2011). Validated LC-MS/MS method for the determination of maackiain and its sulfate and glucuronide in blood: Application to pharmacokinetic and disposition studies. *Journal of Pharmaceutical and Biomedical Analysis*, *55*(2), 288–293. https://doi.org/10.1016/j.jpba.2011.01.015

Gardiner, D. L., Skinner-Adams, T. S., Brown, C. L., Andrews, K. T., Stack, C. M., McCarthy, J. S., Dalton, J. P., & Trenholme, K. R. (2009). *Plasmodium falciparum*: New molecular targets with potential for antimalarial drug

development. *Expert Review of Anti-Infective Therapy*, *7*(9), 1087–1098. https://doi.org/10.1586/eri.09.93

Garza-Tovar, T. F., Sacriste-Hernández, M. I., Juárez-Durán, E. R., & Arenas, R. (2020). An overview of the treatment of cutaneous leishmaniasis. *Faculty Reviews*, *9*, 28. https://doi.org/10.12703/r/9-28

Ghannoum, M. A., & Rice, L. B. (1999). Antifungal Agents: Mode of Action, Mechanisms of Resistance, and Correlation of These Mechanisms with Bacterial Resistance. *Clinical Microbiology Reviews*, *12*(4), 501–517.

Gibaldi, M. (1991). Introduction to Pharmacokinetics. In *Biopharmaceutics and Clinical Pharmacokinetics* (4th ed.). Lea and Febiger.

Golgher, D., Vianna, C. H., & Moura, A. C. (2011). Drugs against leishmaniasis: Overview of market needs and pipeline. *Drug Development Research*, *72*(6), 463–470. https://doi.org/10.1002/ddr.20453

Goto, H., & Lauletta Lindoso, J. A. (2012). Cutaneous and Mucocutaneous Leishmaniasis. *Infectious Disease Clinics of North America*, *26*(2), 293–307. https://doi.org/10.1016/j.idc.2012.03.001

Goto, H., & Lindoso, J. A. L. (2010). Current diagnosis and treatment of cutaneous and mucocutaneous leishmaniasis. *Expert Review of Anti-Infective Therapy*, *8*(4), 419–433. https://doi.org/10.1586/eri.10.19

Gu, H., Liu, G., Wang, J., Aubry, A.-F., & Arnold, M. E. (2014). Selecting the Correct Weighting Factors for Linear and Quadratic Calibration Curves with Least-Squares Regression Algorithm in Bioanalytical LC-MS/MS Assays and Impacts of Using Incorrect Weighting Factors on Curve Stability, Data Quality, and Assay

Performance. *Analytical Chemistry, 86*(18), 8959–8966.

https://doi.org/10.1021/ac5018265

Guidance for Industry, Investigators, and Reviewers: Exploratory IND Studies. (2006).

Biotechnology Law Report, 25(2), 167–174.

https://doi.org/10.1089/blr.2006.25.167

Han, C., Davis, C. B., & Wang, B. (2010). *Evaluation of Drug Candidates for Preclinical*

Development: Pharmacokinetics, Metabolism, Pharmaceutics, and Toxicology.

John Wiley & Sons, Incorporated.

http://ebookcentral.proquest.com/lib/uh/detail.action?docID=479843

Hrycay, E., & Bandiera, S. (2008). Cytochrome P450 Enzymes. In *Preclinical*

Development Handbook: ADME and Biopharmaceutical Properties. John Wiley

& Sons, Incorporated.

Jiamboonsri, P., Pithayanukul, P., Bavovada, R., Leanpolchareanchai, J., Gao, S., & Hu,

M. (2016). In vitro glucuronidation of methyl gallate and pentagalloyl

glucopyranose by liver microsomes. *Drug Metabolism and Pharmacokinetics*,

31(4), 292–303. https://doi.org/10.1016/j.dmpk.2016.04.003

Jones, C. R., Hatley, O. J. D., Ungell, A.-L., Hilgendorf, C., Peters, S. A., & Rostami-

Hodjegan, A. (2016). Gut Wall Metabolism. Application of Pre-Clinical Models

for the Prediction of Human Drug Absorption and First-Pass Elimination. *The*

AAPS Journal, 18(3), 589–604. https://doi.org/10.1208/s12248-016-9889-y

Kang, J.-M., Ju, H.-L., Sohn, W.-M., & Na, B.-K. (2012). Characterization of the

biochemical properties of two methionine aminopeptidases of Cryptosporidium

parvum. *Parasitology International*, *61*(4), 707–710.
https://doi.org/10.1016/j.parint.2012.05.008

Karunaweera, N. D., Ginige, S., Senanayake, S., Silva, H., Manamperi, N.,
Samaranayake, N., Siriwardana, Y., Gamage, D., Senerath, U., & Zhou, G. (n.d.).
*Spatial Epidemiologic Trends and Hotspots of Leishmaniasis, Sri Lanka, 2001–
2018—Volume 26, Number 1—January 2020—Emerging Infectious Diseases
journal—CDC*. https://doi.org/10.3201/eid2601.190971

Kato, K. C., Morais-Teixeira, E., Reis, P. G., Silva-Barcellos, N. M., Salaün, P., Campos,
P. P., Dias Corrêa-Junior, J., Rabello, A., Demicheli, C., & Frézard, F. (2014).
Hepatotoxicity of Pentavalent Antimonial Drug: Possible Role of Residual Sb(III)
and Protective Effect of Ascorbic Acid. *Antimicrobial Agents and Chemotherapy*,
58(1), 481–488. https://doi.org/10.1128/AAC.01499-13

Kaur, G., & Rajput, B. (2014). Comparative Analysis of the Omics Technologies Used to
Study Antimonial, Amphotericin B, and Pentamidine Resistance in Leishmania.
Journal of Parasitology Research, *2014*, 726328.
https://doi.org/10.1155/2014/726328

Keller, B. O., Sui, J., Young, A. B., & Whittal, R. M. (2008). Interferences and
contaminants encountered in modern mass spectrometry. *Analytica Chimica Acta*,
627(1), 71–81. https://doi.org/10.1016/j.aca.2008.04.043

Khalil, E. A., Alkawareek, M. Y., Othman, G., Tbakhi, B., & Al-Bakri, A. G. (2019).
Evaluation of paromomycin sulphate permeation using *ex vivo* human skin model.
Pharmaceutical Development and Technology, *24*(3), 390–393.
https://doi.org/10.1080/10837450.2018.1485697

Knights, K. M., Stresser, D. M., Miners, J. O., & Crespi, C. L. (2016). In Vitro Drug Metabolism Using Liver Microsomes. *Current Protocols in Pharmacology*, *74*(1), 7.8.1-7.8.24. https://doi.org/10.1002/cpph.9

Kosugi, Y., Yamamoto, S., Sano, N., Furuta, A., Igari, T., Fujioka, Y., & Amano, N. (2015). Evaluation of Acid Tolerance of Drugs Using Rats and Dogs Controlled for Gastric Acid Secretion. *Journal of Pharmaceutical Sciences*, *104*(9), 2887–2893. https://doi.org/10.1002/jps.24401

Leishmaniasis. (n.d.). Retrieved October 16, 2021, from https://www.who.int/news-room/fact-sheets/detail/leishmaniasis

Li, F., Ulrich, M. L., Shih, V. F.-S., Cochran, J. H., Hunter, J. H., Westendorf, L., Neale, J., & Benjamin, D. R. (2019). Mouse Strains Influence Clearance and Efficacy of Antibody and Antibody–Drug Conjugate Via Fc–FcγR Interaction. *Molecular Cancer Therapeutics*, *18*(4), 780–787. https://doi.org/10.1158/1535-7163.MCT-18-0977

Li, M., Zhu, L., Chen, L., Li, N., & Qi, F. (2018). Assessment of drug–drug interactions between voriconazole and glucocorticoids. *Journal of Chemotherapy, 30*(5), 296–303. https://doi.org/10.1080/1120009X.2018.1506693

Li, P., Wang, X., Li, J., Meng, Z.-Y., Li, S.-C., Li, Z.-J., Lu, Y.-Y., Ren, H., Lou, Y.-Q., Lu, C., Dou, G.-F., & Zhang, G.-L. (2015). Quantitative and qualitative analysis of the novel antitumor 1,3,4-oxadiazole derivative (GLB) and its metabolites using HPLC-UV and UPLC-QTOF-MS. *Scientific Reports*, *5*(1), 11906. https://doi.org/10.1038/srep11906

Li, X., & Chang, Y. H. (1995). Amino-terminal protein processing in Saccharomyces cerevisiae is an essential function that requires two distinct methionine aminopeptidases. *Proceedings of the National Academy of Sciences*, *92*(26), 12357–12361. https://doi.org/10.1073/pnas.92.26.12357

Li, Y., McCabe, M., Podila, L., Tracy, T. S., & Tweedie, D. J. (2014). Case Study 3. Application of Basic Enzyme Kinetics to Metabolism Studies: Real-Life Examples. In S. Nagar, U. A. Argikar, & D. J. Tweedie (Eds.), *Enzyme Kinetics in Drug Metabolism: Fundamentals and Applications* (pp. 441–460). Humana Press. https://doi.org/10.1007/978-1-62703-758-7_20

Lin, J. H., Chiba, M., & Baillie, T. A. (n.d.). *Is the Role of the Small Intestine in First-Pass Metabolism Overemphasized?* 23.

Lipinski, C. A., Lombardo, F., Dominy, B. W., & Feeney, P. J. (1997). Experimental and computational approaches to estimate solubility and permeability in drug discovery and development settings. *Advanced Drug Delivery Reviews*, *23*(1), 3–25. https://doi.org/10.1016/S0169-409X(96)00423-1

Liu, G., & Aubry, A.-F. (n.d.). Best Practices in Biological Sample Preparation for LC-MS Bioanalysis. In *Handbook of LC-MS/MS Bioanalysis*.

Lynch, T., & Neff, A. P. (2007). The Effect of Cytochrome P450 Metabolism on Drug Response, Interactions, and Adverse Effects. *American Family Physician*, *76*(3), 391–396.

Machado, P. R. L., & Penna, G. (2012). Miltefosine and cutaneous leishmaniasis: *Current Opinion in Infectious Diseases*, *25*(2), 141–144. https://doi.org/10.1097/QCO.0b013e3283509cac

Mannur, V. S., Patel, D., Mastiholimath, V. S., & Shah, G. (2011). Selection of buffers in LC-MS/MS: An overview. *International Journal of Pharmaceutical Sciences Review and Research*, *6*, 34–37.

Mayersohn, M. (2002). Principles of Drug Absorption. In *Modern Pharmaceutics* (Fourth, pp. 23–61). Marcel Dekker, Inc.

McIlwee, B. E., Weis, S. E., & Hosler, G. A. (2018). Incidence of Endemic Human Cutaneous Leishmaniasis in the United States. *JAMA Dermatology*, *154*(9), 1032–1039. https://doi.org/10.1001/jamadermatol.2018.2133

Minodier, P., & Parola, P. (2007). Cutaneous leishmaniasis treatment. *Travel Medicine and Infectious Disease*, *5*(3), 150–158. https://doi.org/10.1016/j.tmaid.2006.09.004

Mitra, A., & Kesisoglou, F. (2013). Impaired Drug Absorption Due to High Stomach pH: A Review of Strategies for Mitigation of Such Effect To Enable Pharmaceutical Product Development. *Molecular Pharmaceutics*, *10*(11), 3970–3979. https://doi.org/10.1021/mp400256h

Mohammadi, J., & Soltani, A. (2019). Epidemiologic Profile of Cutaneous Leishmaniasis Between 2010—2016 in an Endemic Area of Fars Province, South Iran. *Shiraz E-Medical Journal*, *20*(9), Article 9. https://doi.org/10.5812/semj.86445

Mohs, R. C., & Greig, N. H. (2017). Drug discovery and development: Role of basic biological research. *Alzheimer's & Dementia : Translational Research & Clinical Interventions*, *3*(4), 651–657. https://doi.org/10.1016/j.trci.2017.10.005

Navia, M. A., & Chaturvedi, P. R. (1996). Design principles for orally bioavailable drugs. *Drug Discovery Today*, *1*(5), 179–189. https://doi.org/10.1016/1359-6446(96)10020-9

Niazi, S. K. (2019). The Scope of Preformulation Studies. In *Handbook of Preformulation* (2nd ed.). CRC Press.

Nielsen-Kudsk, F., Magnussen, I., Jensen, T. S., & Naeser, K. (2009). Bioavailability and Pharmacokinetics in Man of Orally Administered Theophylline. *Acta Pharmacologica et Toxicologica*, *46*(3), 205–212. https://doi.org/10.1111/j.1600-0773.1980.tb02444.x

Obach, R. S. (n.d.). *PREDICTION OF HUMAN CLEARANCE OF TWENTY-NINE DRUGS FROM HEPATIC MICROSOMAL INTRINSIC CLEARANCE DATA: AN EXAMINATION OF IN VITRO HALF-LIFE APPROACH AND NONSPECIFIC BINDING TO MICROSOMES*. 10.

Obach, R. S. (1999). Prediction of Human Clearance of Twenty-Nine Drugs from Hepatic Microsomal Intrinsic Clearance Data: An Examination of In Vitro Half-Life Approach and Nonspecific Binding to Microsomes. *Drug Metabolism and Disposition*, *27*(11), 1350–1359.

Obach, R. S., Baxter, J. G., Liston, T. E., Silber, B. M., Jones, B. C., Macintyre, F., Rance, D. J., & Wastall, P. (1997). *The Prediction of Human Pharmacokinetic Parameters from Preclinical and In Vitro Metabolism Data*. *283*, 13.

Olaleye, O. A., Bishai, W. R., & Liu, J. O. (2009). Targeting the role of N-terminal methionine processing enzymes in Mycobacterium tuberculosis. *Tuberculosis*, *89*, S55–S59. https://doi.org/10.1016/S1472-9792(09)70013-7

Olaleye, O., Raghunand, T. R., Bhat, S., Chong, C., Gu, P., Zhou, J., Zhang, Y., Bishai, W. R., & Liu, J. O. (2011). Characterization of clioquinol and analogues as novel inhibitors of methionine aminopeptidases from Mycobacterium tuberculosis. *Tuberculosis*, *91*, S61–S65. https://doi.org/10.1016/j.tube.2011.10.012

Olaleye, O., Raghunand, T. R., Bhat, S., He, J., Tyagi, S., Lamichhane, G., Gu, P., Zhou, J., Zhang, Y., Grosset, J., Bishai, W. R., & Liu, J. O. (2010). Methionine Aminopeptidases from Mycobacterium tuberculosis as Novel Antimycobacterial Targets. *Chemistry & Biology*, *17*(1), 86–97. https://doi.org/10.1016/j.chembiol.2009.12.014

Oliveira-Neto, M. P., Schubach, A., Mattos, M., Gonçalves da Costa, S. C., & Pirmez, C. (1997). Intralesional therapy of American cutaneous leishmaniasis with pentavalent antimony in Rio de Janeiro, Brazil – an area of Leishmania (V.) braziliensis transmission. *International Journal of Dermatology*, *36*(6), 463–468. https://doi.org/10.1046/j.1365-4362.1997.00188.x

Pan American Health Organization. (2018). *Leishmaniasis. Epidemiological Report of the America*. https://iris.paho.org/handle/10665.2/34856

Pandey, S. C., Pande, V., & Samant, M. (2020). DDX3 DEAD-box RNA helicase (Hel67) gene disruption impairs infectivity of Leishmania donovani and induces protective immunity against visceral leishmaniasis. *Scientific Reports*, *10*, 18218. https://doi.org/10.1038/s41598-020-75420-y

Pearson, R. D., & Sousa, A. d. Q. (1996). Clinical Spectrum of Leishmaniasis. *Clinical Infectious Diseases*, *22*(1), 1–13. https://doi.org/10.1093/clinids/22.1.1

Piccica, M., Lagi, F., Bartoloni, A., & Zammarchi, L. (2021). Efficacy and safety of
 pentamidine isethionate for tegumentary and visceral human leishmaniasis: A
 systematic review. *Journal of Travel Medicine*, *28*(6), taab065.
 https://doi.org/10.1093/jtm/taab065

Reithinger, R., Dujardin, J.-C., Louzir, H., Pirmez, C., Alexander, B., & Brooker, S.
 (2007). Cutaneous leishmaniasis. *The Lancet Infectious Diseases*, *7*(9), 581–596.
 https://doi.org/10.1016/S1473-3099(07)70209-8

Robinson, K., Mock, C., & Liang, D. (2015). Pre-formulation studies of resveratrol. *Drug
 Development and Industrial Pharmacy*, *41*(9), 1464–1469.
 https://doi.org/10.3109/03639045.2014.958753

Rodriguez, F., John, S. F., Iniguez, E., Montalvo, S., Michael, K., White, L., Liang, D.,
 Olaleye, O. A., & Maldonado, R. A. (2020). *In Vitro* and *In Vivo* Characterization
 of Potent Antileishmanial Methionine Aminopeptidase-1 Inhibitors. *Antimicrobial
 Agents and Chemotherapy*, AAC.01422-19, aac;AAC.01422-19v1.
 https://doi.org/10.1128/AAC.01422-19

Rogge, M. C. (2010). The Scope of Preclinical Drug Development: An Introduction and
 Framework. In *Preclinical Drug Development* (2nd ed.). CRC Press.

Ronald Schoenwal. (2002). Basic Principles. In *Pharmacokinetics in Drug Discovery and
 Development*. CRC Press.

Ronfeld, R. A., & Benet, L. Z. (1977). Interpretation of Plasma Concentration-Time
 Curves after Oral Dosing. *Journal of Pharmaceutical Sciences*, *66*(2), 178–180.
 https://doi.org/10.1002/jps.2600660211

Rostamian, M., & Niknam, H. M. (2019). Chapter One - Leishmania tropica: What we know from its experimental models. In D. Rollinson & J. R. Stothard (Eds.), *Advances in Parasitology* (Vol. 104, pp. 1–38). Academic Press. https://doi.org/10.1016/bs.apar.2018.11.001

Rowland, A., Miners, J. O., & Mackenzie, P. I. (2013). The UDP-glucuronosyltransferases: Their role in drug metabolism and detoxification. *The International Journal of Biochemistry & Cell Biology*, *45*(6), 1121–1132. https://doi.org/10.1016/j.biocel.2013.02.019

Rowland, M. (1972). Influence of Route of Administration on Drug Availability. *Journal of Pharmaceutical Sciences*, *61*(1), 70–74. https://doi.org/10.1002/jps.2600610111

Rudek, M. A., Chau, C. H., Figg, W. D., & McLeod, H. L. (Eds.). (2014). *Handbook of Anticancer Pharmacokinetics and Pharmacodynamics*. Springer New York. https://doi.org/10.1007/978-1-4614-9135-4

Ryan, E. T., & Magill, A. J. (2020). 174—Pentavalent Antimony. In E. T. Ryan, D. R. Hill, T. Solomon, N. E. Aronson, & T. P. Endy (Eds.), *Hunter's Tropical Medicine and Emerging Infectious Diseases (Tenth Edition)* (pp. 1167–1168). Elsevier. https://doi.org/10.1016/B978-0-323-55512-8.00174-5

Saenz, R. E., Paz, H., & Berman, J. D. (1990). Efficacy of ketoconazole against Leishmania braziliensis panamensis cutaneous leishmaniasis. *The American Journal of Medicine*, *89*(2), 147–155. https://doi.org/10.1016/0002-9343(90)90292-L

Scior, T., & Garces-Eisele, S. J. (2006). Isoniazid is Not a Lead Compound for its Pyridyl
Ring Derivatives,Isonicotinoyl Amides, Hydrazides, and Hydrazones: A Critical
Review. *Current Medicinal Chemistry*, *13*(18), 2205–2219.

Scorza, B. M., Carvalho, E. M., & Wilson, M. E. (2017). Cutaneous Manifestations of
Human and Murine Leishmaniasis. *International Journal of Molecular Sciences*,
18(6), 1296. https://doi.org/10.3390/ijms18061296

Séguin, O., & Descoteaux, A. (2016). Leishmania, the phagosome, and host responses:
The journey of a parasite. *Cellular Immunology*, *309*, 1–6.
https://doi.org/10.1016/j.cellimm.2016.08.004

Seibert, E., & Tracy, T. S. (2014). Fundamentals of Enzyme Kinetics. In S. Nagar, U. A.
Argikar, & D. J. Tweedie (Eds.), *Enzyme Kinetics in Drug Metabolism:*
Fundamentals and Applications (pp. 9–22). Humana Press.
https://doi.org/10.1007/978-1-62703-758-7_2

Semalty, A. (2014). Cyclodextrin and phospholipid complexation in solubility and
dissolution enhancement: A critical and meta-analysis. *Expert Opinion on Drug*
Delivery, *11*(8), 1255–1272. https://doi.org/10.1517/17425247.2014.916271

Sensenhauser, C. (2014). In Vitro CYP/FMO Reaction Phenotyping. In *Optimization in*
Drug Discovery. Springer.

Sharma, U., & Singh, S. (2008). Insect vectors of Leishmania: Distribution, physiology
and their control. *J VECTOR BORNE DIS*, 18.

Singh, G. (2018). Preclinical Drug Development. In *Pharmaceutical Medicine and*
Translational Clinical Research (pp. 47–63). Elsevier.

Słoczyńska, K., Gunia-Krzyżak, A., Koczurkiewicz, P., Wójcik-Pszczoła, K., Żelaszczyk, D., Popiół, J., & Pękala, E. (2019). Metabolic stability and its role in the discovery of new chemical entities. *Acta Pharmaceutica*, *69*(3), 345–361. https://doi.org/10.2478/acph-2019-0024

Smith, D. A., Beaumont, K., Maurer, T. S., & Di, L. (2015). Volume of Distribution in Drug Design: Miniperspective. *Journal of Medicinal Chemistry*, *58*(15), 5691–5698. https://doi.org/10.1021/acs.jmedchem.5b00201

Smith, D. A., Di, L., & Kerns, E. H. (2010). The effect of plasma protein binding on in vivo efficacy: Misconceptions in drug discovery. *Nature Reviews Drug Discovery*, *9*(12), 929–939. https://doi.org/10.1038/nrd3287

Solomon, M., Pavlotsky, F., Leshem, E., Ephros, M., Trau, H., & Schwartz, E. (2011). Liposomal amphotericin B treatment of cutaneous leishmaniasis due to Leishmania tropica. *Journal of the European Academy of Dermatology and Venereology*, *25*(8), 973–977. https://doi.org/10.1111/j.1468-3083.2010.03908.x

Song, N.-N., Zhang, S.-Y., & Liu, C.-X. (2004). Overview of factors affecting oral drug absorption. *Asian J Drug Metabolism Pharmacokinetics*, *4*, 167–176.

Soto, J., Arana, B. A., Toledo, J., Rizzo, N., Vega, J. C., Diaz, A., Luz, M., Gutierrez, P., Arboleda, M., Berman, J. D., Junge, K., Engel, J., & Sindermann, H. (2004). Miltefosine for New World Cutaneous Leishmaniasis. *Clinical Infectious Diseases*, *38*(9), 1266–1272. https://doi.org/10.1086/383321

Soto, J., Grogl, M., Berman, J., & Olliaro, P. (1994). Limited efficacy of injectable aminosidine as single-agent therapy for Colombian cutaneous leishmaniasis.

Transactions of the Royal Society of Tropical Medicine and Hygiene, *88*(6), 695–698. https://doi.org/10.1016/0035-9203(94)90235-6

Soto, J. M., Toledo, J. T., Gutierrez, P., Arboleda, M., Nicholls, R. S., Padilla, J. R., Berman, J. D., English, C. K., & Grogl, M. (2002). Treatment of cutaneous leishmaniasis with a topical antileishmanial drug (WR279396): Phase 2 pilot study. *The American Journal of Tropical Medicine and Hygiene*, *66*(2), 147–151. https://doi.org/10.4269/ajtmh.2002.66.147

Soto, J., Toledo, J., Valda, L., Balderrama, M., Rea, I., Parra, R., Ardiles, J., Soto, P., Gomez, A., Molleda, F., Fuentelsaz, C., Anders, G., Sindermann, H., Engel, J., & Berman, J. (2007). Treatment of Bolivian Mucosal Leishmaniasis with Miltefosine. *Clinical Infectious Diseases*, *44*(3), 350–356. https://doi.org/10.1086/510588

Soto-Mancipe, J., Grogl, M., & Berman, J. D. (1993). Evaluation of Pentamidine for the Treatment of Cutaneous Leishmaniasis in Colombia. *Clinical Infectious Diseases*, *16*(3), 417–425.

Sterling, H. J., Batchelor, J. D., Wemmer, D. E., & Williams, E. R. (2010). Effects of Buffer Loading for Electrospray Ionization Mass Spectrometry of a Noncovalent Protein Complex that Requires High Concentrations of Essential Salts. *Journal of the American Society for Mass Spectrometry*, *21*(6), 1045–1049. https://doi.org/10.1016/j.jasms.2010.02.003

Sui, Y., Wu, J., & Chen, J. (2021). The Role of Gut Microbial β-Glucuronidase in Estrogen Reactivation and Breast Cancer. *Frontiers in Cell and Developmental Biology*, *9*, 2067. https://doi.org/10.3389/fcell.2021.631552

Sundar, S., Agrawal, G., Rai, M., Makharia, M. K., & Murray, H. W. (2001). Treatment of Indian visceral leishmaniasis with single or daily infusions of low dose liposomal amphotericin B: Randomised trial. *BMJ : British Medical Journal*, *323*(7310), 419–422.

Sundar, S., & Chakravarty, J. (2013). Leishmaniasis: An update of current pharmacotherapy. *Expert Opinion on Pharmacotherapy*, *14*(1), 53–63. https://doi.org/10.1517/14656566.2013.755515

Sunter, J., & Gull, K. (2017). Shape, form, function and Leishmania pathogenicity: From textbook descriptions to biological understanding. *Open Biology*, *7*(9), 170165. https://doi.org/10.1098/rsob.170165

Takahashi, R. H., Choo, E. F., Ma, S., Wong, S., Halladay, J., Deng, Y., Rooney, I., Gates, M., Hop, C. E. C. A., Khojasteh, S. C., Dresser, M. J., & Musib, L. (2016). Absorption, Metabolism, Excretion, and the Contribution of Intestinal Metabolism to the Oral Disposition of [14C]Cobimetinib, a MEK Inhibitor, in Humans. *Drug Metabolism and Disposition*, *44*(1), 28–39. https://doi.org/10.1124/dmd.115.066282

Temesi, D., Law, B., & Howe, N. (2003). Synthesis and evaluation of PEG414, a novel formulating agent that avoids analytical problems associated with polydisperse vehicles such as PEG400. *Journal of Pharmaceutical Sciences*, *92*(12), 2512–2518. https://doi.org/10.1002/jps.10514

Thakur, C. P., Kumar, M., Kumar, P., Mishra, B. N., & Pandey, A. K. (1988). Rationalisation of regimens of treatment of kala-azar with sodium stibogluconate

in India: A randomised study. *BMJ, 296*(6636), 1557–1561. https://doi.org/10.1136/bmj.296.6636.1557

Tiwari, G., & Tiwari, R. (2010). Bioanalytical method validation: An updated review. *Pharmaceutical Methods*, *1*(1), 25–38. https://doi.org/10.4103/2229-4708.72226

Toma, C.-M., Imre, S., Vari, C.-E., Muntean, D.-L., & Tero-Vescan, A. (2021). Ultrafiltration Method for Plasma Protein Binding Studies and Its Limitations. *Processes*, *9*(2), 382. https://doi.org/10.3390/pr9020382

Trivedi, J. S., & Yue, Z. (2017). Solubilization Using Cosolvent Approach. In *Water-Insoluble Drug Formulation* (3rd ed.). CRC Press.

Tuntland, T., Ethell, B., Kosaka, T., Blasco, F., Zang, R. X., Jain, M., Gould, T., & Hoffmaster, K. (2014). Implementation of pharmacokinetic and pharmacodynamic strategies in early research phases of drug discovery and development at Novartis Institute of Biomedical Research. *Frontiers in Pharmacology*, *5*. https://doi.org/10.3389/fphar.2014.00174

US Food and Drug Administration. (2012). In Vitro Metabolism- and Transporter-Mediated Drug-Drug Interaction Studies Guidance for Industry. *Interaction Studies*, 47.

USFDA. (2018). *Guidance for Industry: Bioanalytical Method Validation*.

van Griensven, J., & Diro, E. (2012). Visceral Leishmaniasis. *Infectious Disease Clinics of North America*, *26*(2), 309–322. https://doi.org/10.1016/j.idc.2012.03.005

van Hees, C. L. M., & Naafs, B. (2016). Cutaneous Leishmaniasis. In J. H. Ólafsson & R. J. Hay (Eds.), *Antibiotic and Antifungal Therapies in Dermatology* (pp. 291–338). Springer International Publishing. https://doi.org/10.1007/978-3-319-39424-4_11

Vélez, I. D., Jiménez, A., Vásquez, D., & Robledo, S. M. (2015). Disseminated Cutaneous Leishmaniasis in Colombia: Report of 27 Cases. *Case Reports in Dermatology*, *7*(3), 275–286. https://doi.org/10.1159/000441120

Vera, A. M., Mantilla, J. C., & Escobar, P. (2021). Anti-leishmanial activity of 29 daily sessions of intralesional-pentavalent antimony administration on Leishmania (Viannia)-infected BALB/c mice. *Revista de Biología Tropical*, *69*(4), 1179–1188. https://doi.org/10.15517/rbt.v69i4.47368

Weinrauch, L., Livshin, R., Even-Paz, Z., & El-On, J. (1983). Efficacy of ketoconazole in cutaneous leishmaniasis. *Archives of Dermatological Research*, *275*(5), 353–354. https://doi.org/10.1007/BF00417211

Wijnant, G.-J., Van Bocxlaer, K., Fortes Francisco, A., Yardley, V., Harris, A., Alavijeh, M., Murdan, S., & Croft, S. L. (2018). Local Skin Inflammation in Cutaneous Leishmaniasis as a Source of Variable Pharmacokinetics and Therapeutic Efficacy of Liposomal Amphotericin B. *Antimicrobial Agents and Chemotherapy*, *62*(10). https://doi.org/10.1128/aac.00631-18

Wortmann, G., Miller, R. S., Oster, C., Jackson, J., & Aronson, N. (2002). A Randomized, Double‐Blind Study of the Efficacy of a 10‐ or 20‐Day Course of Sodium Stibogluconate for Treatment of Cutaneous Leishmaniasis in United States Military Personnel. *Clinical Infectious Diseases*, *35*(3), 261–267. https://doi.org/10.1086/341406

Wright, N. A., Davis, L. E., Aftergut, K. S., Parrish, C. A., & Cockerell, C. J. (2008). Cutaneous leishmaniasis in Texas: A northern spread of endemic areas. *Journal of*

the American Academy of Dermatology, *58*(4), 650–652.

https://doi.org/10.1016/j.jaad.2007.11.008

Wu, B., Kulkarni, K., Basu, S., Zhang, S., & Hu, M. (2011). First-Pass Metabolism via

UDP-Glucuronosyltransferase: A Barrier to Oral Bioavailability of Phenolics.

Journal of Pharmaceutical Sciences, *100*(9), 3655–3681.

https://doi.org/10.1002/jps.22568

Wu, C.-Y., & Benet, L. Z. (2005). Predicting Drug Disposition via Application of BCS:

Transport/Absorption/ Elimination Interplay and Development of a

Biopharmaceutics Drug Disposition Classification System. *Pharmaceutical*

Research, *22*(1), 11–23. https://doi.org/10.1007/s11095-004-9004-4

Yang, G., Ge, S., Singh, R., Basu, S., Shatzer, K., Zen, M., Liu, J., Tu, Y., Zhang, C.,

Wei, J., Shi, J., Zhu, L., Liu, Z., Wang, Y., Gao, S., & Hu, M. (2017).

Glucuronidation: Driving factors and their impact on glucuronide disposition.

Drug Metabolism Reviews, *49*(2), 105–138.

https://doi.org/10.1080/03602532.2017.1293682

Yang, Z., Gao, S., Yin, T., Kulkarni, K. H., Teng, Y., You, M., & Hu, M. (2010).

Biopharmaceutical and pharmacokinetic characterization of matrine as

determined by a sensitive and robust UPLC–MS/MS method. *Journal of*

Pharmaceutical and Biomedical Analysis, *51*(5), 1120–1127.

https://doi.org/10.1016/j.jpba.2009.11.020

Yang, Z., Zhu, W., Gao, S., Xu, H., Wu, B., Kulkarni, K., Singh, R., Tang, L., & Hu, M.

(2010). Simultaneous determination of genistein and its four phase II metabolites

in blood by a sensitive and robust UPLC–MS/MS method: Application to an oral

bioavailability study of genistein in mice. *Journal of Pharmaceutical and Biomedical Analysis*, *53*(1), 81–89. https://doi.org/10.1016/j.jpba.2010.03.011

Yuan, H., Chai, S. C., Lam, C. K., Howard Xu, H., & Ye, Q.-Z. (2011). Two methionine aminopeptidases from Acinetobacter baumannii are functional enzymes. *Bioorganic & Medicinal Chemistry Letters*, *21*(11), 3395–3398. https://doi.org/10.1016/j.bmcl.2011.03.116

Zhang, L., Lin, G., & Zuo, Z. (2006). Position preference on glucuronidation of mono-hydroxylflavones in human intestine. *Life Sciences*, *78*(24), 2772–2780. https://doi.org/10.1016/j.lfs.2005.10.038

Zhu, L., Lu, L., Wang, S., Wu, J., Shi, J., Yan, T., Xie, C., Li, Q., Hu, M., & Liu, Z. (2017). Chapter 11 - Oral Absorption Basics: Pathways and Physicochemical and Biological Factors Affecting Absorption. In Y. Qiu, Y. Chen, G. G. Z. Zhang, L. Yu, & R. V. Mantri (Eds.), *Developing Solid Oral Dosage Forms (Second Edition)* (pp. 297–329). Academic Press. https://doi.org/10.1016/B978-0-12-802447-8.00011-X

(2006). In *The United States Pharmacopeia* (24th ed., p. 3166).